Universität Bremen

MAX-PLANCK-INSTITUT FÜR MARINE MIKROBIOLOGIE

Master of Science Thesis

Seasonal variations of free-living and particle-associated microbial communities in Fram Strait, Arctic Ocean

Ana Carolina Bercini Gusmão

Reviewer: Dr. Christina Bienhold
Second Reviewer: Prof. Dr. Morten Iversen

HGF MPG Joint Research Group for Deep-Sea Ecology and Technology

Max Planck Institute for Marine Microbiology

Bremen, March 2025

Submitted as part of the requirements for the degree of Master in Science in Marine Microbiology to the International Max Planck School of Marine Microbiology (MarMic), program part of Max Planck Society, University of Bremen and Alfred-Wegener Institute for Polar and Marine Research. The thesis was conducted in the HGF MPG joint research group for Deep-Sea Ecology and Technology during September 2024 to March 2025.

Statement

Hiermit versichere ich, dass ich diese Arbeit selbständig verfasst und keine anderen als die angegebenen Quellen und Hilfsmittel verwendet habe.

I herewith confirm that I have written this thesis unaided and that I used no other resources than those mentioned.

_____ _____

(Ort und Datum / Place and Date) (Unterschrift / Signature)

Abstract

The Arctic Ocean experiences extreme seasonality, with variations in solar radiation, temperature and sea-ice cover, influencing biological productivity. In addition, climate change leads to long-term changes in the region marked by sea-ice loss and increasing temperatures. Sinking particles are essential in the biological carbon pump, transporting carbon to deeper ocean layers. Microbial eukaryotes drive primary production and contribute to particle composition or are associate to them as parasites. Prokaryotes (bacteria and archaea) mediate particle transformation by degradation, nutrient availability regulation, and influencing the particle fluxes efficiency. The Fram Strait is a gateway that connects the Arctic Ocean and the Atlantic with two dynamic opposing currents that exchange water masses, nutrients, heat, and sea ice between oceans. This study assessed the composition, structure and environmental drivers of prokaryotic and microbial eukaryotic communities in surface water and sinking particles in the Fram Strait, and focusing in the interplay between microbial communities, particle fluxes and environmental drivers. Seasonality resolved sampling of surface water and sinking particles was conducted over four years (2016-2021) using autonomous samplers at the central station of the Fram Strait, with samples sequenced to generate amplicon data (16S and 18S) as part of the FRAM Molecular Observatory within the long-term ecological observatory HAUSGARTEN. The most dominant families observed were *Bacillariaceae* and *Flavobacteriaceae* for surface water and *Dino-I-1* and *Mycoplasmataceae* for particle-associated. Seasonality influenced richness and structure of surface water communities, whereas the seasonal effects were less pronounced in particle-associated communities. Primary environmental drivers for microbial community structure were temperature, mixed layer depth and sea-ice dynamics, which influenced surface microbial communities and, in turn, sinking particle communities. Interannual variations in environmental parameters, such as changes in sea-ice distance and different stratification regimes between 2017 and 2018, were concomitant with observed variations in the composition of surface and particle-associated microbial communities. The differences between surface and particle-associated communities are likely due to horizontal transfer of particles. A cold anomaly was observed during one of the years with high ice concentration, low temperature, low salinity and a shallow mixed layer depth in the spring. This study provides first insights into a combination of seasonal and interannual variations in a rapidly changing Arctic Ocean and highlights the value of long-term observations at high resolution, in order to assess the interplay between environmental drivers and microbial community structure and function of microbial communities and particle fluxes in the central area of Fram Strait.

TABLE OF CONTENTS

List of Abbreviations

POM	Particulate organic matter
MLD	Mixed layer depth
EGC	East Greenland Current
WSC	West Spitsbergen Current
POC	Particulate organic carbon
PON	Particulate organic nitrogen
CARB	Carbonate
SIL	Silica
SID/ID	Distance to the sea-ice edge
SIC/IC	Sea-ice concentration
TEMP	Temperature
SAL	Salinity
FAW	Fraction of Atlantic Water
FPW	Fraction of Polar Water

1 INTRODUCTION

1.1 Seasonal dynamics in the Arctic Ocean

The Arctic Ocean is a nearly landlocked ocean characterized by strong seasonal patterns of solar radiation, sea-ice cover, river runoff, and atmospheric temperatures (Stein and Macdonald, 2003; Walsh, 2008; Leu et al., 2015). The winter season is marked by low temperatures, the presence of sea ice and very limited or no light available for primary production, depending on the latitude (Berge et al., 2015; Leu et al., 2015). Despite the lack of photosynthetic activity, heterotrophs are sustained by utilizing carbon produced during the previous light period (Sakshaug, 2004, Berge et al, 2015).

As light returns in spring months (April to May), biological productivity sets in, fueled by winter nutrients, primarily based on sea-ice algae and phytoplankton (Sakshaug, 2004). The production period is short, ending in late summer or autumn, and is regulated by light and nutrient availability (Berge et al., 2015; Wiedmann et al., 2020). The transition from winter to spring is marked by sea-ice algae vernal blooms occurring as soon as light conditions become favorable (Leu et al., 2015), with phytoplankton blooms occurring only later, after sea-ice melt (Leu et al., 2015; Wiedmann et al., 2020). The ice algae act as an important food source in early spring for pelagic grazers and under-ice fauna (Werner, 1997; Poltermann, 2001; Leu et al., 2015). After their release from the ice, they can form aggregates and contribute to fast-sinking particulate organic matter (POM) (Wiedmann et al., 2020).

Sea-ice dynamics influence the stratification of the Arctic water column (von Appen et al, 2021), which is regulated by salinity rather than by temperature (Rudels and Carmack, 2022). The melting of sea ice in summer, together with river runoff, introduces a significant input of freshwater into the system, creating a low salinity surface layer with low density, resulting in a stratified water column (Ekwurzel et al., 2001; von Appen et al, 2021). Sea ice can also influence the biota, as strong stratification can lead to rapid bloom development and nutrient depletion due to the limitation of the supply of nutrients by vertical mixing (Stein and Macdonald, 2003; Oldenburg et al., 2024b). The extent of stratification, most importantly the

mixed layer depth (MLD), influences the ecosystem by keeping phytoplankton in the surface layer of the ocean (von Appen et al, 2021). Moreover, sea-ice also influences the timing of phytoplankton blooms and, consequently, the proportion and quality of the sinking particles (Hodal et al., 2012).

The Arctic is one of the most sensitive regions to the effects of the changing climate (Walsh, 2008; Pörtner et al., 2019). In recent decades, a decline in sea ice coverage, thickness, and extent has been observed (Comiso et al., 2008; Kwok et al., 2009), with approximately 12% reduction in sea-ice extent during September in the Artic (Figure 1) (Spreen et al., 2008). The retreat of sea ice can affect carbon flux characteristics (Fadeev et al., 2021). Additionally, there has been an increase in sea surface temperature and in the inflow of warmer water masses into the Arctic region (Beszczynska-Moller et al., 2012; Polyakov et al., 2017; Pörtner et al., 2019; AMAP, 2021). Increase in sea surface temperatures, light availability, along with changes in sea-ice dynamics, will alter the seasonal cycle in the Arctic Ocean, with an increase in primary production projected (Arrigo et al., 2008; Lewis et al., 2020). However, a water column more stratified in summer limiting the nutrient supply in the euphotic zone, eventually will lead to a reduction of net primary productivity (Arrigo et al., 2008; Carton, Ding and Arrigo, 2015; Lewis et al., 2020). Additionally, an earlier break-up of sea-ice, leading to an earlier spring phytoplankton bloom, can increase sinking export due to a mismatch between the timing of phytoplankton and zooplankton cycles (Dunweber et al., 2010; Sejr et al., 2007).

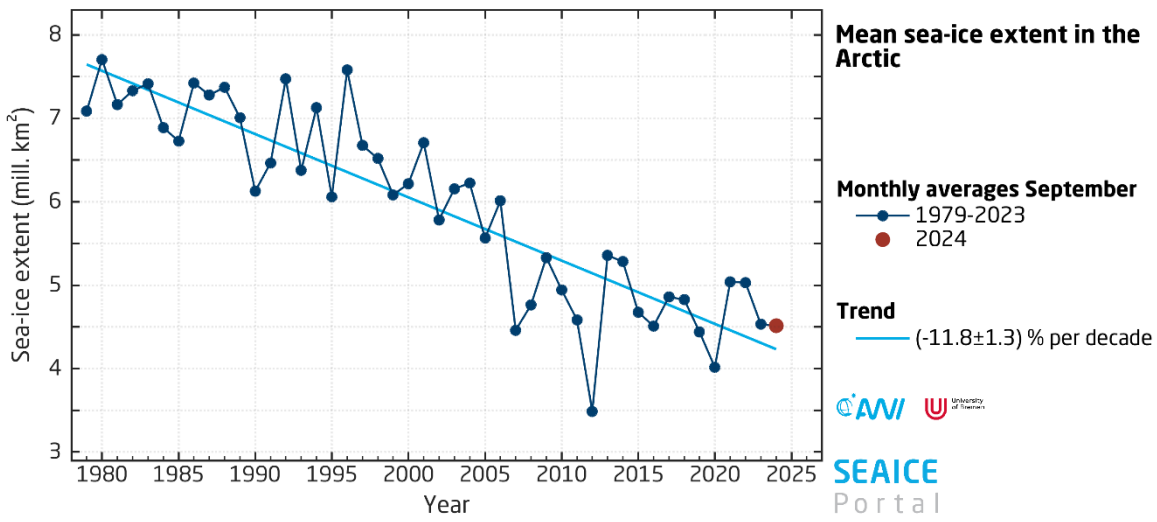

Figure 1: Mean sea-ice extent (in million square kilometers) in the Artic during September from 1979 to 2023. Sea ice data obtained from meereisportal.de (Spreen et al., 2008)

Heterotrophic prokaryotes play an essential role mediating fluxes of nutrient and carbon in marine ecosystems (Arrigo et al., 2005; Azam and Malfatti, 2007). In this thesis, the term 'prokaryotes' refers collectively to bacteria and archaea and will be used throughout the text. Despite some taxa that are abundant worldwide, marine polar environments have unique microbial assemblages (Ghiglione et al., 2012). In the Arctic environment, the key taxa composing primary producers are diatoms, mainly *Melosira arctica* and *Nitzschia frigida*, and pico- or nano-phytoplankton (Wiedmann et al., 2020). The diatoms dominate spring blooms, often co-occuring with *Micromonas pusilla* and *Phaeocystis pouchetti*, which are abundant in summer (Berge et al, 2015; Leu et al., 2015). Other microbial eukaryotes such as cryptophytes has also been previously reported in Artic waters (Lovejoy et al., 2011).

The abundance of surface marine prokaryotic communities is described as strongly influenced by seasonality, primarily due to light availability and phytoplankton blooms (Pedrós-Alió, Potvin and Lovejoy, 2015; Wilson et al., 2017), as well as spatial differences (Lee at al., 2019). During summer and early fall, the most abundant classes are Alphaproteobacteria, Gammaproteobacteria and Flavobacteriia (Pedrós-Alió, Potvin and Lovejoy, 2015; Wilson et al., 2017; Lee at al., 2019; Öztürk et al., 2024). Alphaproteobacteria are associated with open-water, oligotrophic conditions (Pedrós-Alió, Potvin and Lovejoy, 2015), whereas Gammaproteobacteria and Flavobacteriia are linked to high light availability and increased phytoplankton levels (Wilson et al., 2017). During winter, an increase in microbial diversity and archaeal taxa have been reported (Wilson et al., 2017).

Due to the presence of sea-ice and other winter conditions, continuous observations are difficult in high-latitude environments. However, the use of autonomous technologies allows year-round studies in polar environments (Herfort et al., 2016; Wietz et al 2021), unveiling seasonal transitional phases. Coupled with DNA sequencing, the use of autonomous technologies, such as sediments traps (Cardozo-Mino et al., 2023) and Remote Access Samplers (RAS) (Metfies et al., 2017; Wietz et al., 2022), allows the linkage between particle fluxes and microbial diversity, even in remote areas like the Arctic Ocean. Understanding the

seasonal patterns and environmental drivers of microbial communities in the Arctic is essential for comprehending the variability in their taxonomy composition, resilience and gaining insights into their responses to the ongoing changes in the Arctic Ocean.

1.2 Sinking particles and the Biological Carbon Pump

The array of processes that capture, distribute and store carbon, thereby regulating the CO_2 balance in the ocean, are referred to as carbon pump (Ducklow et al, 2001; Turner, 2015), with sinking particles playing a key role in its biological counterpart (Dugdale and Goering, 1967) (Figure 2). Only a small percentage of net primary production escapes the euphotic zone (De La Rocha and Passow, 2007; Iversen, 2023). Nevertheless, sinking particles are responsible for removing more than 6 Gt of carbon from surface waters annually (Nowicki et al., 2022). The sinking particles are a mixture of organic and inorganic matter, including living and carcasses of phyto-, zoo- and bacterioplankton, biological remains (e.g. abandoned larvacean houses, zooplankton molts), fecal pellets, shells, and minerals (Simon et al, 2002) (Figure 2). These particles connect the surface to the deeper layers of the ocean, transporting organic matter mainly produced in the euphotic zone by the primary producers (Turner, 2015). They also transport nutrients (e.g. C, N, P, S, Fe) and trace elements vertically and horizontally, thereby nourishing the deep-sea ecosystem (Volk and Hoffert, 1985; Fowler and Knauer 1986; McDonnell et al. 2015, Boeuf et al, 2019).

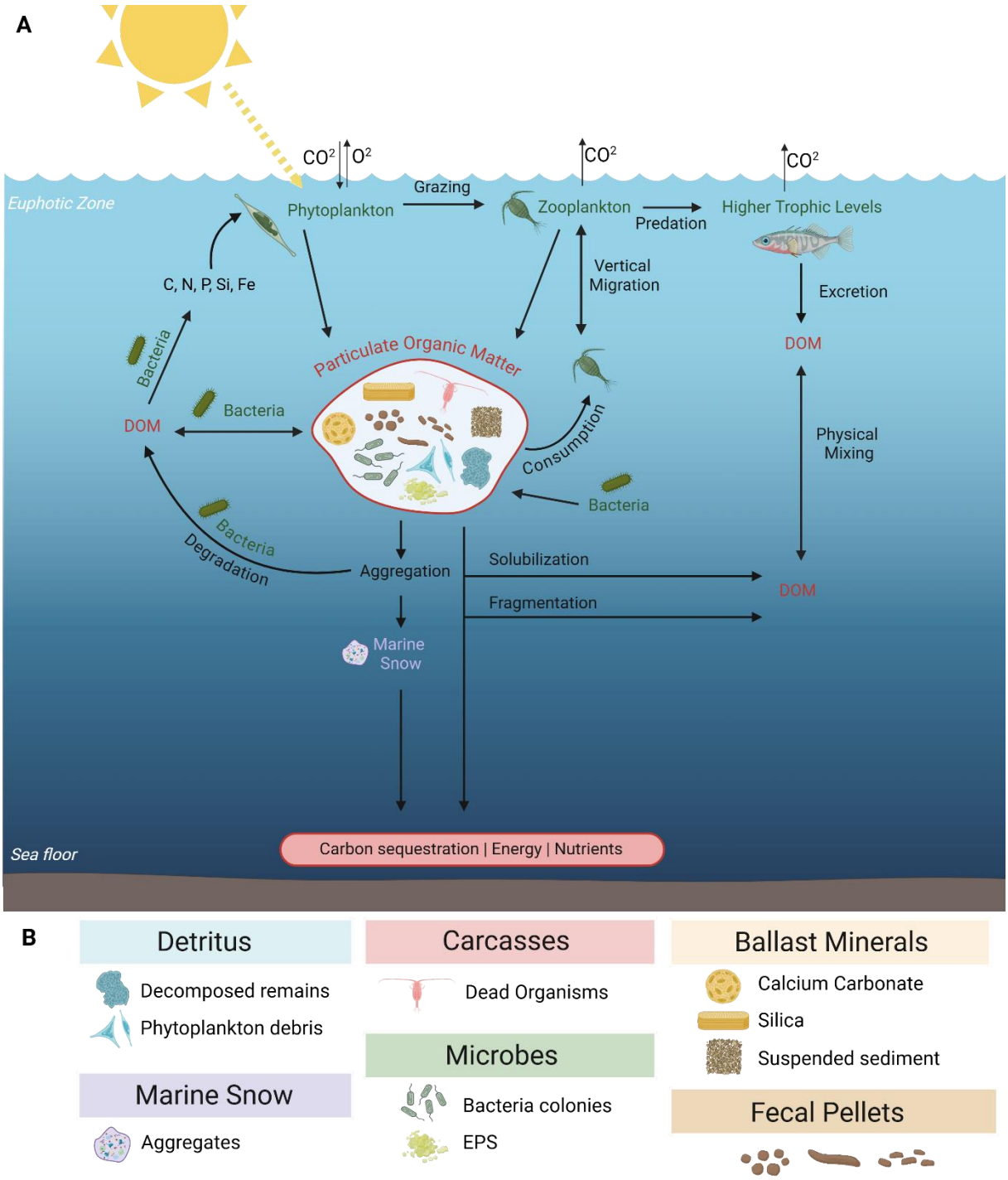

Figure 2: Overview of (A) Biological Carbon Pump and (B) sinking-particle composition. Arrows represent the direction of organic matter. DOM = Dissolved Organic Matter.

During their descent, the particles undergo rapid colonization and ecological succession by prokaryotes (Datta et al., 2016). These prokaryotes mediate particle transformations, such as the breakdown and degradation of organic matter, facilitate the aggregation of small particles into marine snow, or contribute to remineralization and

consequently, trophic transfer of nutrients, carbon and energy through the microbial loop (Simon et al, 2002, Buesseler et al, 2007; Steinberg et al, 2008; Turner, 2015, Nguyen et al., 2022). Other organisms such as flagellates and ciliates consume large fractions of the organic matter (Calbet and Landry, 2004). These processes can strongly attenuate the vertical transport of sinking particles (Martin et al. 1987).

The quantity and quality of particles are highly variable due to geographic differences, seasonality, and the vertical distribution of organisms that interact with and produce particles in the water column (Francois et al., 2002; Henson, Sanders and Madsen, 2012). Particle type also influences the efficiency of carbon transport to the deep-sea due to differences in sinking rates (Buesseler and Boyd et al., 2009; Mestre et al., 2018). Larger particles and fecal pellets sink faster, increasing their chances of reaching deeper layers (Mestre et al., 2018; Fadeev et al., 2021). Additionally, environmental surface conditions affect the timing and duration of phytoplankton blooms, consequently influencing particle composition, abundance, and distribution (Simon et al., 2002; Buesseler and Boyd, 2009; Guidi et al., 2009)

1.3 Sinking particle microbiota

It is well known that sinking particles provide a unique habitat enriched with reduced chemical substrates and elevated extracellular activity, fueling a wide range of microbial metabolisms (Kirchman et al., 2010). These particles often harbor distinct microbial taxa compared to the surrounding seawater (Fontanez et al., 2015; Leu et al., 2022). Additionally, sinking particles can act as dispersal vectors for viable microbes from the surface, influencing microbial community structure and function in the deep sea (Mestre et al, 2018, Preston et al., 2020; Fadeev et al., 2021). Some microbial taxa, considered rare in surface waters, can become more abundant at deeper layers due to vertical transport, the so-called “seed” taxa (Mestre et al., 2018; Fadeev et al., 2021).

The size of particles influences microbial composition and transport efficiency, with larger particles being more efficient at carrying particle-attached microbes to deeper layers (Mestre et al., 2018; Durkin et al., 2022). The quality of particles also plays a role in shaping

particle-attached heterotrophic microbial communities, enhancing specific taxa (Stephens et al., 2024). Moreover, these microbial communities undergo compositional shifts with increasing water column depth (Mestre et al., 2018) and progressive particle degradation (Durkin et al., 2022).

The taxonomic composition and microbial dynamics of particle-associated microbes has been studied worldwide, including the Pacific (Mestre et al., 2018; Boeuf et al, 2019; Preston, Durkin and Yamahara, 2020; Preston et al., 2020; Durkin et al., 2022; Stephens et al., 2024), Atlantic and Indian oceans (Mestre et al., 2018), and polar regions (Balmonte, Teske and Arnosti, 2018; Cardozo-Mino et al.,2023). In deep oligotrophic waters, sinking particle microbial communities were dominated by *Arcobacter* and *Sulfurovum*, *Colwellia, Moritella and Shewanella*, with lower contribution of archaea (Boeuf et al., 2019). In a sub-artic region, Stephens et al (2024) found an overlap of free-living and particle-attached communities, including taxa such as *Pirellulaceae, Alteromonadaceae* and *Vibrionaceae.* The Vibrionaceae specifically, was identified as a proxy of freshly produced zooplankton fecal pellets, with a replacement by other taxa during degradation and sinking of the particles (Stephens et al., 2024). In the Central Arctic, some taxa such as Alphaproteobacteria, Flavobacteria and Gammaproteobacteria highly present in surface seawater were found in sinking particles at 500 meters (Balmonte et al., 2018).

Microbial eukaryote communities within sinking particles are described as more variable, including grazers, protists, parasites and surface-water-derived foraminifera and radiolarians (Boeuf et al., 2019). The latter ones are sporadically found in deeper region, related to higher inputs through fast-sinking particles (Boeuf et al, 2019). Similar to the findings in the central Arctic by Balmonte et al. (2018), Cardozo-Mino et al. (2023) found Alphaproteobacteria and Gammaproteobacteria strongly dominating bacterial communities of sinking particles in another Arctic region, the Fram Strait, together with other phytoplankton-associated taxa, such as Bacteroidia and Verrucomicrobiae during high carbon export events. Also, a high dominance of diatoms (Bacillariophyta), dinoflagellates (Syndiniales), and radiolarians (Acantharea) were described (Cardozo-Mino et al., 2023)

Identifying the microbiota associated with sinking particles and understanding their seasonal and temporal dynamics is crucial for gaining insights into local carbon export fluxes, biogeochemical cycles, nutrient dynamics and ecosystem resilience. This information is particularly valuable for highly climate-sensitive environments like the Arctic (Walsh, 2008; Pörtner et al., 2019), as sinking particles play a key role in the BCP (Dugdale and Goering, 1967; Iversen 2023), which is responsible for the majority of organic matter transport to deeper ocean layers (Turner, 2015).

1.4 Fram Strait and Long-Term Ecological Research observatory HAUSGARTEN

The Fram Strait (77°N/81°N), located between Greenland and Svalbard, connects the central Arctic to the North Atlantic, acting as a gateway between the two ocean basins. The exchange of water masses occurs in both directions (Rudels, 2015) (Figure 3). The inflow of warmer and salty Atlantic water (2.7 to 8°C) flows toward the central Arctic via the West Spitsbergen Current (WSC) (Beszczynska-Möeller et al., 2011; Nöthig et al, 2015), with some recirculation in the central region of the strait (Hattermann et al., 2016). At the same time, it is also where the majority of the Arctic ice export occurs, along with the outflow of the cold and less saline polar water (-1.7 to 0°C) via the East Greenland Current (EGC) (Beszczynska-Möeller et al., 2011; Nöthig et al, 2015). These water masses harbor different microbial communities, including eukaryotes, plankton communities, and bacteria (Nöthig et al, 2015; Wietz et al., 2021).

An average of 2800 km^3 of ice is exported through the Fram Strait each year via the Transpolar Drift, with significant interannual variability (Dickson et al 2000). Between 1990 and 2010, this export increased by 10% per decade due to enhanced ice melt in the Central Arctic (Zamani et al., 2019). Sea-ice dynamics play a key role in sinking-particle processes in the region, with ice-covered regions exhibiting higher export efficiency and enhanced microbial connectivity (Fadeev et al., 2021). It also influences the composition and timing of zooplankton (Ramondec et al., 2022), as well as the composition, structure and functionality of bacterial communities (Priest et al., 2023). For phytoplankton, only minor changes in bloom

timing or duration were observed, however the seasonal variability increased (Nöthig et al, 2015).

In addition to sea ice, the influx of Atlantic water also influences the Fram Strait ecosystem. Priest et al. (2023) identified metabolically distinct microbial populations associated with varying levels of ice coverage and Atlantic water influx. In the past, two warm anomaly periods were observed in the region (1999-2000 and 2005-2007) (Beszczynska-Möller et al., 2012). The warm anomaly of 2005-2007 had temperatures exceeding 1°C from the usual, along with a decrease in the ice extent and biogenic matter fluxes (Beszczynska-Möller et al., 2012; Lalande et al., 2013). This warm anomaly led to changes in species composition and abundance of the dominant phytoplankton taxa in the region (Nöthig et al, 2015; Onda et al., 2020). It caused a shift from the dominance of large diatoms to smaller cells, such as coccolithophores, later replaced by an increase in the flagellates *Phaeocystis pouchetti* that persisted in the next years (Lalande et al., 2013; Nöthig et al, 2015). Atlantic water influxes are also related to the northward expansion of subarctic habitats which bring invasive species with the potential to replace Arctic communities, the “Atlantification” phenomenon, with consequences throughout the entire Arctic food web (Polyakov et al., 2017)

Seasonal pattern in surface water microbial communities in the region of Fram Strait have been previously described (Oldenburg et al., 2024a, Priest et al., 2025). Microeukaryotic communities were described exhibiting a recurring structure, starting in early spring with primary producers, transitioning to mixotrophs in autumn, and eventually leading to the dominance of heterotrophs and parasites in winter (Oldenburg et al., 2024a). Key taxa identified by Oldenburg et al. (2024a) include Ochrophyta dominating primary production, with a shift to Chlorophyta in autumn. Dinoflagellates, such as Syndiniales and Dinophyceae, are dominant in the transitional phases of spring and autumn (Oldenburg et al., 2024a). Other key groups include Ciliophora in summer, Cryptophyta in summer and autumn, and Radiolaria in winter and spring (Oldenburg et al., 2024a).

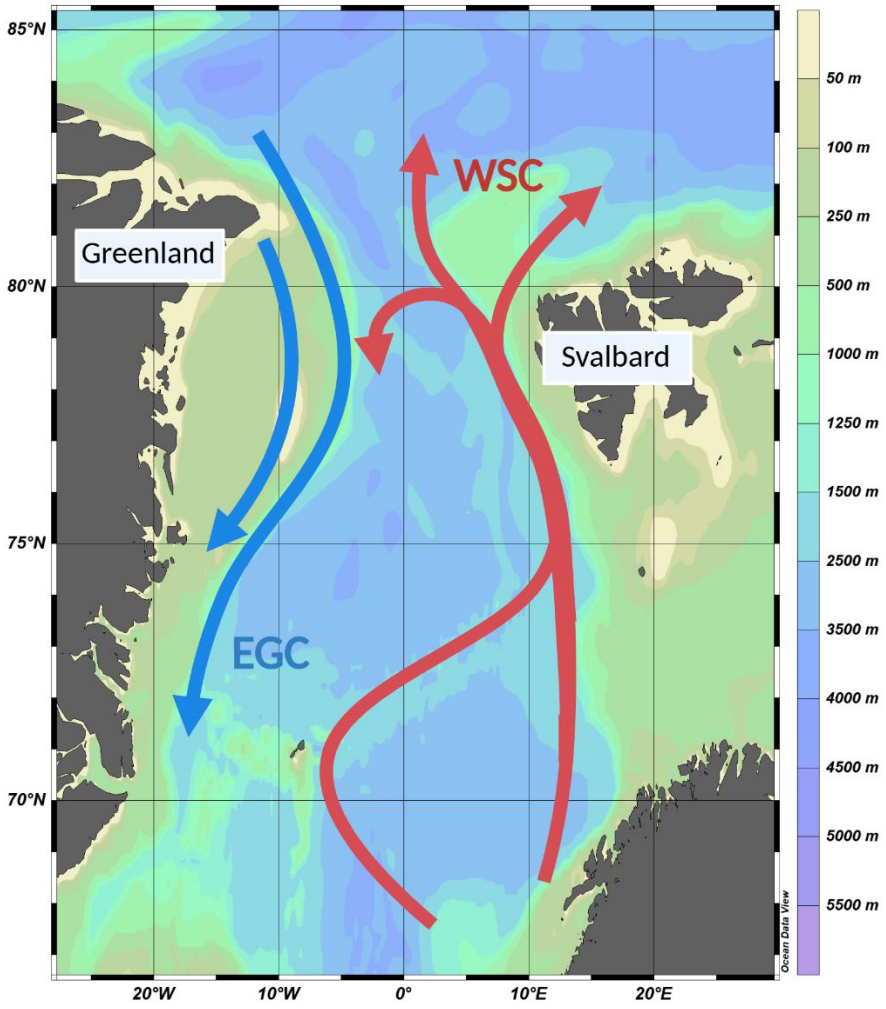

Figure 3: Bathymetric map of the Fram Strait with main currents. Flow directions are indicate by arrows, where the red arrows indicate the West Spitsbergen Current carrying Atlantic Water into the region and the blue arrows the East Greenland Current with cold polar water exiting the Arctic Ocean**.**

The Fram Strait is a key Arctic region due the interaction of water masses from the Artic and Atlantic Oceans (Beszczynska-Möller et al., 2011; Nöthig et al, 2015), and as a polar region, it is also subject to extreme seasonality. Even though the region has been studied for over 20 years (Soltwedel et al., 2016), the use of amplicons sequencing analysis coupled with sediment traps is recent (Cardozo-Mino et al., 2020). Understanding the seasonal dynamics, environmental drivers and interactions between sinking particle-attached microbes with free-living surface microbial communities is essential in this highly seasonal environment. Moreover, characterizing the composition of these communities provide valuable insights into the microbial connectivity throughout the water column, and the impact of seasonal changes and interannual variations on carbon cycling in the Arctic. A previous study identified the

prokaryotic communities associated with sinking particles in the Fram Strait region (Cardozo-Mino et al., 2023). However, this study was focused on high export events in spring and summer and spring between 2000 and 2012. An seasonally resolved study of sinking-particle microbial communities in the Fram Strait is essential to better understand the transitional phases and seasonal dynamics within these communities and contrast them to interannual dynamics.

This study was conducted in the framework of the FRAM Molecular Observatory at the Long-Term Ecological Research (LTER) Site HAUSGARTEN operated by the Alfred Wegener Institute Helmholtz Center for Polar and Marine Research. Sequences from surface waters were available from the FRAM Molecular Observatory. Sinking particle samples were sequenced as part of the EU Project AtlantECO (European Union's Horizon 2020 research and innovation programme, grant agreement number 862923). Resources were provided by the Alfred Wegener Institute Helmholtz Centre for Polar and Marine Research (AWI) and the Max Planck Institute for Marine Microbiology.

1.5 Aims of the project

This project investigates the composition of bacterial and eukaryotic communities in surface waters and on sinking particles across four years, using seasonally resolved amplicon sequencing data collected with autonomous samplers in the Fram Strait. The major goal was to identify and explore seasonal and interannual variations of surface water free-living and particle-attached microbial communities in their environmental context, including sea ice cover, water properties and particulate organic carbon flux.

We hypothesized that:

1. The strong seasonal dynamics in the Arctic are reflected not only in annually recurring seasonal patterns of free-living but also of sinking-particle associated microbial communities
2. Strong interannual environmental variations, such as sea ice or water temperature anomalies, lead to observable shifts in the composition of both surface water and particle-associated communities.
3. Sea ice dynamics are a major driver for shaping surface microbial communities, and subsequent microbial particle composition

2 MATERIAL AND METHODS

2.1 Sampling

Surface water and sinking-particle samples were collected at the Long-Term Ecological Research Observatory (LTER) HAUSGARTEN station HGIV, located in the central area of the Fram Strait (79°0'25.92" N, 4°20'3.12" E), Arctic (Figure 4). The sampling occurred during RV Polarstern expeditions PS99, PS107, PS114 and PS121. The deployment and collection dates, as well as the sampling depths of sediments traps and moored Remote Access Samplers (RAS) can be found in Appendix 1.

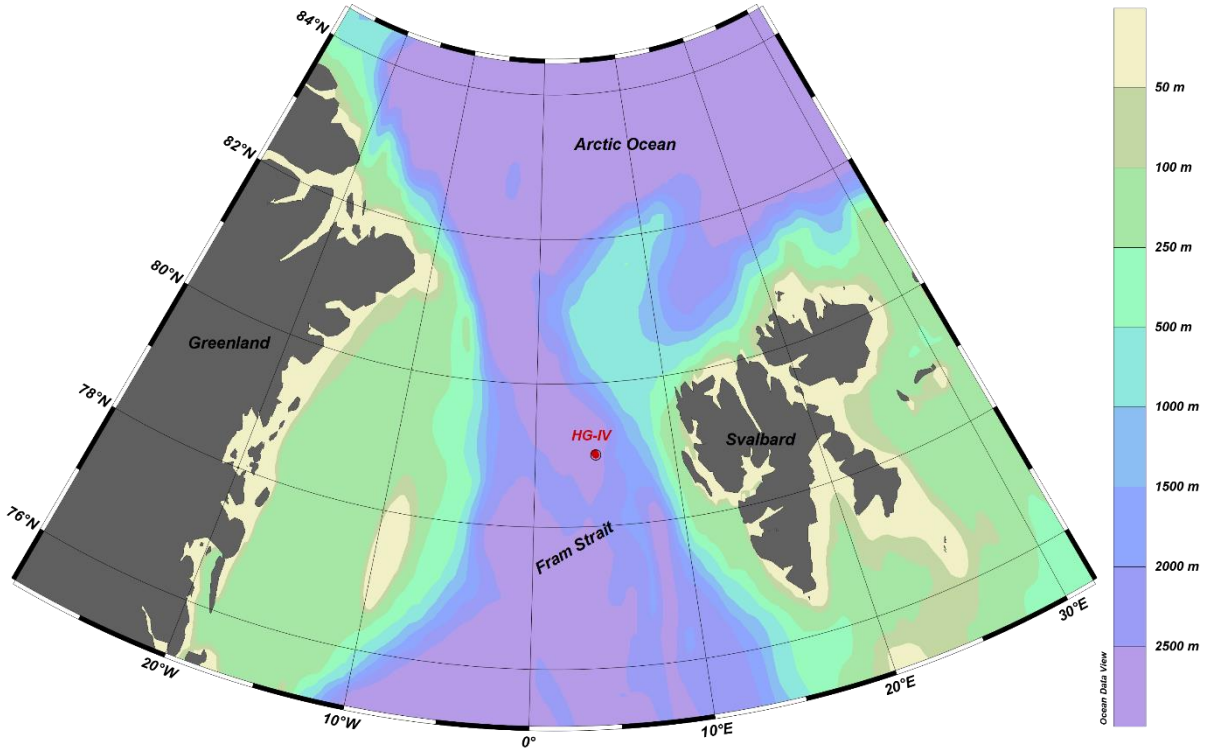

Figure 4: Location of the HG-IV station at the LTER HAUSGARTEN observatory in Fram Strait. In black the name of the main regions. At side, the color gradient represents the bathymetry of the region.

Sinking particles were sampled using automatic sediment traps (K.U.M trap type K/MT 234, Kiel Germany) and surface water was sampled using Remote Access Samplers (RAS; McLane Research Laboratories) (Figure 5). Both systems were anchored by seafloor moorings, deployed and recovered as part of AWI-led expeditions over four complete years (mid-2016 – mid-2021). Deployments usually lasted 1 year, except for RAS and sediment traps recovered

during PS121, which remained in the water for 2 years (2019-2021). Due to water movement, the sampling depth of RAS varied between 24 and 131 meters. For the sediment traps, the average deployment depth was around 200 m.

Sediment traps had a sampling area of 0.5 m^2 with 20 collection cups. Each cup was filled with sterile-filtered North Sea seawater (40 PSU) and mercuric chloride (0.14% final concentration), which served as fixation for the samples (Wietz et al., 2022). Sampling cups rotated at intervals that varied between 8 and 91 days, depending on the anticipated magnitude of particulate organic matter (POM) flux. After recovery, samples were refrigerated at 4°C for later analysis. The samples corresponding to the period of spring and summer of 2019 were not collected due to a failure in the sediment trap mechanism. In the laboratory, zooplankton (swimmers) larger than 0.5 mm were removed with forceps under a dissecting microscope (AWI Polar Biological Oceanography Group). Then, samples were split using a wet splitting procedure (Bodungen et al, 1991) for different measurements and stored at 4 °C. All samples were checked for signs of decomposition in the original cups, including rotten or sulfidic smell, black color and zooplankton decomposition.

The RAS contained 48 sterile sampling bags (500 ml), filled with 700 µL of mercuric chloride solution (7.5% w/v). The sampling events were previously programmed, with two samples per event with an hour apart. At an event, approximately 500 ml of water were automatically pumped and fixed by the mercuric chloride (0.01% final concentration). After recovery and subsampling for distinct analysis, two sampling bags were combined and filtered using 0.22 µm Sterivex filters and refrigerated at -20°C for later analysis.

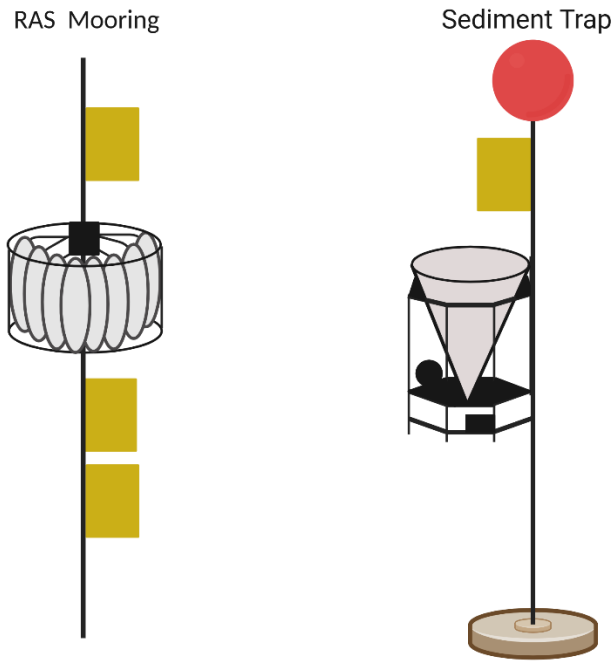

Figure 5: Scheme of (A) Remote Access Sampler (RAS) and (B) Sediment Trap. Yellow squares represent CTD sensors.

2.2 DNA extraction and sequencing

DNA extractions from sinking particle and surface water samples were done using the DNeasy PowerWater Kit (QIAGEN, Germany) by the AWI Polar Biological Oceanography and Deep-sea Ecology and Technology groups, following the manufacturer's protocol. For prokaryotes the 16S hypervariable V4–V5 rRNA region was amplified using primers 515F (5'-GTG YCA GCM GCC GCC GTA A-3') and 926R (5'-CCG YCA ATT YMT TTR AGT TT-3') (Parada et al. 2016). For microbial eukaryotes, the hypervariable V4 region of the 18S rRNA gene was amplified using primers 528iF (5'-GCG GTA ATT CCA GCT CC A-3') and 964iR (5'-AC TTT CGT TCT TGA TYR R-3') (Metfies et al., 2020). Sequencing was performed by Genoscope (National Center of Sequencing, France) for the sinking-particle samples and by the Alfred-Wegener Intitute for the surface water samples, both using Illumina MiSeq platform in 2 × 300 bp paired-end runs (Wietz et al., 2021; Cardozo-Mino et al., 2023). Negative controls of PCR amplification were available for surface water samples, but were not provided for sinking-particle samples. Some samples were unsuccessful in the sequencing process. The samples for the sediment trap, Fevi34 cups 4, 12 and 15, and Fevi40 cups 7, 10, 11 and 12, failed in the sequencing of microbial eukaryotic organisms, while Fevi 40 cup 9, failing for both prokaryotic

and eukaryotic sequencing. An overview of samples can be visualized on the Appendix 1. For the RAS samples, the HS2_PS114_E9 (corresponding to the first half of February 2018) and HS2_PS114_E11 (corresponding the first half of March 2018) failed in the sequencing of microbial eukaryotic organisms. The sequences for the water column are deposited in the European Nucleotide Archive under umbrella project FRAM/HAUSGARTEN with accession number PRJEB43905. The sequences for the sinking particles are uploaded in the same repository under umbrella project AtlantECO with accession number PRJEB78421.

2.3 Environmental parameters

Biogeochemical measurements of the particles, such as particulate organic matter (POM), particulate organic carbon (POC), particulate organic nitrogen (PON), silica (dissolved and particulate), and calcium carbonate ($CaCO_3$), were provided by the Polar Biological Oceanography group at AWI (pers. comm. M.Iversen). Briefly, triplicate subsamples for POC and PON analyses were measured using an elemental analyzer after filtration through pre-combusted GF/F filters (0.7 µm, 500 °C for 4 h) and an acid treatment (0.1 N HCL) to remove inorganic carbon and drying (60°C for 12 h). The $CaCO_3$ content was estimated by measuring inorganic carbon and converting it to carbonate values using correction factors when calcium carbonate-containing organisms were present in the samples. Finally, subsamples for biogenic silica measurements were filtered on cellulose acetate filters (0.8 µm pore size) and determined by a wet-alkaline digestion process followed by an extraction for 2h at 85°C in a shaking water bath. All procedures were conducted following the methodology described in Bodungen et al (1991), which provides more details for each procedure. Fluxes were calculated using the average of triplicates in milligrams (mg) and converted to daily fluxes per square meter. The Dixon's Q test (Dean and Dixon, 1951) was used to identify outliers, resulting in the removing of one replica from POM from Fevi34 cup12.

Environmental parameters of the CTD sensors (SeaBird SBE37-ODO and Microcat) attached to the moorings, including temperature, depth, salinity, oxygen and chlorophyll concentrations measurements, were recovered from PANGAEA repository from von Appen (2019) and Hoppmann et al (2023). The proportion of Atlantic (AW) and Polar water (PW) were

determined based on the physico-chemical characteristics of the water masses, using the environmental parameters collected with the CTD (see Wietz et al. 2021 for details). The polar water comprises both the outflowing water from the Arctic through the East Greenland Current (EGC) and other sources of fresh, cold water, including meltwater. A water mass was considered as pure fraction when its relative proportion exceeded 80%, otherwise it was classified as a mixture. Sea ice concentration is an updated version of Melsheimer et al (2019) in the PANGAEA repository (https://doi.org/10.1594/PANGAEA.898399) that can be recovered from https://seaice.uni-bremen.de/data/amsr2/asi_daygrid_swath/. Distance of sea-ice edge was calculated based on the distance from the mooring to the 20% sea-ice concentration (in km), with negative values indicating that the sea-ice concentration exceeded 20%. Mixed Layer Depth (MLD) was determined by multiple CTD sensors along the mooring. The Physical Oceanography group at AWI (W.-J. von Appen, pers. comm.) provided all the calculations. Finally, the environmental parameters originally in hourly resolution were averaged for daily resolution. Environmental parameters of the surface were associated to the sinking-particle samples with a 4-days delay, assuming particle sinking velocities of 60 m d^{-1} (Fadeev et al., 2021). The definition of seasons followed the seasonal divisions previously established by Wietz et al. (2021) for the Fram Strait: spring (mid-April to mid-June), summer (mid-June to late-July), autumn (August to October), and winter (November to mid-April).

2.4 Bioinformatic and statistical analyses

Statistical analysis was performed using R v.4.4.1 (R Core Team, 2024) and RStudio v.2024.04.2 (Posit team, 2024). The DADA2 workflow and cleaning process followed modified scripts (DataLoad and DataProcessing) for the RAS-1617 repository from https://github.com/matthiaswietz/RAS-1617 (Wietz et al., 2021) and from Pauli et al, 2021. The complete set of scripts used to produce the images in this project can be found at https://github.com/acgusmao32/MSc_FStrait. Primers were removed from the raw paired-end reads using Cutadapt (Martin, 2011). The DADA2 package (Callahan et al., 2016) was used for quality checking of the sequences and taxonomic assignment into amplicon sequence variants (ASVs). The four datasets (prokaryotes and microeukaryotes from the sediment trap, prokaryotes and microeukaryotes from the water column) were analysed separately, and later

merged into two datasets, one for all 16S sequences and one for all 18S sequences. After filtering and truncation (Table 1), error models were calculated from the quality profiles, followed by dereplication, denoising and merging of the sequences. Then, chimeras, junk sequences (sequences outside the expected amplicon length range) and singletons (sequences that appear only once across the entire dataset) were removed. The length range used was 354-412 bp for 16S dataset and 318-403 bp for 18S. Taxonomic assignment were done using the databases SILVA v.138.2 (Quast et al., 2013) and PR2 v.5.0 (Guillou et al., 2013) for 16S and 18S datasets, respectively.

Table 1: Truncation parameters used in DADA2 pipeline for each dataset

Dataset	Trunc values Forward	Trunc values Reverse
16S Sinking Particles	250 bp	190 bp
18S Sinking Particles	260 bp	200 bp
16S Water Column	250 bp	190 bp
18S Water Column	230 bp	216 bp

An additional cleaning step removed for the 16S dataset the ASVs unclassified at phylum level and classified as mitochondria, chloroplasts or considered human contaminants, such as: *Propionibacteriaceae, Weeksellaceae, Corynebacteriaceae, Streptococcaceae, Xanthobacteraceae, Staphylococcacea and Burkholderiaceae* from the 16S dataset. For the 18S dataset, ASVs unclassified at the kingdom level or classified as metazoans were removed. The negative controls of PCR amplification were removed from the surface water samples. Two samples (Fevi36 Up09 and Fevi36 Up15) of the 16S dataset were also removed due to the higher relative abundance of the family *Sulfurimonadaceae.* This taxon is composed by sulfur-oxidizing members (Han and Perner, 2015), which could indicate fixation issues.

The sampling effort was checked using rarefaction curves of the observed species for each dataset, created with iNEXT package v.3.0.1 (Hsieh et al, 2016). Alpha-diversity analysis included the number of observed ASVs, as well as Chao1, Shannon and Inverse Simpson metrics, calculated using the raw ASV table (including singletons and unclassified taxa at phylum or kingdom level) through phyloseq R package v. 1.48.0 (McMurdie and Holmes, 2013). The normalization was achieved by rarefaction using the lowest possible number higher than 10.000 reads. As result, some samples with an insufficient number of reads were

removed, those being Fevi36_Up09, Fevi36_Up15 and HS3_PS121_E35 for microbial eukaryotes and HS1_PS107_E39 for prokaryotes (Appendix 1). Samples were collapsed by season in each dataset, and tested for significance with Kruskal-Wallis and pairwise Wilcoxon tests using the ggpubr package v. 0.6.0 (Kassambara, 2023).

The datasets were further subdivided into particle-attached and surface water categories. For visualization, each subset was then grouped at the family level for prokaryotes and at the class level for microbial eukaryotes, with sample counts transformed into relative abundance percentages. The five most abundant taxa at a specific taxonomic level were identified by the sum of counts across all samples with the grouped file and calculation of relative abundance. Then, all taxa at that specific level with mean abundance lower than 2% were considered rare and removed or collapsed as a new group called “Others”.

To evaluate compositional differences and visualize patterns in the microbial communities, non-metric multidimensional scaling (NMDS) with Bray-Curtis dissimilarity was performed after Hellinger transformation (Wietz et al., 2022). The function envfit also from vegan package, was used to assess the influence of environmental variables on community structure (Oksanen et al., 2007). The method tested significance of each variable through 999 permutations, where variables with low p-value ($p < 0.05$) were considered significantly associated with the structure of the microbial community in the direction of the vector. It was also tested the analysis of variance using distance matrices (ADONIS). The Mantel tests were used to assess the influence of each environmental parameter on microbial community dissimilarity, and between prokaryotic and microbial eukaryotic communities’ dissimilarities. The Mantel test was calculated using vegan package v.2.6.8 (Oksanen et al., 2017) and linkET package v.0.0.7.4 (Huang, 2021), with Euclidean distance for environmental parameters, Bray-Curtis for microbial communities, method Spearman and 999 permutations. Finally, shared and exclusive ASVs were analyzed to identify habitat-specific microbial communities and overlap between habitats at the ASV level, using the ggvenn package v. 0.1.10 (Yan, 2023). Other R packages used during analyses for plot creation included dplyr, ggplot2, gridExtra and tidyverse.

3 RESULTS

3.1 Oceanographic conditions overview

The oceanographic conditions varied across years, with the evident differences observed in the proportion of Atlantic Water (AW) and Polar Water (PW) in 2019 and 2020 (Figure 6). The average proportion of PW in the time-series was 30%, with specific periods reaching 100%. The period from January 2020 to September 2020 reached the highest proportion of PW more frequently, although intermittently. Also, it was observed a record-breaking marine cold air outbreak in early 2020 in Fram Strait, where the intensified cold air interacting in the sea-air interface likely enhanced heat loss, promoting surface cooling (Dahlke, Solbès and Maturilli, 2022). We termed the period between January and September 2020 as a cold anomaly event (McPherson pers. comm.)

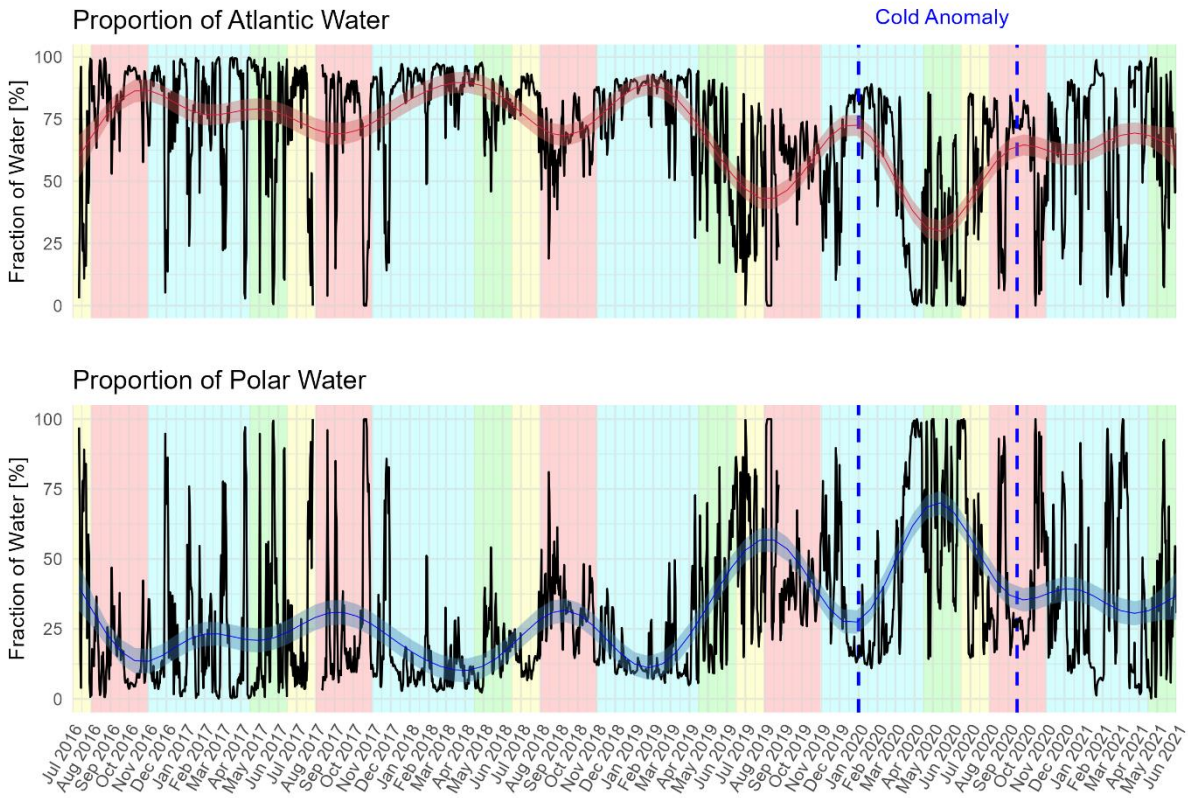

Figure 6: Proportions of water fractions (%) at HG-IV station from July 2016 to June 2021. Trend lines and confidence intervals (95%) are shown in red for Atlantic Water and blue for Polar Water fractions. Background colors represent the seasons: yellow for summer, red for autumn, blue for winter and green for spring. Blue dashed lines indicate the cold anomaly event. The original data (hourly resolution) was averaged per day.

Water temperature varied seasonally, with values dropping during winter and starting to increasing again during spring (Figure 7). With an average of 3.1 ± 1.9 (SD), the lowest recorded temperature was -1.7°C in spring 2020, during the cold anomaly, and the highest value of 7°C was reached in autumn 2016. Salinity was more stable and was 34.8 ± 0.2 (SD), on average, with a decrease between May 2019 and August 2019, as well as between February 2020 and May 2020, also co-occurring with the cold anomaly (Figure 7). Sea-ice concentration is a reflection of the sea-ice transported from other regions through the Fram Strait (Zamani et al., 2019) with peaks usually during spring and summer. An unusual peak (96% coverage) can be observed in late winter, in April 2020, during the cold anomaly event. This higher sea-ice concentration, linked with the higher proportion of polar water, could represent a stronger and earlier melt season. The Mixed Layer Depth (MLD) also presented seasonal trends, reaching higher depths during winter and early spring, with a maximum of 415 m in 2017. A different pattern can be observed between March and April 2020, likely influenced by the lower salinity during the cold anomaly event, which made the water column more stratified, resulting in a shallower MLD.

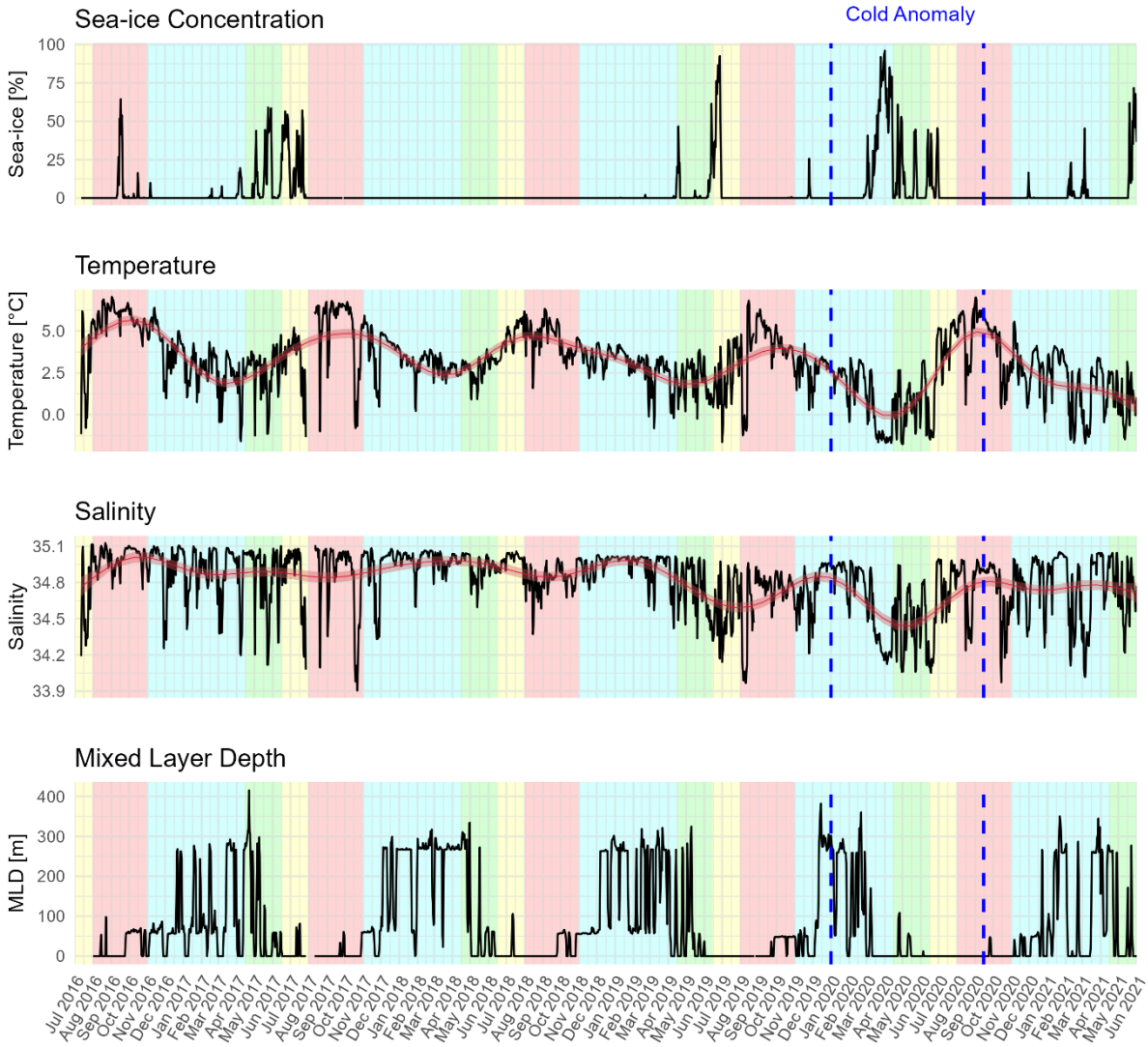

Figure 7: Temperature (°C), Salinity, Sea-ice concentration (% coverage) and Mixed Layer Depth (meters) at station HG-IV from July 2016 to June 2021. Background colors represent the seasons: yellow for summer, red for autumn, blue for winter and green for spring. The trend line and confidence intervals (95%) are shown in red on the two middle plots. Blue dashed lines indicate the cold anomaly event. The original data (hourly resolution) was averaged per day.

Chlorophyll concentrations presented clear seasonal trends (Figure 8), with higher values during spring and summer, reflecting the increase in primary productivity. The cold anomaly does not appear to have an effect on chlorophyll concentrations. However, since the values are uncalibrated, this conclusion cannot be confirmed. The average distance of the sea-ice edge from the mooring was 66.5 ± 17.9 (SD) km, with the distance usually shorter in spring for most of the time-series (Figure 8). A different pattern was observed in spring 2018 with the sea-ice edge being more distant compared to other years. Dissolved oxygen concentrations also presented seasonal variations, as shown by the trend line (Figure 8), with

values increasing during spring as a result of photosynthesis and decreasing during autumn. The concentrations ranged from 283 to 416 µmol/L, with an average of 316.2 ± 17.9 (SD) µmol/L.

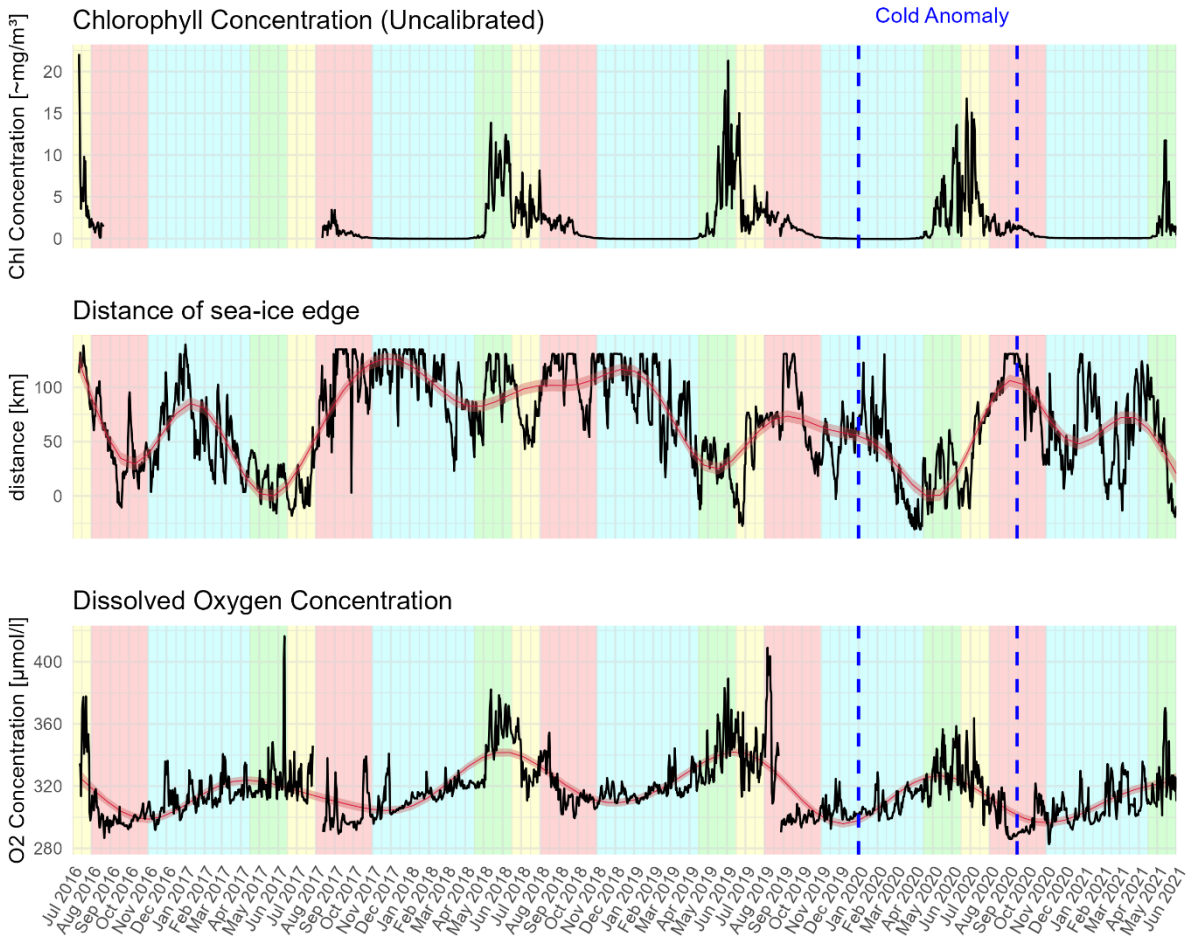

Figure 8: Chlorophyll concentration (mg/m^3), distance of sea-ice edge (km) from the mooring and dissolved oxygen concentration (µmol L^{-1}) at station HG-IV from July 2016 to June 2021. Background colors represent the seasons: yellow for summer, red for autumn, blue for winter and green for spring. The trend line and confidence intervals (95%) are shown in red on the last two plots Blue dashed lines indicate the cold anomaly event. The original data (hourly resolution) was averaged per day.

3.2 Sinking particle fluxes in Fram Strait (2016-2021)

The particle fluxes followed a bi-modal annual export of particulate organic carbon (POC) linked with the productive season (spring, summer/autumn) (Figure 9 - A). The magnitude of POC flux ranged from 0.31 to 35 mg m^{-2} d^{-1}, with the first export event (usually 5 to 10 mg m^{-2} d^{-1}) occurring during the transition from winter to spring and the second, more

intense (> 10 mg m^{-2} d^{-1}), peaking in summer/autumn. Particulate organic nitrogen (PON) remained low for most of the dataset, surpassing 3 mg m^{-2} d^{-1} ± 1 three times, during September of 2016, August 2017 and July 2020. The carbonate flux had an average of 12.6 mg m^{-2} d^{-1} ± 7.6. Overall, the PON and carbonate fluxes followed similar trends to the POC events (Figure 9 – B, C). The exported flux of biogenic silica (BSi), combined with particulate silica (Figure 9 – D), also remained low (< 5 mg m^{-2} d^{-1}) for most of the time series. However, sporadic higher export events (> 10 mg m^{-2} d^{-1}) were observed annually during one of the productive seasons, indicating the development and export of diatom blooms.

There was notable interannual variability in the fluxes observed, with some differences in the timing and magnitude of exports. In 2017, the highest silica export event was not recorded. Also, during this year, the PON flux reached its highest magnitude (4.78 mg m^{-2} d^{-1}) in the time series. In 2018, the higher silica export event occurred earlier, coinciding with the first POC export event, unlike in other years, where it aligned with the second peak in POC export. Also during spring of 2018, the station was more distant of the sea-ice edge than in other years. Finally, deviating from the typical pattern, the second POC export event in 2020 was lower than the first. No significant difference were found in the magnitude of the POC, and carbonate fluxes during the year of the cold anomaly compared to 2017 and 2018 (T-test, $p>0.05$). The higher silica export event was also tested against the events in 2018 and 2016, with no significant difference observed (Wilcoxon, $p>0.05$). For PON, the only significant difference (Wilcoxon, $p<0.05$) was observed with 2017.

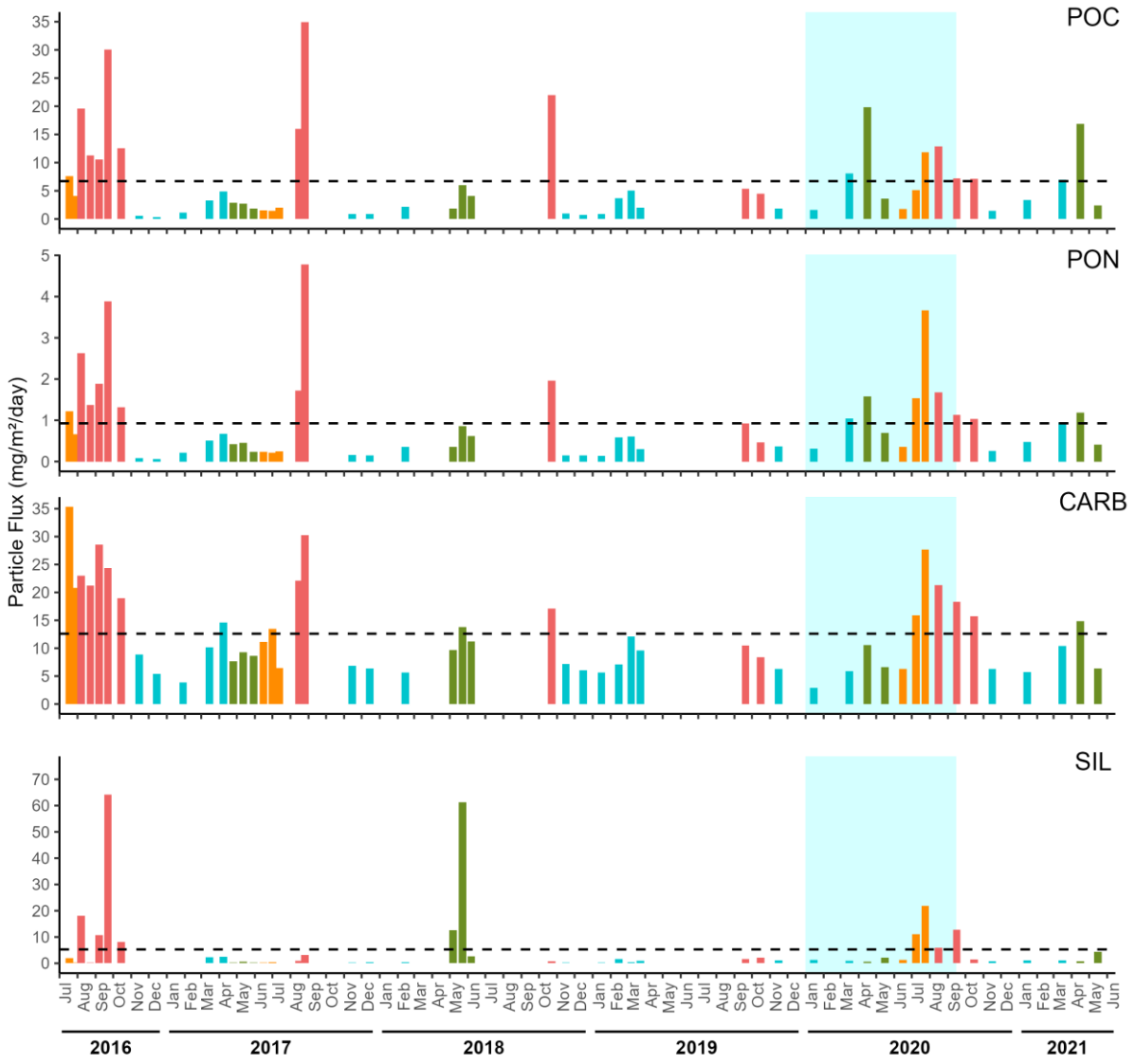

Figure 9: Particle fluxes (mg m^{-2} d^{-1}) at station HG-IV in Fram Strait from 2016 to 2021. The fluxes are (A) POC = Particulate Organic Carbon, (B) PON = Particulate Organic Nitrogen, (C) CARB = Carbonate and (D) SIL = Silica (BSi + Particulate). The black dashed line represents the mean of daily flux rates across the entire period. The blue area indicates the cold anomaly event. Color of the bars represent the seasons: summer (orange), autumn (red), winter (blue) and spring (green).

3.3 Richness and Diversity of microbial communities

We recovered 15084 ASVs for prokaryotes, which after filtering, totalized 13658 ASVs, with 13222 associated with Bacteria and 436 with Archaea. For microbial eukaryotes, 12348 ASVs were identified, with 10635 ASVs remaining after the filtering, with the protist group TSAR with the highest amount of ASVS (8639). The average sequence reads for samples were 126762 ± 94932 for prokaryotes and 108602 ± 66873.

Rarefaction curves showed that diversity was sufficiently covered in most microbial eukaryote samples. Although the full diversity may not have been captured for prokaryotes, the overall coverage indicated that most of the community diversity was captured (Appendix 2). The number of observed ASVs per sample ranged from 311 to 1656 (mean: 876 ± 343 SD) for prokaryotes, with microbial eukaryotes presenting a lower variation in richness, ranging from 64 to 909 (mean: 342 ± 127 SD). Chao1 richness estimates presented a similar pattern as the observed ASVs, with higher variation in prokaryotes (mean: 1289 ± 520 SD) compared to microbial eukaryotes (mean: 402 ± 159 SD). Shannon and Inverse Simpson indices presented an average of 4.6 ± 0.8 SD and 46 ± 37 SD for prokaryotes, and 3.8 ± 0.6 SD and 18.5 ± 12.4 SD for microbial eukaryotes, respectively.

Richness differed significantly across seasons (Kruskal-Wallis, $p \leq 0.05$) for all metrics in surface water prokaryotic communities, highlighting the importance of seasonal variability for the diversity of these communities. For particle-associated communities, only observed ASVs and Chao1 presented significant differences across seasons (Figure 10). These results suggest the presence of unique ASVs per season, which, however, do not affect community evenness. The winter was the season with highest richness and diversity, being significantly different from the other seasons in most pairwise comparisons (Wilcoxon test, $p \leq 0.05$). These elevated values are likely due the mixture of deep and surface waters that occurs during winter, which inflates richness.

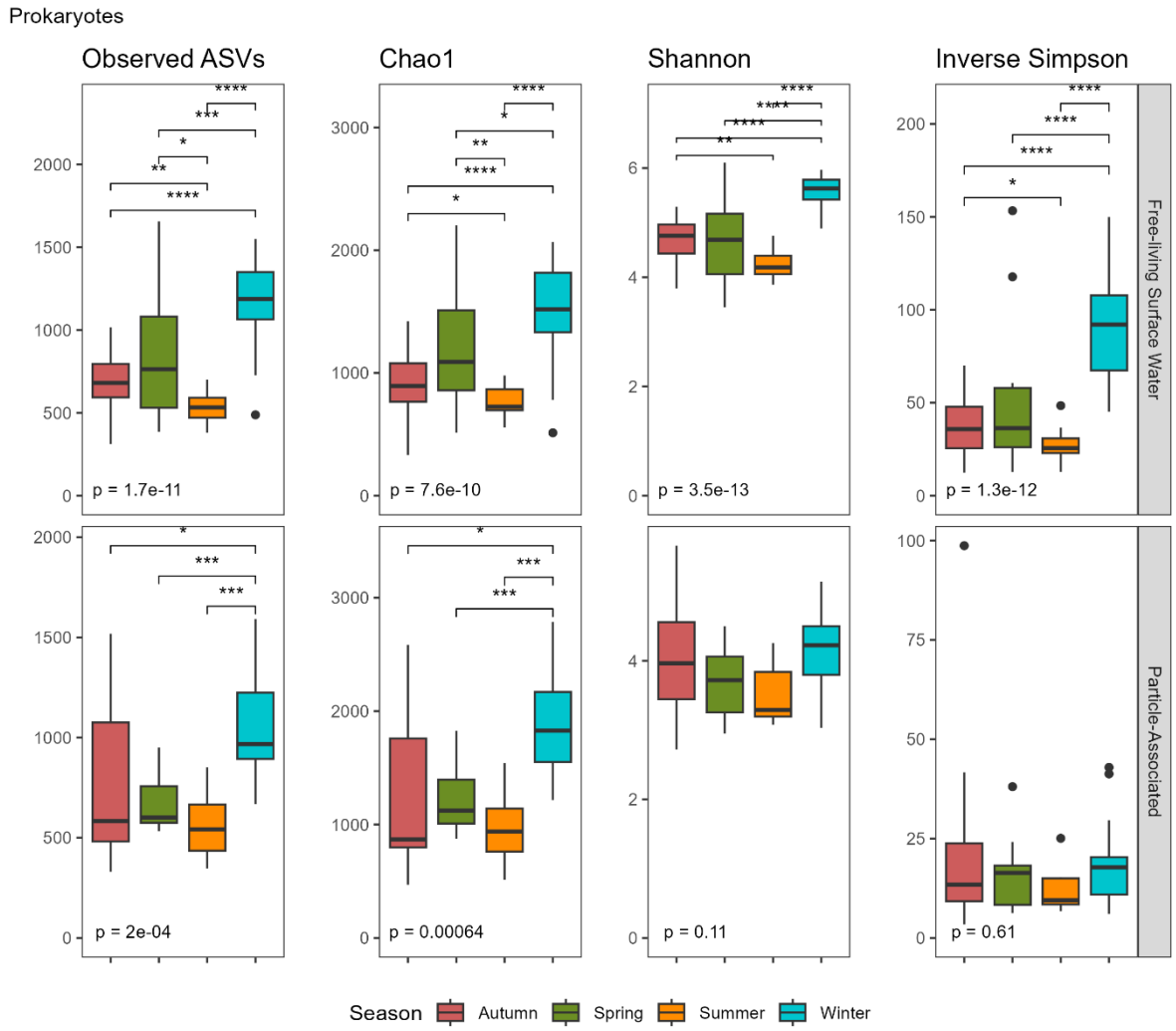

Figure 20: Alpha-diversity metrics for prokaryotes. Each column is an alpha-diversity metric (Observed ASVs, Chao1, Shannon and Inverse Simpson). The upper section corresponds to surface water, while the lower section corresponds particle-attached communities. Boxplot colors indicate seasons: red for autumn, green for spring, orange for summer, and blue for winter. The p-value is derived from the Kruskal-Wallis test. Asterisks represent significant pairwise comparisons by Wilcoxon test: * ($p \leq 0.05$), ** ($p \leq 0.01$), *** ($p \leq 0.001$), and **** ($p \leq 0.0001$).

Microbial eukaryotes showed significant difference (Kruskal-Wallis, $p \leq 0.05$) in richness (observed ASVs and Chao1), but not for the evenness. The inverse Simpson metric was not significant in both habitats (surface water and particle-associated), whereas, the Shannon diversity presented a significant, but weak, difference in the particle-attached communities (Kruskal-Wallis, $p = 0.04$) (Figure 11). This suggests a stable community across the seasons for both habitats, where, despite variations in richness, the distribution of individuals across taxa remained comparable.

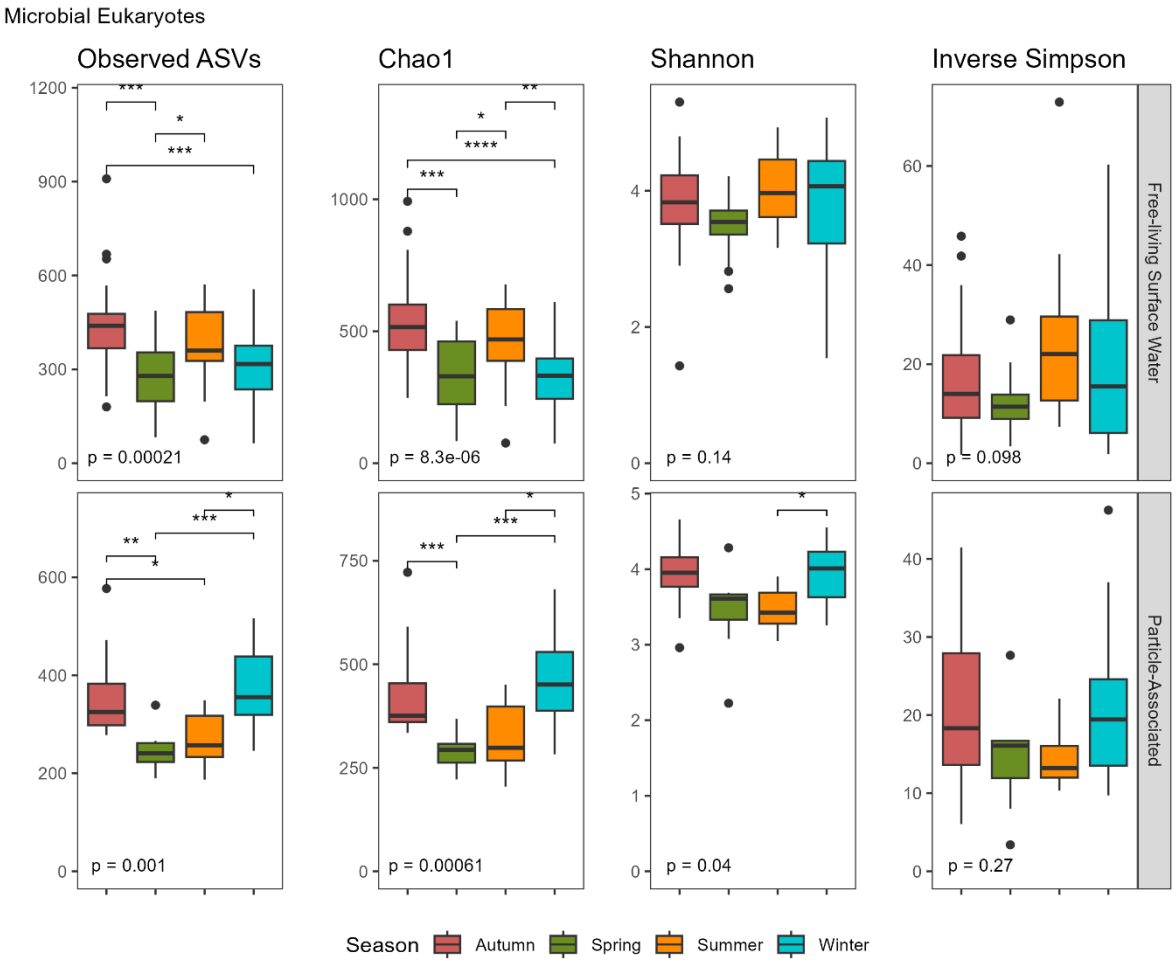

Figure 11: Alpha-diversity metrics for microbial eukaryotes. Each column is an alpha-diversity metric (Observed ASVs, Chao1, Shannon and Inverse Simpson). The upper section corresponds to surface water, while the lower section corresponds particle-attached communities. Boxplot colors indicate seasons: red for autumn, green for spring, orange for summer, and blue for winter. The p-value is derived from the Kruskal-Wallis test. Asterisks represent significant pairwise comparisons by Wilcoxon test: * ($p \leq 0.05$), ** ($p \leq 0.01$), *** ($p \leq 0.001$), and **** ($p \leq 0.0001$).

The comparison of alpha-diversity metrics between seasons over time revealed few significant differences between years, with most occurring between winters for both prokaryotes and microbial eukaryotes in both habitats (surface and particle-associated) (Appendix 3 and 4). Specifically, the winter of 2020, during the cold anomaly, showed only one significant difference in the observed ASVs metric for the particle-associated prokaryotic community compared to the winter of 2018.

3.4 Microbial composition of surface waters in Fram Strait

Eleven microbial eukaryotic families from eight classes were found with more than 2% of relative abundance in surface water samples (Figure 12). Families of diatoms (*Chaetocerotaceae, Thalassiosiraceae* and *Bacillariaceae*), dinoflagellates (*Gymnodiniaceae*, *Suessiaceae* and unclassified *Dinophyceae*), intracellular parasites (*Dino-I-1*), ciliates (*Ephelotidae* and *Strombidiidae*), radiolarians (*RAD-C*) and microalgae (*Phaeocystaceae*) dominated the microbiome. The most abundant family was *Bacillariaceae* (10%), followed by *Ephelotidae* (9%), *Dino-I-1* (8%) and *Phaeocystaceae* (5%). The most abundant genera of *Bacillariaceae* was *Pseudo-nitzschia*, comprising 45% of the family.

For surface prokaryotic communities, it was found thirteen families of four classes with relative abundance more than 2% (Figure 12). The most abundant families of prokaryotes were the *SAR11 Clade 1* (14%), followed by *Flavobacteriaceae* (13%). Other families composing the microbiome were common marine families (SAR11 Clade II, and SAR 86), and, *Thioglobaceae, Porticoccaceae*, *Paracoccaceae*, *Nitrosopumilaceae*, *Nitrincolaceae*, *Methylophilaceae*, *Magnetospiraceae*, *HOC36* and *AEGEAN-169*. The most abundant genera within the *Flavobacteriaceae* family is *Polaribacter*, comprising 30% of the total abundance of the family.

Seasonal patterns were observed for some microbial eukaryotic families, but not all (Figure 12). *Dino-I-1* (class Syndiniales), *RAD-C* and *Ephelotidae* showed an increase in relative abundance during winter, whereas *Phaeocystaceae*, diatoms families and *Strombidiidae* exhibited increase in relative abundance during the productive seasons (spring, summer and autumn). The dinoflagellates from the Dinophyceae class did not showed a clear seasonal pattern, as their relative abundance fluctuated across different seasons. Interannual variability was also observed. The *Ephelotidae* showed an increase in relative abundance, but only every other year. *Bacillariaceae* typically peaked in autumn, however, in 2018 a peak was observed in spring. That same year *Phaeocystaceae* showed a different dynamic, with a decline in relative abundance compared to other years. The diatom family *Chaetocerotaceae* showed a decline in relative abundance during the spring of 2019, in contrast to previous years, and this trend continued into the spring in 2020. Finally, RAD-C exhibited a decline in

the winter of 2020 and Dino-I-1 that usually peaks in winter, showed an increase in relative abundance in spring of 2021.

The majority of the prokaryotic families showed clear seasonal patterns (Figure 12). *Flavobacteriaceae* and *Nitrincolaceae* increased in relative abundance during spring-summer, while *Paracoccaceae* showed peaks in autumn. The *Porticoccaceae* was the only family that did not show a seasonal pattern, maintaining low relative abundance across all seasons for the most of the dataset. All other families, including *Nitrosopumilaceae*, uncultured *HOC 36*, *AEGEAN-169*, *Magnetospiraceae*, *Methylophilaceae*, *SAR11 (Clade I and II)*, *SAR 86* and *Thioglobaceae*, had higher sequence proportions in autumn and winter. Interannual variability was observed in *Porticoccaceae*, *Nitrincolaceae* and *HOC36. Porticoccaceae* exhibited an increase in relative abundance during the spring and summer of 2020. *Nitrincolaceae* showed a decline in relative abundance during the spring and summer of 2017, while *HOC36* declined in winter of 2019-2020.

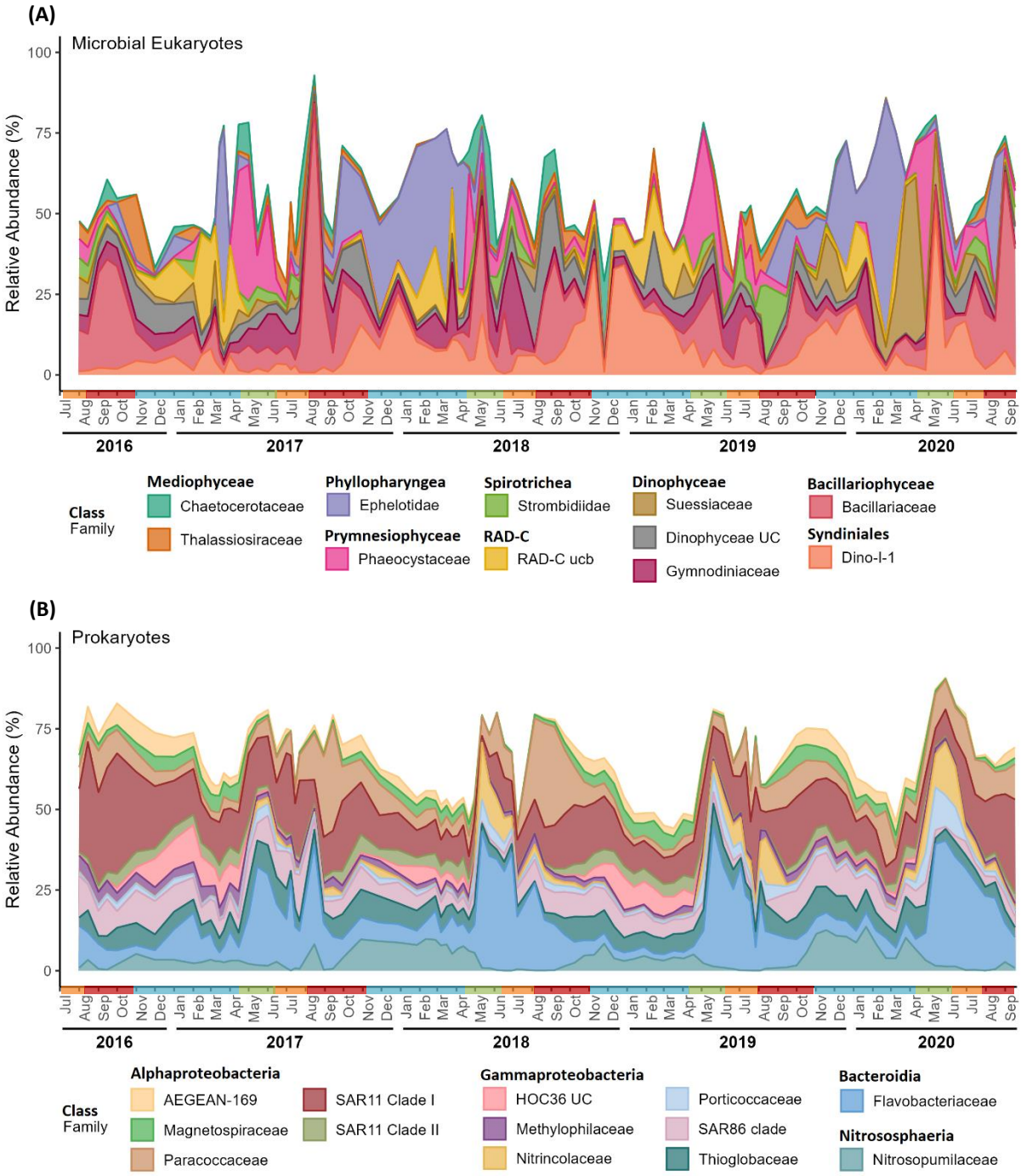

Figure 12: Relative abundance and taxonomic affiliation of surface water microbial communities in Fram Strait from 2016 to 2020. Relative abundance (%) of (A) microbial eukaryotes and (B) prokaryotes, filtered to include only the most abundant families (>2%). Taxonomic classification at the family level is also grouped by class. The colored bar at the bottom of the plots represents the seasons: winter is blue, autumn is red, summer is orange and spring is green.

3.5 Microbial composition of sinking particles in Fram Strait

Fourteen families above 2% relative abundance (Figure 13) comprised the microbiome of sinking-particle microbial eukaryotes. It included radiolarians (*Acantharea C3*), diatoms (*Chaetocerotaceae*), stramenopiles (*MAST-9*), green algae (*Chloropicaceae*), intracellular parasites (unclassified *Microsporida, Dino-I-1*, *Dino-I-2 and Dino-I-3*), dinoflagellates (*Dinophyceae*) and other heterotrophic protists (*Cryothecomonas*, *Protaspa* and *Pirsoniales*). The most abundant families was *Dino-I-1* (13%), followed by unclassified *Microsporida* (10%), *Dino-I-2* (9%) and *Chaetocerotaceae* (4%). Four families were shared between sinking-particle communities and surface water, being them the *Chaetocerotaceae*, *Dino-I-1*, *Suessiaceae* and unclassified *Dinophyceae*.

A seasonal trend was observed in the family *MAST-9* and *Dino-I-2*, with an increase in relative abundance during winter. Unclassified *Microsporida* showed an increase in relative abundance during the winter-spring transition. *Acantharea C3*, *Chaetocerotaceae*, *Protaspa* and unclassified *Gymnodiniales* showed an increase in relative abundance during the productive seasons (spring, summer and/or autumn). No seasonal trend was observed for *Cryothecomonas*, *Chloropicaceae*, unclassified *Pirsoniales*, *Suessiaceae*, unclassified *Dinophyceae*, *DINO-I-1* and *Dino-I-3*. Variability between years was also observed. *MAST-9* and unclassified *Microsporida* showed a decline in relative abundance during the winter of 2016-2017 compared to the following years. Also in 2017, the unclassified *Pirsoniales* exhibited an increase in relative abundance and *Dino-I-2*, which usually peaks in winter, instead peaked in autumn. A peak of *Cryothecomonas* was observed in the summer and autumn of 2018, while *Acantharea C3* was absent during this year. *Chloropicaceae* showed an increase in relative abundance only during 2019 and 2020. *Chaetocerotaceae* exhibited an increase in abundance during the summer-autumn of 2020 compared with to previous years, maintaining high relative abundance throughout the following winter.

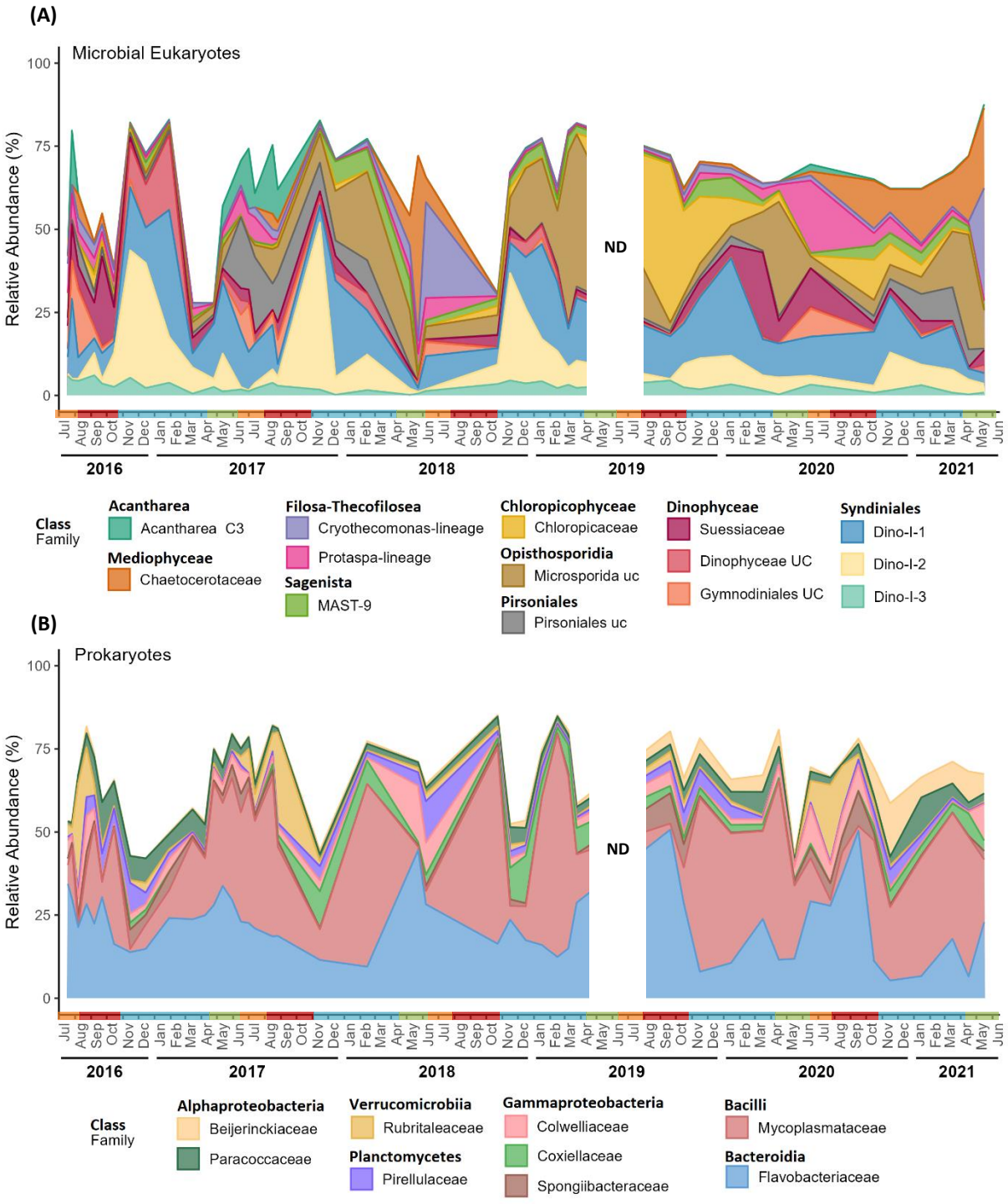

Figure 13: Relative abundance and taxonomic affiliation of particle-associated microbial communities in Fram Strait from 2016 to 2021. Relative abundance (%) of (A) microbial eukaryotes and (B) prokaryotes, filtered to include only the most abundant families (>2%). Taxonomic classification at the family level is also grouped by class. The colored bar at the bottom of the plots represents the seasons: winter is blue, autumn is red, summer is orange and spring is green. ND = No data available.

There were nine prokaryotic families with more than 2% relative abundance of six classes (Figure 14). *Mycoplasmataceae* were the most abundant (24%), followed by

Flavobacteriaceae (22%). Other families present in the sinking-particle prokaryotic community are associated with organic matter degradation, including *Colwelliaceae, Coxiellaceae,* and *Rubritalaceae.* The *Flavobacteriaceae* together with *Paracoccaceae* were the only two relative abundant families from the surface water also present in the sinking-particle samples. Even though the families are shared between habitats, they differ in the most abundant lower taxonomic levels. Unlike in the surface habitat, where the most abundant genera within these families were *Polaribacter* for *Flavobateriaceae* and *Amylibacter* for *Paracoccaceae*, the dominant genera in sinking-particle samples were *Aurantivirga* and *Sulfitobacter*, repectively, accounting for 32% and 27% of the total abundance of their respective families

The majority of the families did not follow any apparent seasonal trends, such as *Flavobacteriaceae*, *Mycoplasmataceae*, *Spongiibacteriaceae*, *Coxiellaceae*, *Colwelliaceae*, *Pirellulaceae* and *Beijerinckiaceae*. Only *Rubritalaceae* and *Paracoccaceae* showed an apparent seasonal pattern. *Rubritalaceae* showed an increase in relative abundance during the summer-autumn, whereas *Paracoccaceae* tended to increase in relative abundance during winter. Interannual variability was observed for *Pirellulaceae*, that showed an increase in relative abundance during 2018 and a decline in 2020. The family *Flavobacteriaceae*, rather than presenting a seasonal pattern, seems to follow an inverse correlation with the microbial eukaryote families Dino-I-1 and Dino-I-2 of the Syndiniales class. This can be clearly observed in the spring of 2018, with a strong decrease in the both Syndiniales families and a concurrent increase in *Flavobacteriaceae*. *Beijerinckiaceae* showed an interesting temporal pattern, with increased abundances starting in 2019, followed by a decline during the cold anomaly, and then a subsequent rise in the autumn of 2020. This trend closely mirrors the dynamics of the green algae *Chloropicophyceae,* which also exhibited a bloom in 2019 and followed a similar fluctuation thereafter. The parallel dynamics suggest a possible ecological link between *Beijerinckiaceae* and *Chloropicophyceae* blooms.

3.6 Similarities and differences in microbial communities across habitats and seasons

Microbial communities were distinct across habitats (surface water and sinking particles), sharing only 15% and 10% of the ASVs for prokaryotes and microbial eukaryotes, respectively (Figure 14). For prokaryotes, the particle-associated communities had the highest number of exclusive ASVs (5561), accounting for 50% of the dataset. For microbial eukaryotes, the surface water community had the most exclusive ASVs (6046), representing 68.5% of the total. The distinct composition of the communities in both datasets suggest a high degree of specialized communities. This pattern is further supported by NMDS analysis (Appendix 6) and ANOSIM tests ($R = 0.9$, $p < 0.05$ for prokaryotes and $R= 0.7$, $p < 0.05$ for microeukaryotes), which shows a clear separation between the two habitats.

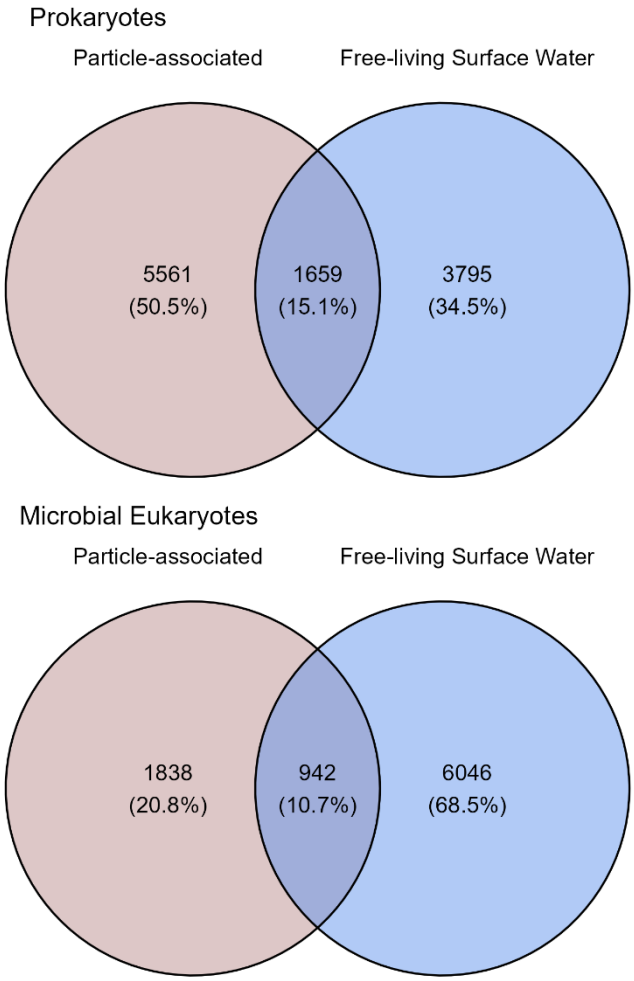

Figure 14: Venn Diagrams of exclusive and shared ASVs between surface water and particle-attached microbial communities for (A) prokaryotes and (B) Microbial Eukaryotes. The values were rarefied by sequencing depth using the lowest number of sequences higher than 10,000.

Particle-associated prokaryotic communities shared 17.4% of ASVs between all seasons, whereas, microbial eukaryotes shared 11.3% of ASVs. The highest overlap between two seasons occurred between autumn and winter for both domains, with 16.2% of prokaryotic ASVs and 8.4% of microbial eukaryotic ASVs shared (Figure 15). High community turnover between seasons was also observed for surface water microbial communities (Appendix 7), with the only difference being that, for prokaryotes, the second-largest overlap after the ASVs shared across all seasons (22%) was between winter and spring (17.8%). The winter showed the highest numbers of exclusive ASVs (Figure 15 and Appendix 7).

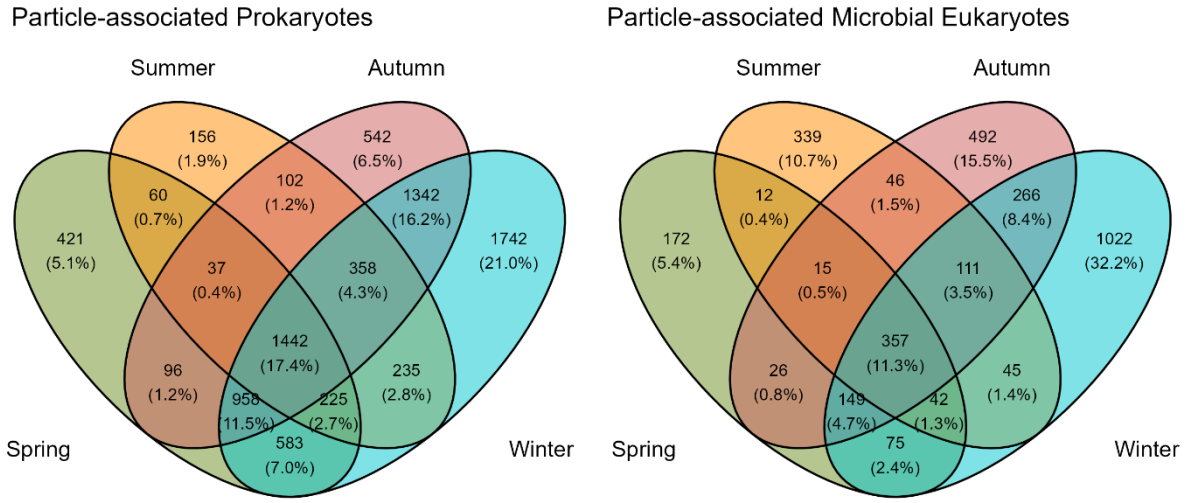

Figure 15: Venn Diagrams of exclusive and shared ASVs between seasons for particle-associated (A) prokaryotes and (B) microbial eukaryotes. The values were rarefied in each dataset by sequencing depth using the lowest number of sequences higher than 10,000.

The seasonal cycle in water column communities is clearly discernable for prokaryotes and microbial eukaryotes in the non-metric multidimensional scaling (NMDS) ordinations (Figure 15). This seasonal trend remains detectable in microbial eukaryotes (PERMANOVA p = 0.001) (Appendix 8 and 9) associated with the sinking particles, as these communities largely constitute the particles generated in the surface. However, the seasonal trend within the sinking-particle microbial eukaryotic communities appears less pronounced than for the communities in the water column, with seasons explaining 12% of the variation in the sinking-particle communities, and the samples for late summer (July) more dispersed. The particle-attached prokaryotic communities exhibited overlap between seasons, with only one distinct cluster of late summer and early autumn samples (Figure 15 – B), suggesting that seasons are

less reflected in the composition of particle associated communities. Also, the samples were more dispersed within each season, indicating greater variability in community composition. Despite the overlap, PERMANOVA (Appendix 8 and 9) revealed significant differences between seasons (p = 0.001), with seasons explaining 13% of the variation.

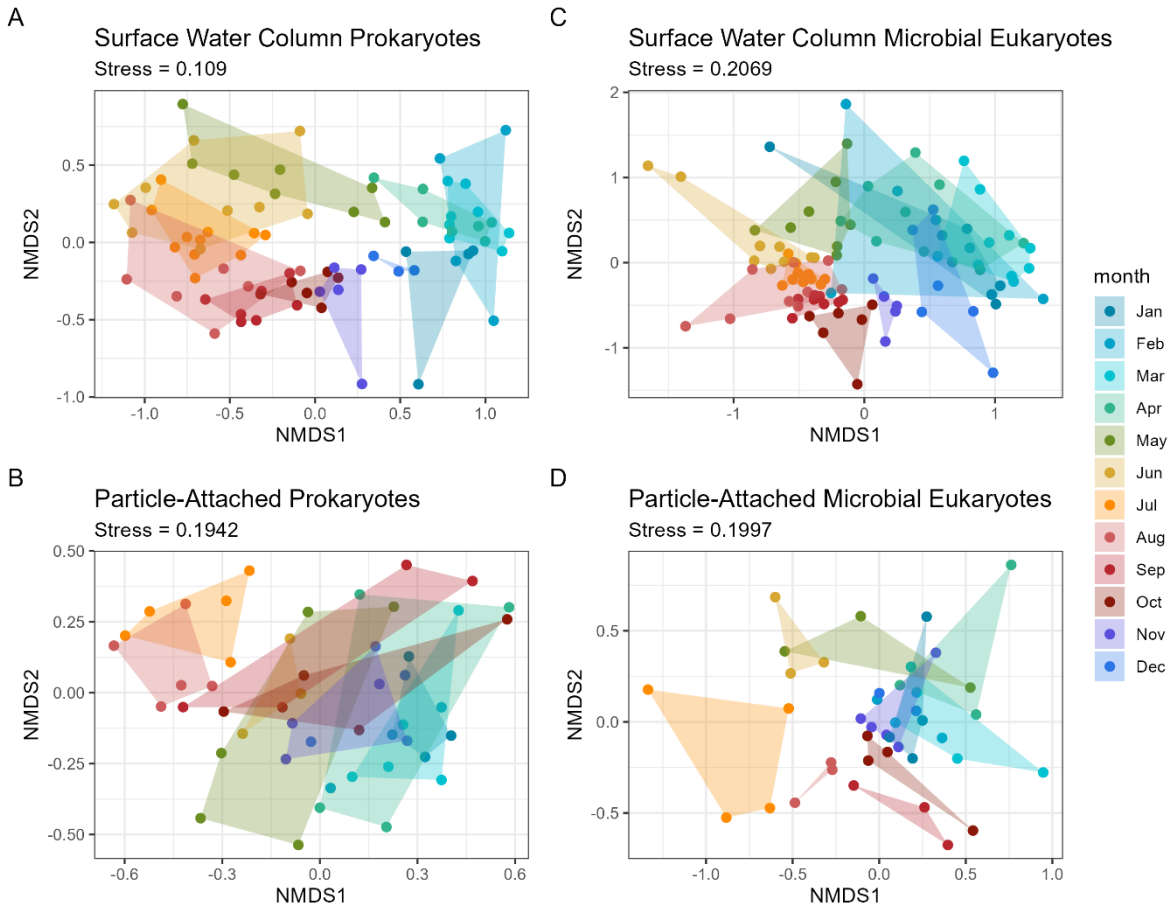

Figure 15: Two-dimensional NMDS of Bray-Curtis dissimilarity for (A) surface water and (B) particle-attached prokaryotes, as well as (C) surface water and (D) particle-attached microbial eukaryotes. Dissimilarities were calculated after Hellinger transformation. Colors represent months, with different shades indicating seasons (blue for winter, green for spring, yellow for summer, and red for autumn).

3.7 Correlation with environmental parameters

The variation of surface water prokaryotic communities was significantly correlated (Mantel tests, $p < 0.05$) (Figure 16) with temperature, salinity, fraction of Atlantic and Polar water and dissolved oxygen. However, only temperature and dissolved oxygen were correlations with moderate strength (Mantel test, R = 0.2 – 0.4), whereas all the other

correlations were weak (Mantel test, R < 0.2). For surface water microbial eukaryotes, the variation of communities were only significantly (Mantel test, p < 0.05) correlated with temperature and distance of the sea-ice edge, with both correlations weak (Mantel test, R < 0.02).

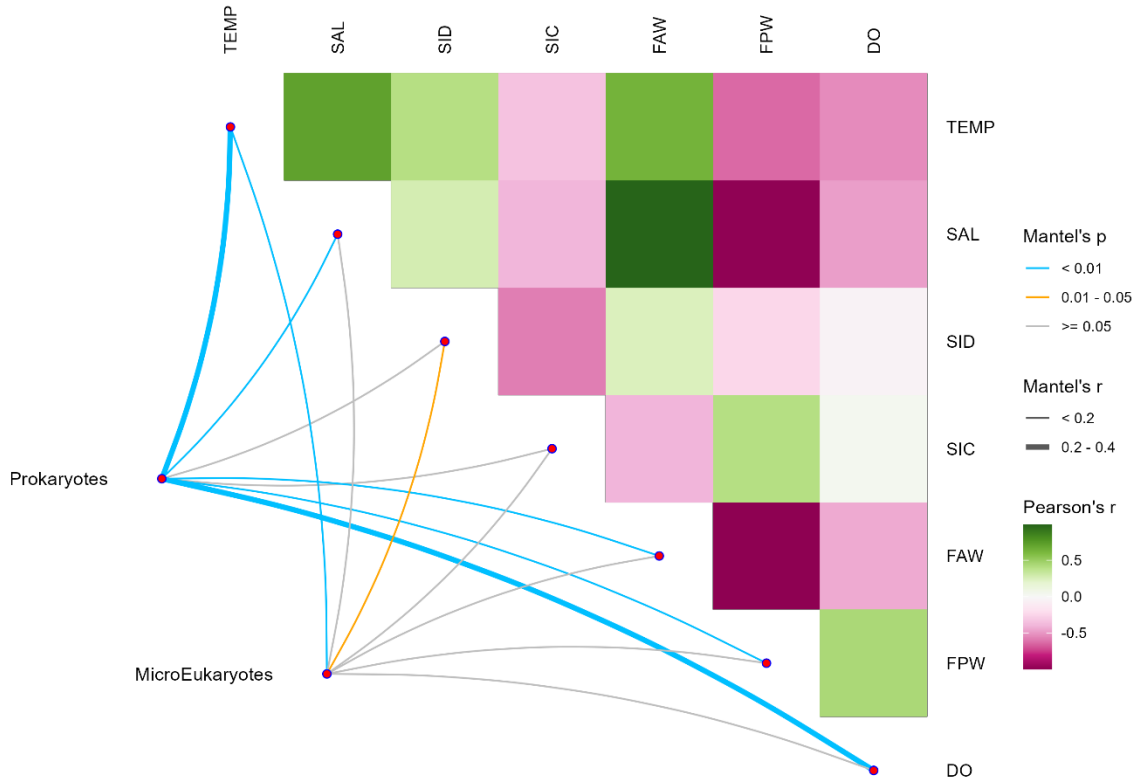

Figure 16: Mantel test of free-living surface water prokaryote and microbial eukaryote community dissimilarity (Bray-Curtis) and various environmental factors (Euclidean Distance). Curved line width and color represent the correlation coefficients of the Mantel Tests. The heatmap shows pairwise correlations between environmental variables. TEMP = Temperature; SAL = salinity; SID = Sea ice distance; SIC = Sea ice concentration; FAW = Fraction of Atlantic Water; Fraction of Polar Water; DO = Dissolved Oxygen.

The variation of prokaryotic particle-associated communities was significantly correlated (Mantel tests, p < 0.05) (Figure 17) with temperature, sea ice dynamics (distance of the edge and concentration), oxygen, POC, PON, carbonate and silica. Except for sea-ice concentration and dissolved oxygen, which showed weak correlations, all other significant relationships were moderate in strength (R = 0.2 – 0.4), indicating that prokaryotic communities are strongly driven by organic matter availability. For particle-associated microbial eukaryotes, community variation was correlated to variations in sea-ice dynamics (concentration and distance of the edge), oxygen and fluxes of silica and carbonate. Due to

the moderate strength of the correlations between microbial eukaryotic communities with both sea ice properties, the sea ice seasonal dynamics may play a significant role shaping these communities.

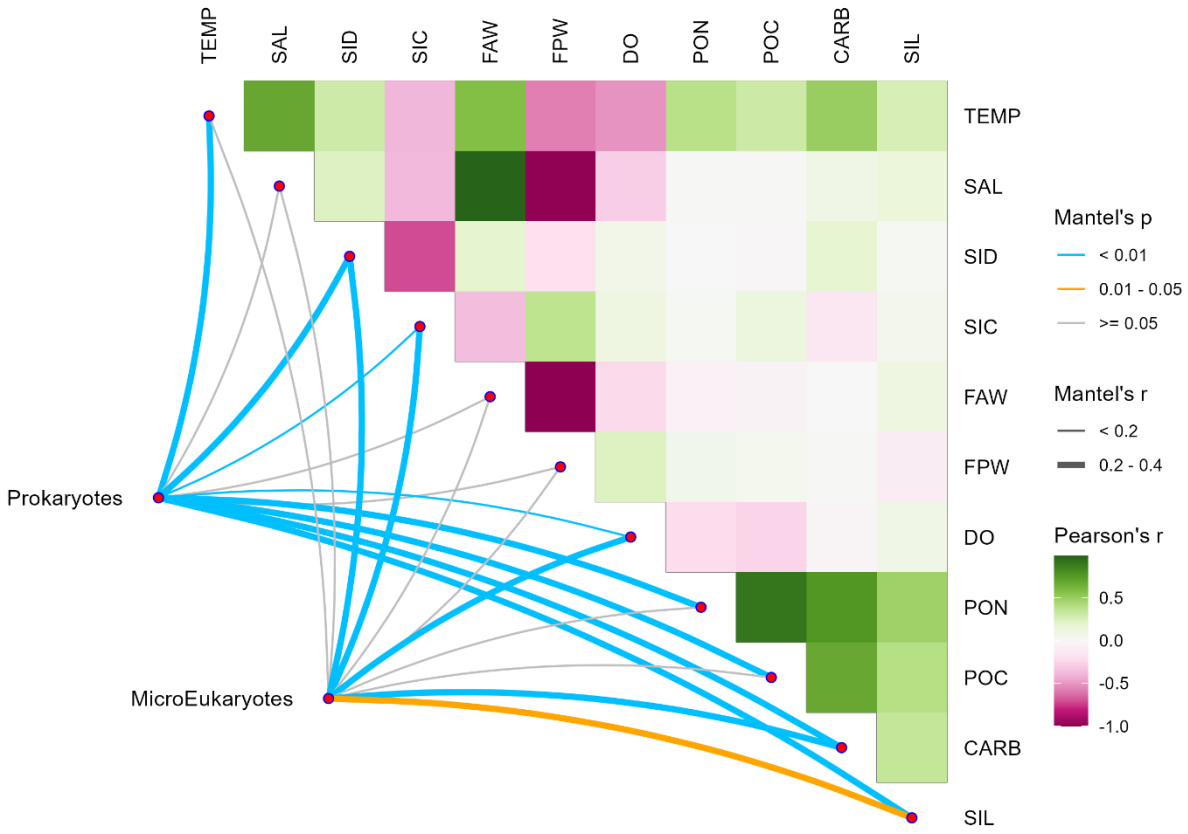

Figure 17: Mantel test of sinking-particle prokaryote and microbial eukaryote community dissimilarity (Bray-Curtis) and various environmental factors (Euclidean Distance). Curved line width and color represent the correlation coefficients of the Mantel Tests. The heatmap shows pairwise correlations between environmental variables. TEMP = Temperature; SAL = salinity; SID = Sea ice distance; SIC = Sea ice concentration; FAW = Fraction of Atlantic Water; Fraction of Polar Water; DO = Dissolved Oxygen; PON = Particulate Organic Nitrogen; POC = Particulate Organic Carbon; CARB = Carbonate; SIL = Silica (BSi + Particulate Silica).

A strong, positive and significant correlation (Mantel test, R = 0.6, p = 0.001) was observed between variations in sinking-particle associated prokaryotic and sinking-particle associated microbial eukaryotic communities (Figure 18).

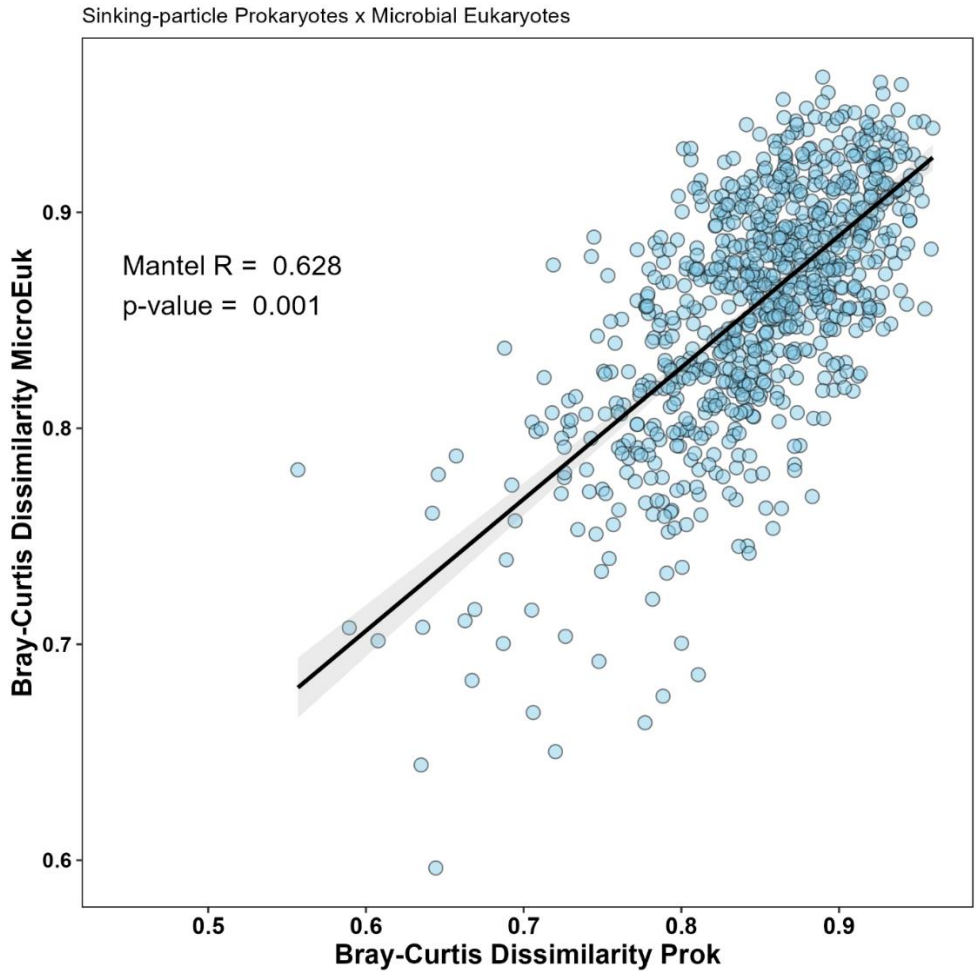

Figure 18: Mantel test between community dissimilarity of sinking-particle prokaryotes and microbial eukaryotes. Dissimilarities were calculated by Bray-Curtis. The smooth line used linear mode.

Variations in microbial community structure across all datasets were strongly correlated with MLD and temperature (Figure 19 and 20) for winter and autumn communities, respectively ($p \leq 0.01$). Each of these parameters explained approximately 20-43% of the variation in the microbial communities. Due to their consistent presence and strong representation across the datasets, these environmental parameters are likely the primary drivers for microbial communities in the central region of Fram Strait.

Besides the MLD, winter samples in surface waters were significantly correlated ($p < 0.01$) with the fraction of Atlantic Water and salinity. The Atlantic Water is characterized as a saline water mass (Beszczynska-Möeller et al., 2011; Nöthig et al, 2015) compared to Polar

Water (Figure 19), which explain both parameters (AW and salinity) with vectors to the same direction. Sea-ice distance to the edge was correlated to the surface water microbial communities in early winter for microbial eukaryotes and late autumn for prokaryotes. Spring samples in surface water showed a significant correlation with dissolved oxygen and fraction of Polar Water.

Sinking-particle microbial eukaryotes were not only significantly correlated with temperature in autumn, but also with particle fluxes (carbonate, carbon and nitrogen) (Figure 20). For prokaryotes, even with the overlap of the seasons in the NMDS, the vectors still indicate correlations. The distance of sea-ice edge significantly correlated with spring, likely due to the sea-ice dynamics during this season. Carbonate fluxes were positively correlated with summer communities, reflecting higher export fluxes during this season. Temperature also correlated with summer samples.

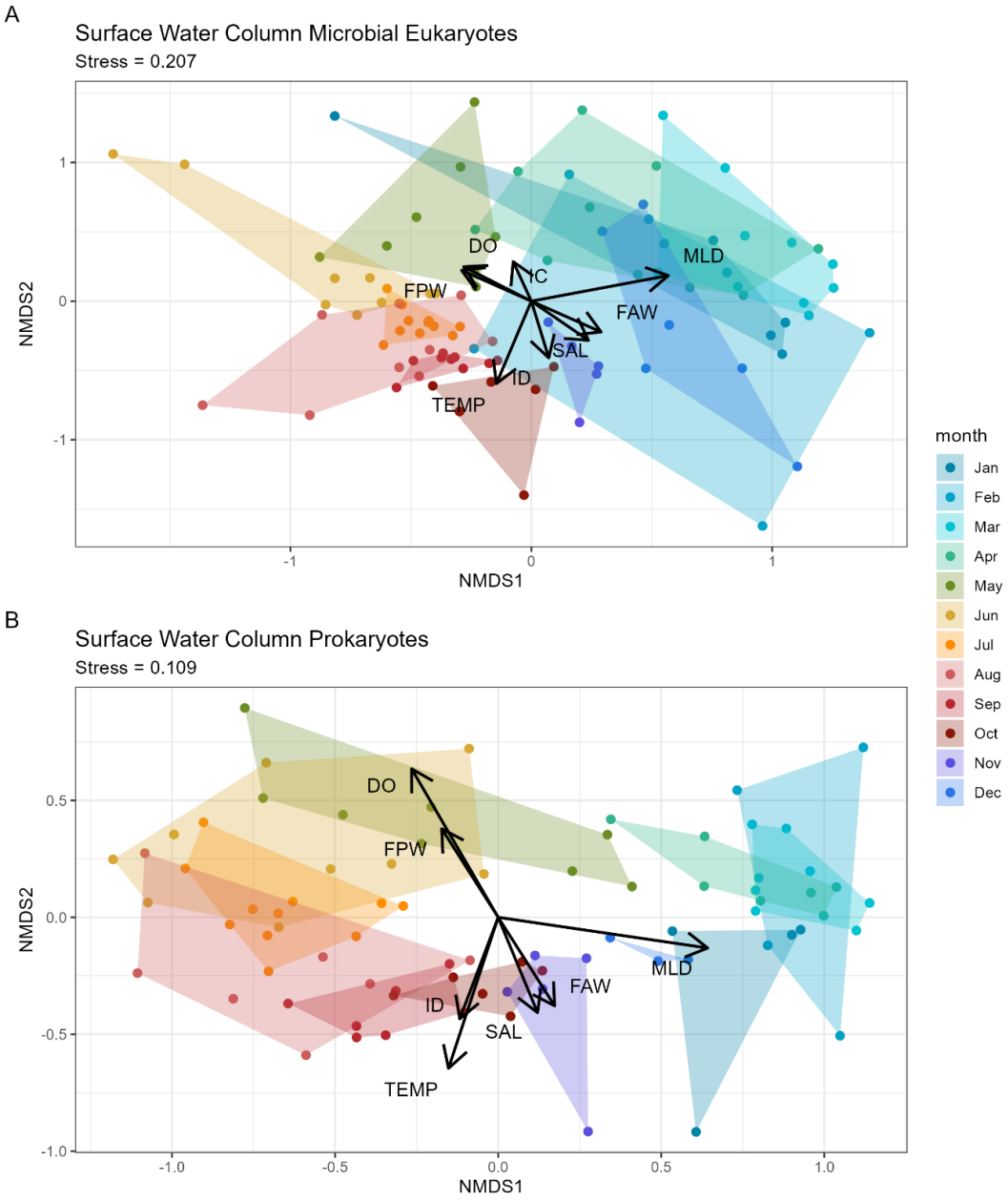

Figure 19: Two-dimensional NMDS of Bray-Curtis dissimilarity (A) microbial eukaryotes and (B) prokaryotes from surface water with fitted significant environmental variables. The environmental variables include: Dissolved Oxygen Concentration (DO), Polar Water Fraction (FPW), Mixed Layer Depth (MLD), Atlantic Water Fraction (FAW), Salinity (SAL), Sea-ice Concentration (IC), Distance of the sea-ice edge (ID) and Temperature (TEMP). Dissimilarities were calculated after Hellinger transformation. Colors represent months, with different shades indicating seasons (blue for winter, green for spring, yellow for summer, and red for autumn).

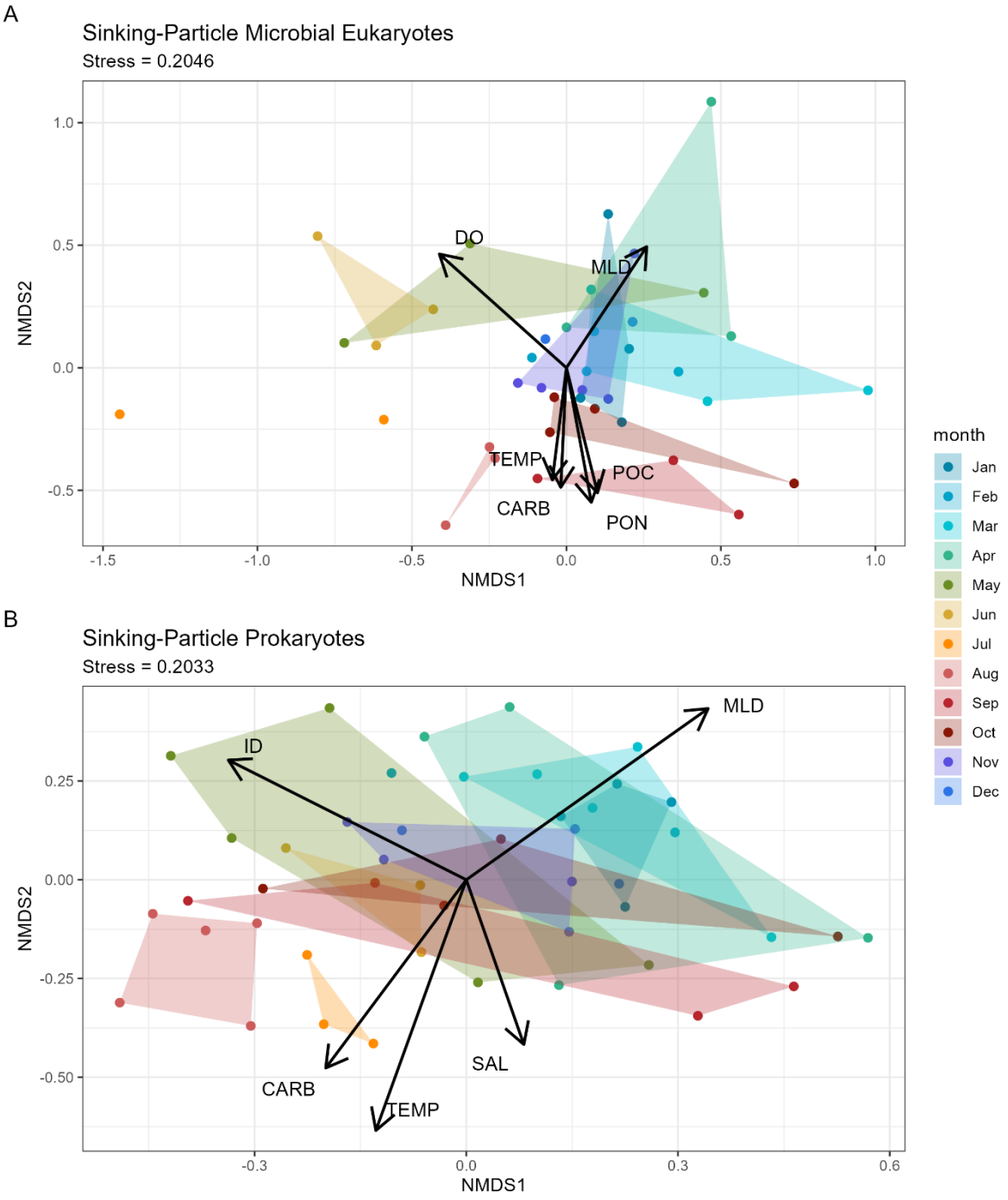

Figure 20: Two-dimensional NMDS of Bray-Curtis dissimilarity (A) microbial eukaryotes and (B) prokaryotes from sinking particles with fitted significant environmental variables. The environmental variables include: Dissolved Oxygen Concentration (DO), Mixed Layer Depth (MLD), Salinity (SAL), Distance of the sea-ice edge (ID), Carbonate (CARB), Particulate Organic Carbon (POC) and Particulate Organic Nitrogen (PON) and Temperature (TEMP). Dissimilarities were calculated after Hellinger transformation. Colors represent months, with different shades indicating seasons (blue for winter, green for spring, yellow for summer, and red for autumn).

4 DISCUSSION

This thesis provides insights into the seasonal microbial dynamics of particle-associated microbial communities and the connections with the free-living counterpart in the ocean surface in Fram Strait, Arctic. A total of 13658 ASVs were recovered for prokaryotes and 10635 ASVs for microbial eukaryotes over four seasonally resolved years, allowing an overview of composition, richness, structure and environmental drivers of microbial communities associated with the biological carbon pump in a key Arctic region.

4.1 Seasonality shapes surface microbes with limited impact on particle-associated communities

The Arctic region experiences strong seasonal variations with fluctuations in environmental parameters such as light availability, temperature and sea-ice presence in each season (Stein and Macdonald, 2003; Walsh J, 2008; Leu et al., 2015), all of which can affect microbial communities (Pedrós-Alió, Potvin and Lovejoy, 2015; Wilson et al., 2017). Previous work on seasonal microbial dynamics (Wietz et al., 2021; Priest et al 2025) has highlighted the significant role of seasonality in shaping microbial communities in the surface waters of the Arctic. The effects of seasonality, particularly in microbial communities associated with sinking particles in Fram Strait, remain poorly understood. Investigating seasonal microbial dynamics provides valuable ecological insights into ecosystem structure, revealing how the communities cope with annual environmental fluctuations.

Over the study period (2016-2021) physico-chemical environmental parameters varied across each annual cycle. The variations were primarily driven by seasonality, likely influenced by light availability and temperature, as the winter differed from the productive seasons (spring, summer and early autumn), as expected in Arctic regions (Berge et al., 2015; Wietz et al., 2021). Particle fluxes followed a bimodal carbon export pattern during the productive season, which has been previously described for the region (Fadeev et al., 2021; Ramondec et al., 2022; Cardozo-Mino et al., 2023). This pattern was observed along with annual differences

in the magnitude of particle fluxes. Overall, the average flux values were consistent with previous studies for the region (Lalande et al., 2013; Fadeev et al., 2021; Cardozo-Mino et al., 2023). POC ranged from 0.31 to 35 mg m^{-2} d^{-1}, PON generally low (<3 mg m^{-2} d^{-1}), carbonate averaging 12.6 ± 7.6 mg m^{-2} d^{-1} and silica mostly low (< 5 mg m^{-2} d^{-1}) but with sporadic higher export events (> 10 mg m^{-2} d^{-1}).

Seasonality was also a significant driver of surface microbial communities, influencing both the richness and composition of surface prokaryotic communities, as well as richness of surface microbial eukaryotic communities. Seasonality was also visible in the variation of relative abundances over seasons for most of the surface prokaryotic families and for some of the microbial eukaryotes, such as the radiolarians *RAD-C*. These results corroborate with other previous studies that evaluated the seasonality for surface microbial communities conducted in the Fram Strait (Wietz et al., 2021; Priest et al., 2025). *Flavobacteriaceae* and *Bacillariaceae* families dominated the productive season (spring, summer and autumn) in prokaryotes and microbial eukaryotes, respectively. Wietz et al (2021) identified the orders Flavobacteriales and Bacillariophyta, of which *Flavobacteriaceae* and *Bacillariaceae* families are members, as dominant during the productive season in other regions of the Strait. Then, these families represent the microbiome of the productive season in the Fram Strait, composed by photosynthetic phytoplankton and opportunistic heterotrophic bacteria. In this study, other taxa increased in relative abundance concomitant with *Flavobacteriaceae*, such as *Nitrincolaceae*. The *Nitrincolaceae* family is commonly associated with sea-ice algae blooms capable of a high diversity of carbon metabolisms (Thiele et al., 2022), thereby contributing to varied carbon cycling processes during the productive season in the region. For the winter season, Wietz et al (2021) identified certain prokaryotes as contributors to nutrient replenishment. Among these, *Nitrosopumilaceae* and *Magnetospiraceae* were also detected here in the surface waters with an increase in relative abundance during winter.

In contrast to the strong seasonality shaping free-living surface microbial communities, the effects on sinking-particle communities were less pronounced, but still significant, influencing richness with a high turnover in community composition throughout the year. Seven out of nine (~77%) of the particle-associated prokaryotic families and seven out of

fourteen (50%) of the particle-associated microbial eukaryotic families identified as abundant in this study did not show any apparent seasonality. Still, some families presented a seasonal pattern, such as *MAST-9* increasing in relative abundance in winter, or *Acantharea C3* and *Chaetocerotaceae* in the productive seasons. Cardozo-Mino et al (2023) previously assessed the composition of sinking-particle microbiota in the same region and identified seasonal differences between spring and summer high export event for microbial communities. By incorporating fall and winter data, which were not included in their study, this research complements their work, providing a comprehensive understanding of seasonal shifts in particle-associated microbial communities across the entire annual cycle.

Considering the seasonal patterns in both surface and sinking-particle microbial communities, winter showed as the most rich and diverse season for prokaryotic communities in both habitats (surface water and sinking particles). Similar results were observed in other studies (Wilson et al., 2017; Wietz et al., 2021; Priest et al., 2025). This increased richness and diversity during winter is likely a result of the vertical mixing of waters during this season. During winter, brine released from ice formation and wind-driven mixing in ice-free regions both promote the mixing of surface and deeper waters, reducing stratification (Stein and Macdonald, 2003). Since different water masses in the Fram Strait harbor distinct microbiomes (Fadeev et al. 2021), the mixing could introduce new ASVs into surface communities. Moreover, in this thesis the mixed layer depth as the strongest environmental driver for all winter microbial communities, reinforcing the idea of vertical mixing influencing microbial richness and variations in composition.

The results partially support the initial hypothesis that strong seasonal dynamics in the Arctic would lead to annually recurring patterns in both free-living surface and sinking-particle-associated microbial communities. The seasonality had a stronger influence on structuring free-living surface communities compared to particle-associated ones. This may be due to the direct exposure of surface communities to environmental variations, whereas sinking-particle communities are indirectly influenced, as they depend on the production and export of particles from the surface.

4.2 Interannual variability and its impacts on microbial community composition

Interannual variability in environmental conditions, such as fluctuations in sea-ice extent, water temperature anomalies or changes in primary productivity, can significantly influence microbial community composition and dynamics (Ramondec et al., 2022; Priest et al., 2023). Then, is essential to characterize these communities, define their similarities and differences to better identify patterns in community responses to environmental variability.

One key aspect of this characterization is examining the composition. Surface water microbial eukaryotic community was composed of a variety of organisms, including diatoms, dinoflagellates, intracellular parasites, microalgae, ciliates and radiolarians. The most abundant family was the diatom *Bacillariaceae*, more specifically the genus *Pseudo-nitzschia. Pseudo-nitzschia* is a globally distributed diatom, of which some members can produce a biotoxin harmful for marine organisms and shown to accumulate when organisms feed on phytoplankton (Harðardóttir et al., 2015). In contrast, only four classes of prokaryotes composed the surface prokaryotic microbiota, with the *Flavobacteriaceae*, more specifically the genus *Polaribacter*, as the most abundant. *Polaribacter* are commonly described in surface seawaters of polar environments (Gosink et al., 1998) associated with diatom blooms (Avcı et al. 2020). Other families present at the prokaryotic surface communities were ubiquitous and commonly marine taxa, such as SAR11 and SAR86 (Giovannoni, 2017; Hoarfrost et al., 2020), as described in other studies in the Arctic surface water column (Wietz et al., 2021).

In comparison, particle-associated microbial eukaryotic communities were composed of radiolarians, stramenopiles, green algae, intracellular parasites, dinoflagellates and other heterotrophic protists, with the most abundant family being the *Dino-I-1*, member of the Syndiniales class. This class comprises a diverse group of marine parasites that play a significant role in controlling plankton populations (Cleary and Durbin, 2016; Clarke et al., 2019). They have also been commonly described in the surface waters of Fram Strait (Fadeev et al., 2018; Wietz et al., 2021; Cardozo-Mino et al., 2023), and sinking particles (Cardozo-Mino

et al., 2023), which highlight their importance for phytoplankton dynamics in the region (Cleary and Durbin, 2016; Clarke et al., 2019). Ramondenc et al. (2025) who studied sinking particles in the Fram Strait from 2000 to 2012, reported an abundance of diatom lineages in sediments traps at 200 meters, including *Chaetoceros sp* and *Thalassiosira sp.* Both of these diatom families, were also relative abundant (> 2%) in this study, however only *Chaeotocerotaceae* appears as relative abundant in both surface water and sinking particles.

For the particle-associated microbial prokaryotic community, the most abundant families were *Mycoplasmataceae* and *Flavobacteriaceae.* The *Mycoplasmataceae* family is composed of wall-less bacteria commonly found in the gut microbiome of fishes (Blanton et al 2022). Cardozo-Mino et al. (2023) also identified the *Mycoplasmataceae* as one of the most abundant families of the class Bacilli in the Fram Strait, related to high export events in spring. The taxon is also associated as symbiont of meso- and macro-zooplankton (Jaspers et al., 2020). Other families that were abundant in sinking particles were linked to organic matter degradation, such as *Colwelliaceae*, *Rubritalaceae* and *Coxiellaceae*. *Colwelliaceae* is commonly associated with sinking particles for their role in decomposing organic matter (Bowman, 2014). The family is ubiquitous in polar marine ecosystems and can be found associated with sea ice (Bowman, 2014) or with dinoflagellates (Seibold et al. 2001). *Rubritalaceae* are chemoheterotrophs, with some strains contributing to polysaccharide degradation (Martinez-Garcia et al., 2012; Rosenberg, 2014) and *Coxiellaceae* is known for decomposing organic matter of intermediate complexity (e.g. hydrocarbons) and are also widespread in polar oceans, where they can be associated with sea ice (Bowman, 2014). The most abundant genus within *Flavobacteriaceae* family in particle-associated communities was *Aurantivirga,* a known heterotrophic bacteria associated with phytoplankton blooms (Priest et al., 2025). The particle-associated prokaryotic and microbial eukaryotic communities presented a strong positive correlation of their variations between them. Since sinking particles can consist of microbial eukaryote remains (Simon et al, 2002), is likely that the availability of microbial eukaryotic communities will have an influence in prokaryotic communities. It also could be due to possible co-variations or co-ocurrences. Some coupled dynamics observed were an inverse relationship of *Flavobacteriaceae* and *Dino-I-1*, and an

increase in *Beijerinckiaceae* concomitant with *Chloropicophyceae*. However, further analyses are necessary to confirm these observations.

Only few ASVs (~10 to 15%) were shared between surface water and sinking particles, contrary to other observations (Mestre et al., 2018). Mestre et al. (2018) identified vertical connectivity between surface water and sinking particles occurring mainly by rare surface species that act as seeds, increasing in abundance as particles sink. The distinct communities found here could be due the successional pattern of communities as the particle sink (Datta et al. 2016) or due horizontal transport of particles. Sediment traps collect particles over a larger spatial area, then integrating the particles over time and space, meaning that the particles caught by the traps may have originated from different locations and depths (Wekerle et al., 2018), which would explain differences in the community. Some of the communities observed in both habitats in this study are widespread in the Fram Strait, being described in different points of the strait, such as Dino-I-1, Chaetocerotaceae and *Flavobacteriaceae* (Wietz et al., 2021). Also, some of the previously identified abundant communities in sediment traps at the same depth and in the same station, such as *Thalassiosiraceae* family (Ramondenc et al., 2025), here it was only abundant in the surface.

The microbial composition also exhibited interannual differences that co-varied with variations in particle fluxes or environmental parameters. The years 2017 and 2018 presented variations in sea ice dynamics, as previously reported by von Appen et al. (2021). The ice export area of 2018 it was anomalously small (von Appen et al. 2021), which was also identified here by the very low ice concentration. Also, *Bacillariaceae* that showed peaks in autumn in the others years, peaked earlier in spring, representing the earlier silica export flux in the Fram Strait and highlighting the importance of *Bacillariaceae* for the export fluxes in the Fram Strait. Following the very low ice concentration, a subsequent higher distance of the HG-IV station to the sea-ice edge occurred in the next seasons, spring and summer of 2018. During these seasons, a decline in relative abundance of *Phaeocystaceae*, the absence of *Acantharea C3* and an increase in relative abundance of *Cryothecomonas, Pirellulaceae* and *Colweliaceae* was identified. Also, *Nitrincolaceae* showed a very low relative abundance in 2017, but an increase in the relative abundance in 2018, whereas *Rubritalaceae* showed an increase in

relative abundance in 2017. These communities variations are likely related to the two different stratification regimes identified by von Appen et al. (2021), where 2017 was under meltwater-stratified conditions and 2018 was under mixed layer regime. It also highlight the importance of sea-ice dynamics to the composition of both surface and particle-associated communities in the Fram Strait.

The year of 2020 also presented interannual variation, with a cold anomaly occuring from January to September 2020. Lower temperatures, salinity, higher sea ice concentrations and a shallower MLD marked the cold anomaly. While silica and POC fluxes were lower compared to other years, the differences were no significant. Unlike the decline in biogenic matter fluxes observed during the warm anomaly (2006-2007) in the Fram Strait (Lalande et al., 2013), no substantial changes were detected here, suggesting a weaker impact of the cold anomaly on biogenic fluxes. Microbial species richness also remained stable compared to other years. Specific taxa showed changes in abundance, with increases in *Beijerinckiaceae*, *Porticoccaceae* and *Nitrincolaceae*, and declines in radiolarians (RAD-C) and the uncultured *HOC36* bacteria. The warm anomaly studied by Lalande et al. (2013) occurred between 2005 and 2007, being much more prolonged than the cold anomaly investigated here (January 2020 to September 2020), which may explain the differences in the results. Additionally, the nature of the anomaly could also be an explanation, where a higher and frequent input of colder waters might not create the same environmental stress level required to drives changes in export fluxes or in the microbial composition, which needs to be further investigated

The results support the hypothesis that strong interannual environmental variation lead to observable shifts in the composition of both surface water and particle-associated. However, the magnitude of these observable shifts depends on the environmental parameter, here the sea-ice dynamics showed more important to shifts in the composition that the cold anomaly that occurred in 2020.

4.3 Microbial communities in Fram Strait are driven by mixed layer depth, temperature and sea-ice dynamics

Environmental parameters are known for influencing microbial communities in marine environments. In the Arctic, these conditions fluctuate throughout the annual cycle, with sea-ice dynamics and light availability marking the strong seasonality (Stein and Macdonald, 2003). Identifying which environmental factors shape microbial communities is essential for understanding seasonal and interannual variations. In this study, the mixed layer depth (MLD) and temperature were the primary drivers influencing microbial communities across both habitats (surface water and sinking particles). Similarly, Priest et al. (2025) identified MLD as a key environmental driver for prokaryotic communities, and Nöthig et al (2015) identified temperature, sea-ice concentration and stratification as the phytoplankton environmental drivers in the eastern region of the strait.

Specifically for the surface water microbial communities, the temperature was the most consistent environmental factor that correlated with variations in both surface water prokaryotic and microbial eukaryotic communities, though the strength of the correlations were weak to moderate. When evaluating by season, the spring correlated with dissolved oxygen concentrations and polar water fraction for both surface prokaryotes and microbial eukaryotes. Dissolved oxygen increases in spring because of photosynthetic activity, whereas the fraction of polar water likely represents meltwater, directly linking with stratification of the water column. The input of meltwater increases stratification by adding freshwater that is less dense to the surface layer, which reduces vertical mixing between surface and deeper waters (Stein and Macdonald, 2003). The stronger stratification keeps cells in the surface layer (von Appen et al 2021) boosting primary production initially, however, it also limit nutrient upwelling, leading to a fast nutrient depletion and limiting the bloom duration, and primary production (Arrigo et al., 2008; Carton, Ding and Arrigo, 2015; Lewis et al., 2020).

Besides the stratification that is related with the sea-ice concentration, the distance to the sea-ice edge was also an important driver, but for early winter surface microbial eukaryotes and for late autumn surface prokaryotes, suggesting the importance of this parameter to the transitional period of autumn-winter for both free-living surface water communities (prokaryotes and microbial eukaryotes). In Fram Strait, sea ice extent is highly

variable due to the export of ice from Central Arctic that pass through the strait, resulting in fluctuating ice-edge positions (Dickson et al 2000; Fadeev et al., 2021). The sea-ice edge marks the boundary between ice-covered and ice-free regions, and it is during the transitional autumn-winter phase that sea-ice formation is occurring, constantly changing the boundary (Stein and Macdonald, 2003), with consequences on primary production and community dynamics. In winter, surface communities correlated with MLD, salinity and Atlantic Water. During the winter, low temperatures and high salinity allowed the vertical mixing of the water column, reducing stratification. The Atlantic water is a warmer and more saline water mass compared with Polar water (Beszczynska-Möeller et al., 2011), and then its input during the winter could disturb the cold-adapted communities.

In contrast, particle-associated prokaryotes and particle-associated microeukaryotes responded differently to environmental parameters. Prokaryotes were more sensitive to organic matter availability, whereas microbial eukaryotes were more influenced by sea-ice dynamics. Some of the most abundant families of sinking-particle prokaryotic microbiota were described as playing a role in organic matter degradation. This is also widely known, as observed in other surveys about sinking particles worldwide (Grossart et al., 2003; Fontanez et al., 2015). Microbial eukaryotes were sensitive to sea-ice dynamics, a pattern that directly influences Arctic primary production, including the Strait (Fadeev et al., 2021). Specifically for seasonal patterns, the correlation of particle-associated prokaryotic communities during spring with sea-ice distance to the edge was likely influenced by the effects of sea-ice dynamics on eukaryotic communities and primary production, with an indirect impact in the particle-associated prokaryotic communities. Additionally, von Appen et al (2021) identified that sea-ice distance of the edge as an important driver influencing the timing of ice-associated blooms. Then, these findings link the sinking-particle communities with sea-ice dynamics during the spring season. Other significant environmental drivers included salinity and temperature for the transitional seasons signaling the beginning or end of the winter.

The results support the hypothesis that sea ice dynamics are the primary driver shaping surface microbial communities. Besides the sea ice dynamics, the MLD, which is also influenced by sea-ice dynamics, and temperature were other main environmental drivers

structuring microbial communities in the Fram Strait. Additionally, sea-ice dynamics indirectly affected the composition of particle-associated microbial communities.

4.4 Method discussion and potential biases

One potential source of bias in this study is the variability in how seasons are defined across different Arctic studies (Wietz et al., 2021; Salter et al., 2023), which can influence comparisons across studies. To ensure consistency and comparability, we followed the seasonal classification used by Wietz et al., (2021), who previously studied the Fram Strait at two distinct locations. Additionally, sediment traps do not provide high and consistent resolution, with sampling intervals varying depending on the magnitude of particle production during the season, which can potentially miss short-term fluctuations in the microbial communities. Despite these limitations, our approach remains valid because it captures seasonal trends at a resolution sufficient to identify major patterns in microbial dynamics. A third consideration is the time lag used to associate environmental parameters with sinking-particle communities. While a four-day lag may not fully account for the formation time of the particles, a pragmatic approach is necessary due to the complexity of particle production process, together with the variety of particle types. Here, the study was based on an estimated sinking rate of 60 m per day (Wekerle et al., 2018), method that was previously applied by Cardozo-Mino et al (2023) that studied sinking particles in the same region.

5 CONCLUSIONS AND OUTLOOK

This study provided an overview and comprehensive analysis of seasonal dynamics and environmental drivers structuring surface free-living and particle-associated microbial communities at a long-term observatory in the central Fram Strait over four years.

During the study period (2016-2021), seasonal shifts in environmental conditions in the Fram Strait were mainly driven by polar night and day dynamics, with a bimodal carbon export pattern and annual variations. The dominant taxa of surface microbial communities during the productive season were *Bacillariaceae* and *Flavobacteriaceae*, whereas parasites and taxa related to nutrient replenishment were observed in surface waters during winter. Diatoms (*Bacillariaceae)* were important contributors to export fluxes in 2018, a year characterized by low ice concentration where the diatoms showed an earlier and high export of silica. Additionally, the parasitic Syndiniales likely play a role for plankton blooms control in the region. Seasonal dynamics were reflected in recurring seasonal patterns of free-living surface communities, but were less pronounced in particle-associated microbial communities. Likely, it is a reflection of the direct and continuous exposure of surface communities to the highly variability of environmental parameters in the surface, whereas sinking-particle communities are indirectly influenced, as they depend on the production and export of particles from the surface.

Sea ice dynamics, temperature and the mixed layer depth were the most important environmental parameters driving variations in surface microbial communities and indirectly affecting sinking-particle communities. Sea-ice dynamics were the main environmental factor leading to the most observable shifts in microbial composition. This is evident in the differences between 2017 and 2018, which exhibited distinct stratification regimes influenced by sea-ice presence. These differences resulted in shifts in the composition of both surface and particle-associated microbial communities. In contrast, the cold anomaly (January 2020 – September 2020) with higher ice presence around the station, had a weaker impact on microbial communities and particle fluxes compared to previous temperature anomalies

(warm anomalies), with only slight shifts in microbial community composition and no significant changes in particle fluxes. A contrast that can be related to the duration of the anomaly and consequently time of exposition of microbial communities to stress factors.

The ongoing climate change in the Arctic region, particularly the reduction in sea-ice extent and changes in stratification patterns, could significantly alter microbial community dynamics in the Fram Strait. As sea-ice cover decreases and stratification regimes shift, these changes in the seasonality will likely drive shifts in the surface microbial composition of the Fram Strait, affect the export of particle fluxes due to shifts in surface communities and consequently affecting the availability of organic matter for sinking-particle communities. Additionally, the sensitivity of particle-associated prokaryotes to organic matter availability, and of microbial eukaryotes to sea-ice dynamics, indicates that ongoing sea-ice loss could lead to long-term changes in particle-associated community structures. This may result in a reduced capacity for organic matter degradation and altered nutrient recycling processes.

As the next steps, the focus will be on integrating ecological co-occurrence network analysis for the identification of microbial modules and confirm the associated dynamics between families that was observed here, which could provide insights into ecological roles, and connections between prokaryotic and eukaryotic microorganisms. Additionally, time-shifted analyses will be used to detect microbial responses to environmental fluctuations, and indicator species will be used to track ecosystem transitions. These approaches will contribute to a fully comprehensive understanding of the interconnections and seasonal patterns of particle-attached and surface free-living microbial communities in the Fram Strait

REFERENCES

AMAP, 2021. **Arctic Climate Change Update 2021: Key Trends and Impacts**. Summary for Policy-makers. Arctic Monitoring and Assessment Programme (AMAP), Tromsø, Norway. 16 pp

Arrigo KR (2005) **Marine microorganisms and global nutrient cycles**. Nature. 437, 349–355.

Arrigo KR, van Dijken GL, Pabi S (2008), **Impact of a shrinking Arctic ice cover on marine primary production**, Geophys. Res. Lett., 35, L19603, Doi: 10.1029/2008GL035028.

Avcı B, Krüger K, Fuchs BM, Teeling H, Amann RI (2020) **Polysaccharide niche partitioning of distinct Polaribacter clades during North Sea spring algal blooms**. ISME J 14(6):1369–1383

Azam F, Malfatti F (2007) **Microbial structuring of marine ecosystems**. Nat Rev Microbiol 5, 782–791 Doi: 10.1038/nrmicro1747

Balmonte JP, Teske A, Arnosti C (2018) **Structure and function of high Arctic pelagic, particle-associated and benthic bacterial communities.** Environ Microbiol, 20: 2941-2954. Doi:10.1111/1462-2920.14304

Berge J, Renaud PE, Darnis G, Cottier F, Last Kim, Gabrielsen TM, Johnsen G, et al. (2015) **In the dark: A review of ecosystem processes during the Arctic polar night.** Progress In Oceanography. 139. 10.1016/j.pocean.2015.08.005.

Beszczynska-Möller A, Fahrbach E, Schauer U, Hansen E (2012) **Variability in Atlantic water temperature and transport at the entrance to the Arctic Ocean**, 1997–2010, ICES Journal of Marine Science, Volume 69, Issue 5, July 2012, Pages 852–863, Doi: 10.1093/icesjms/fss056

Beszczynska-Möller A, Woodgate RA, Lee C, Melling H, and Karcher M (2011) **A synthesis of exchanges through the main oceanic gateways to the Arctic Ocean.** Oceanography 24(3):82–99, Doi:10.5670/oceanog.2011.59.

Bodungen BV, Wunsch M, and Fürderer H (1991) **Sampling and analysis of suspended and sinking particles in the northern North Atlantic.** American Geophysical Union, Washington. 63, 5-6. doi: 10.1029/GM063p0047

Boeuf D, Edwards BR, Eppley JM, Hu SK, Poff KE, Romano AE, Caron DA, Karl DM, DeLong EF, **Biological composition and microbial dynamics of sinking particulate organic matter at abyssal depths in the oligotrophic open ocean**, Proc. Natl. Acad. Sci. U.S.A. 116 (24) 11824-11832. Doi: 10.1073/pnas.1903080116 (2019).

Bowman JP (2014). **The Family *Colwelliaceae***. In: Rosenberg, E., DeLong, E.F., Lory, S., Stackebrandt, E., Thompson, F. (eds) The Prokaryotes. Springer, Berlin, Heidelberg. Doi: 10.1007/978-3-642-38922-1_230

Buesseler KO, Boyd PW (2009). **Shedding light on processes that control particle export and flux attenuation in the twilight zone of the open ocean**. Limnol. Oceanogr. 54, 1210–1232. Doi: 10.4319/lo.2009.54.4.1210.

Buesseler KO, Lamborg CH, Boyd PW, Lam PJ, Trull TW, Bidigare RR, Bishop JKB, Casciotti KL, et al (2007) **Revisiting carbon flux through the ocean's twilight zone**. Science, 316 (5824), 567–570. Doi: 10.1126/science.1137959

Callahan BJ, McMurdie PJ, Rosen MJ, Han AW, Johnson AJA, Holmes SP (2016) **DADA2: High-resolution sample inference from Illumina amplicon data**. Nat Methods. 13:581–3.

Cardozo-Mino MG, Salter I, Nöthig E-M, Metfies K, Ramondec S, Wekerle C, Krumpen T, Boetius A and Bienhold C (2023) **A decade of microbial community dynamics on sinking particles during high carbon export events in the eastern Fram Strait.** Front Mar. Sci. 10:1173384. Doi: 10.3389/fmars.2023.1173384

Carton JA, Ding Y, and Arrigo KR (2015) **The seasonal cycle of the Arctic Ocean under climate change**, Geophys. Res. Lett., 42, 7681–7686. Doi:10.1002/2015GL064514.

Clarke LJ, Bestley S, Bissett A, et al. (2019) **A globally distributed Syndiniales parasite dominates the Southern Ocean micro-eukaryote community near the sea-ice edge**. ISME J 13, 734–737. Doi: 10.1038/s41396-018-0306-7

Comiso JC, Parkinson CL, Gersten R, Stock L (2008) **Accelerated decline in the Arctic sea ice cover**, Geophys. Res. Lett., 35, L01703. Doi:10.1029/2007GL031972.

Dahlke S, Solbès A, Maturilli M (2022). **Cold air outbreaks in Fram Strait: Climatology, trends, and observations during an extreme season in 2020**. Journal of Geophysical Research: Atmospheres, 127, e2021JD035741. Doi: 10.1029/2021JD035741

Datta MS, Sliwerska E, Gore J, Polz MF, Cordero OX (2016) **Microbial interactions lead to rapid micro-scale successions on model marine particles**. Nat. Commun. 7, 1–7.Doi: 10.1038/ncomms11965

De La Rocha CL, Passow U (2007) **Factors influencing the sinking of POC and the efficiency of the biological carbon pump.** Deep-Sea Res. II 54:639–58

Dean RB and Dixon WJ (1951) **Simplified Statistics for Small Numbers of Observations**. Anal. Chem., 23 (4), 636–638.

Ducklow HW, Steinberg DK, Buesseler KO (2001) **Upper ocean carbon export and the biological pump**. Oceanography 14:50–58. Doi: 10.5670/oceanog.2001.06

Dugdale RC, Goering JJ (1967) **Uptake of new and regenerated forms of nitrogen in primary productivity**. Limnol. Oceanogr, 12, 196–206. Doi: 10.4319/lo.1967.12.2.0196.

Dunweber M, Swalethorp R, Kjellerup S, Nielsen TG, Arendt KE, Hjorth M, Tonnesson K, Moller EF, (2010). **Succession and fate of the spring diatom bloom in Disko Bay, western Greenland**. Marine Ecology Progress Series 419, 11–29.

Durkin CA, Cetinić I, Estapa M, Ljubešić Z, Mucko M, Neeley A, Omand M (2022) **Tracing the path of carbon export in the ocean though DNA sequencing of individual sinking particles**. The ISME Journal. Volume 16, Issue 8, August 2022, Pages 1896–1906. Doi: 10.1038/s41396-022-01239-2

Ekwurzel B, Schlosser P, Mortlock RA, Fairbanks RG, and Swift JH (2001). **River runoff, sea ice meltwater, and Pacific water distribution and mean residence times in the Arctic Ocean.** J. Geophys. Res. Ocean. 106, 9075–9092. Doi: 10.1029/1999JC000024.

Fadeev E, Rogge A, Ramondenc S, Nöthig E-M, Wekerle C, Bienhold C, et al (2021) **Sea Ice presence is linked to higher carbon export and vertical microbial connectivity in the Eurasian Arctic ocean**. Commun. Biol. 4, 1255. Doi: 10.1038/s42003-021-02776-w

Fontanez KM, Eppley JM, Samo TJ, Karl DM, DeLong EF (2015) **Microbial community structure and function on sinking particles in the North Pacific Subtropical Gyre.** Front. Microbiol. 6, 469.

Fowler SW, Knauer GA (1986) **Role of large particles in the transport of elements and organic compounds through the oceanic water column.** Progress in Oceanography 16: 147–194. Doi:10.1016/0079-6611(86)90032-7

Francois R, Honjo S, Krishfield R, Manganini S (2002) **Factors controlling the flux of organics carbon to the bathypelagic zone of the ocean.** Global Biogeochem. Cycles, 16(4), 1087. Doi: 10.1029/2001GB001722

Fuhrman, J., Cram, J. & Needham, D (2015). **Marine microbial community dynamics and their ecological interpretation**. Nat Rev Microbiol, 13, 133–14. Doi: 10.1038/nrmicro3417

Ghiglione J-F, Galand PE, Pommier T, Pedrós-Alió C, Maas EW, Bakker K, Bertilson S, Kirchman DL, Lovejoy C, Yager PL, Murray AE (2012) **Pole-to-pole biogeography of surface and deep marine bacterial communities**. Proceedings of the National Academy of Sciences of the United States of America 109, 17633–17638. Doi: 10.1073/pnas.1208160109.

Giovannoni SJ (2017) **SAR11 Bacteria: the Most Abundant Plankton in the Oceans. Annual Review of Marine Science.** v.9, p.231-255, issn 1941-0611. Doi: 10.1146/annurev-marine-010814-015934

Gosink JJ, Woese CR, Staley JT (1998) **Polaribacter gen. nov., with three new species, P. irgensii sp. nov., P. franzmannii sp. nov. and P. filamentus sp. nov., gas vacuolate polar marine bacteria of the Cytophaga-Flavobacterium-Bacteroides group and reclassification of 'Flectobacillus glomeratus' as Polaribacter glomeratus comb. Nov**. Int J Syst Evol Microbiol 48(1):223–235

Grossart H-P, Kiørboe T, Tang K, Ploug H (2003) **Bacterial colonization of particles: growth and interactions.** Appl. Environ. Microbiol. 69, 3500–3509. Doi: 10.1128/aem.69.6.3500-3509.2003

Guidi L, Stemmann L, Jackson GA, Ibanez F, Claustre H, Legendre L, et al (2009) **Effects of phytoplankton community on production, size and export of large aggregates: A world-ocean analysis.** Limnol. Oceanogr. 54, 1951–1963. Doi: 10.4319/lo.2009.54.6.1951.

Guillou L, Bachar D, Audic S, Bass D, Berney C, Bittner L, et al (2013) **The Protist Ribosomal Reference database (PR2): a catalog of unicellular eukaryote Small Sub-Unit rRNA sequences with curated taxonomy**. Nucleic Acids Res. 41:D597–D604.

Han Y and Perner M (2015) **The globally widespread genus Sulfurimonas: versatile energy metabolisms and adaptations to redox clines**. Front. Microbiol. 6:989. Doi: 10.3389/fmicb.2015.00989

Harðardóttir S, Pančić M, Tammilehto A, Krock B, Møller EF, Nielsen TG, Lundholm N (2015) **Dangerous Relations in the Arctic Marine Food Web: Interactions between Toxin Producing *Pseudo-nitzschia* Diatoms and *Calanus* Copepodites**. *Marine Drugs*. 2015; 13(6):3809-3835. Doi: 10.3390/md13063809

Hattermann T, Isachsen PE, von Appen W-J, Albretsen J, Sundfjord A (2016) **Eddy-driven recirculation of Atlantic Water in Fram strait**. Geophys. Res.Lett. 43, 1–9.

Henson SA, Sanders R, Madsen E (2012). **Global patterns in efficiency of particulate organic carbon export and transfer to the deep ocean.** Global Biogeochem. Cycles 26. Doi: 10.1029/2011GB004099.

Herfort L, Seaton C, Wilkin M, Roman B, Preston CM, Marin R III, et al (2016) **Use of continuous, real-time observations and model simulations to achieve autonomous, adaptive sampling of microbial processes with a robotic sampler**. Limnol. Oceanogr. Methods 14, 50–67. Doi: 10.1002/lom3.10069

Hoarfrost A, Nayfach S, Ladau J. *et al.* (2020) **Global ecotypes in the ubiquitous marine clade SAR86.** *ISME J* 14, 178–188. Doi: 10.1038/s41396-019-0516-7

Hodal H, Falk-Petersen S, Hop H, Kristiansen S, Reigstad M (2012) **Spring bloom dynamics in Kongsfjorden, Svalbard: nutrients, phytoplankton, protozoans and primary production**. Polar Biology 35, 191–203.

Hoppmann, M: **Collection of raw data from oceanographic moorings in the Fram Strait, Greenland Sea, and central Arctic Ocean, 2018-2025 [dataset publication series].** PANGAEA, https://doi.pangaea.de/10.1594/PANGAEA.959812

Hsieh TC, Ma KH, Chao A (2016**) iNEXT: an R package for rarefaction and extrapolation of species diversity (Hill numbers)**. Methods Ecol Evol. 7:1451–6.

Huang H (2021). **linkET: Everything is Linkable.** R package version 0.0.7.4.

Iversen M (2023) **Carbon Export in the Ocean: A Biologist's Perspective**. Annual Review of Marine Science, v.15, p357-381. Doi: 10.1146/annurev-marine-032122-035153

Jaspers C, Weiland-Bräuer N, Rühlemann MC, Baines JF, Schmitz RA, Reusch TBH (2020) **Differences in the microbiota of native and non-indigenous gelatinous zooplankton organisms in a low saline environment.** Sci. Total Environ. 734, 139471. Doi: 10.1016/j.scitotenv.2020.139471

Kassambara A (2023) **ggpubr: ggplot2 Based Publication Ready Plots.** R package version 0.6.0 <<https://CRAN.R-project.org/package=ggpubr>>

Kwok R, Cunningham GF, Wensnahan M, Rigor I, Zwally HJ, Yi D (2009) **Thinning and volume loss of the Arctic Ocean sea ice cover: 2003–2008.** Journal of Geophysical Research 114, C07005, Doi: 10.1029/2009JC005312.

Lee J, Kang S-H, Yang EJ, Macdonald AM, Joo HM, Park J, Kim K, Lee GS, Kim JH, Yoon JE, Kim SS, Lim J-H, Kim I-N (2019) **Latitudinal Distributions and Controls of Bacterial Community Composition during the Summer of 2017 in Western Arctic Surface Waters (from the Bering Strait to the Chukchi Borderland).** Scientific Reports, 9(1), 16822. Doi: 10.1038/s41598-019-53427-4

Leu E, et al. (2015) **Arctic spring awakening – steering principles behind the phenology of vernal ice algal blooms**. Progress in Oceanography 139, 151–170. Doi: 10.1016/j.pocean.2015.07.012.

Lewis KM, et al. (2020) **Changes in phytoplankton concentration now drive increased Arctic Ocean primary production.** Science 369, 198-202. Doi:10.1126/science.aay8380

Lovejoy C, Galand PE, Kirchman DL (2011) **Picoplankton diversity in the Arctic Ocean and surrounding seas**. Mar Biodiv 41, 5–12. Doi: 10.1007/s12526-010-0062-z

Martin M (2011) **Cutadapt removes adapter sequences from high-throughput sequencing reads**. EMBnet.journal. 17:10–2. Doi: 10.14806/ej.17.1.200

Martinez-Garcia M, Brazel DM, Swan BK, Arnosti C, Chain PSG et al (2012) **Capturing single cell genomes of active polysaccharide degraders: an unexpected contribution of Verrucomicrobia**. PLoS One 7(4):e35314

McDonnell AMP, Lam PJ, Lamborg CH, et al (2015) **The oceanographic toolbox for the collection of sinking and suspended marine particles.** Progress in Oceanography 133: 17–31. Doi:10.1016/j.pocean.2015.01.007

McMurdie PJ, Holmes S (2013) **phyloseq: An R package for reproducible interactive analysis and graphics of microbiome census data**. PLoS ONE 8(4):e61217.

Melsheimer, Christian; Spreen, Gunnar (2019): **AMSR2 ASI sea ice concentration data, Arctic, version 5.4 (NetCDF) (July 2012 - December 2019)** [dataset]. PANGAEA. https://doi.org/10.1594/PANGAEA.898399

Mestre M, Ruiz-González C, Logares R, Duarte CM, Gasol JM, Montserrat Sala M (2018) **Sinking particles promote vertical connectivity in the ocean microbiome**. PNAS. 115(29):E6799–6807. Doi: 10.1073/pnas.180247011

Metfies K, Bauerfeind E, Wolf C, Sprong P, Frickenhaus S, Kaleschke L, et al (2017) **Protist communities in moored long-term sediment traps (Fram Strait, Arctic)–preservation with mercury chloride allows for PCR-based molecular genetic analyses**. Front. Mar. Sci. 4:301. Doi:10.3389/fmars.2017.00301

Metfies K, Hessel J, Klenk R, Petersen W, Wiltshire KH, Kraberg A (2020) **Uncovering the intricacies of microbial community dynamics at Helgoland roads at the end of a spring bloom using automated sampling and 18S meta-barcoding**. PloS One 15, e023392. doi: 10.1371/journal.pone.0233921

Nguyen TTH, Zakem EJ, Ebrahimi A, Schwartzman J, Caglar T, Amarnath K, et al (2022) **Microbes contribute to setting the ocean carbon flux by altering the fate of sinking particulates**. Nat. Commun. 13:1657. Doi: 10.1038/s41467-022-29297-2

Nöthig E-M, Bracher A, Engel A, Metfies K, Niehoff B, Peeken I, Bauerfeind E, et al. (2015) **Summertime plankton ecology in Fram Strait—a compilation of long- and short-term observations**. Polar Research, 34:1, 23349, DOI: 10.3402/polar.v34.23349

Nowicki M, DeVries T,Siegel DA (2022) **Quantifying the carbon export and sequestration pathways of the ocean's biological carbon pump**. Global Biogeochemical Cycles 36, e2021GB007083. Doi: 10.1029/2021GB007083

Oksanen J, Kindt R, Legendre P, O'Hara B, Stevens MHH, Oksanen MJ, et al. (2007) **The Vegan Package. Community Ecology Package**. 10 p. 719.

Oldenburg E, Kronberg RM, Metfies K. *et al.* (2024a) **Beyond blooms: the winter ecosystem reset determines microeukaryotic community dynamics in the Fram Strait.** Commun Earth Environ 5, 643. Doi: 10.1038/s43247-024-01782-0

Oldenburg E, Popa O, Wietz M, von Appen W-J, Torres-Valdes S, Bienhold C, Ebenhöh O, Metfies K (2024b) **Sea-ice melt determines seasonal phytoplankton dynamics and delimits the habitat of temperate Atlantic taxa as the Arctic Ocean atlantifies.** ISME Comm, 4(1), Doi: 10.1093/ismeco/ycae027

Öztürk RÇ, Terzi Y, Rodríguez-Machado S, Başar E, Feyzioğlu AM, Ustaoğlu D, Ağırbaş E, Chakrabarty P (2024) **Metabarcoding the Arctic Ocean Helps Reveal Its Hidden Microbial Community Composition**. Turkish Journal of Fisheries and Aquatic Sciences, 24(SI), TRJFAS27181. Doi: 10.4194/TRJFAS27181

Parada AE, Needham DM, Fuhrman JA (2016) **Every base matters: assessing small subunit rRNA primers for marine microbiomes with mock communities, time series and global field samples**. Environ Microbiol. 18:1403–14.

Pauli NC, Metfies K, Pakhomov EA et al (2021) **Selective feeding in Southern Ocean key grazers—diet composition of krill and salps**. Commun Biol 4, 1061 (2021). Doi: 10.1038/s42003-021-02581-5

Pedrós-Alió C, Potvin M, Lovejoy C (2015) **Diversity of planktonic microorganisms in the Arctic Ocean**, Progress in Oceanography, V. 139, p.233-243, ISSN 0079-6611, Doi: 10.1016/j.pocean.2015.07.009.

Poltermann M (2001) **Arctic sea ice as feeding ground for amphipods – food sources and strategies**. Polar Biology 24, 89–96.

Polyakov IV, et al., (2017) **Greater role for Atlantic inflows on sea-ice loss in the Eurasian Basin of the Arctic Ocean**. Science 356: 285–291. Doi:10.1126/science.aai8204

Pörtner H, at al., (2019) **IPCC special report on the ocean and cryosphere in a changing climate**. IPCC Intergovernmental Panel on Climate Change: Geneva, Switzerland, 1(3).

Posit team (2024). **RStudio: Integrated Development Environment for R.** Posit Software, PBC, Boston, MA. URL http://www.posit.co/.

Priest T, von Appen WJ, Oldenburg E et al (2023) **Atlantic water influx and sea-ice cover drive taxonomic and functional shifts in Arctic marine bacterial communities**. ISME J 17, 1612–1625. Doi: 10.1038/s41396-023-01461-6

Priest, T., Oldenburg, E., Popa, O. *et al.* **Seasonal recurrence and modular assembly of an Arctic pelagic marine microbiome.** *Nat Commun* **16**, 1326 (2025). https://doi.org/10.1038/s41467-025-56203-3

Preston CM, Durkin CA, Yamahara KM (2020) **DNA Metabarcoding reveals organisms contributing to particulate matter flux to abyssal depths in the north East pacific ocean**. Deep. Res. Part II Top. Stud. Oceanogr. 173, 104708. Doi: 10.1016/j.dsr2.2019.104708

Quast C, Pruesse E, Yilmaz P, Gerken J, Schweer T, Yarza P, et al (2013) **The SILVA ribosomal RNA gene database project: improved data processing and web-based tools**. Nucleic Acids Res. 41:D590–596.

R Core Team (2024) **R: A Language and Environment for Statistical Computing.** R Foundation for Statistical Computing, Vienna, Austria. https: //www.R-project.org/

Ramondenc S, Nöthig E-M, Hufnagel L, Bauerfeind E, Busch K, Knüppel N, Kraft A, Schröter F, Seifert M, Iversen MH (2023) **Effects of Atlantification and changing sea-ice dynamics on zooplankton community structure and carbon flux between 2000 and 2016 in the eastern Fram Strait**. Limnol Oceanogr, 68: S39-S53. Doi: 10.1002/lno.12192

Rosenberg E (2014). **The Family *Rubritaleaceae***. In: Rosenberg, E., DeLong, E.F., Lory, S., Stackebrandt, E., Thompson, F. (eds) The Prokaryotes. Springer, Berlin, Heidelberg. Doi: 10.1007/978-3-642-38954-2_146

Rudels B, Carmack E. (2022) **Arctic Ocean Water Mass Structure and Circulation.** Oceanography 35. Doi:10.5670/oceanog.2022.116.

Sakshaug E (2004) **Primary and secondary production in the Arctic Seas**. In: Stein R, Macdonald RW (eds) The organic carbon cycle in the Arctic Ocean. Springer, Berlin, pp 57–81

Salter I, Bauerfeind E, Fahl K, Iversen MH, Lalande C, Ramondenc S, Von Appen W-J, Wekerle C and Nöthig E-M (2023), **Interannual variability (2000–2013) of mesopelagic and bathypelagic particle fluxes in relation to variable sea ice cover in the eastern Fram Strait**. Front. Earth Sci. 11:1210213. Doi: 10.3389/feart.2023.1210213

Seibold A, Wichels A, Schutt C (2001) **Diversity of endocytic bacteria in the dinoflagellate Noctiluca scintillans.** Aquat Microb Ecol 25:229–235

Sejr MK, Nielsen TG, Rysgaard S, Risgaard-Petersen N, Sturluson M, Blicher ME (2007) **Fate of pelagic organic carbon and importance of pelagic–benthic coupling in a shallow cove in Disko Bay, West Greenland**. Marine Ecology Progress Series 341, 75–88.

Simon M, Grossart H, Schweitzer B, Ploug H (2002) **Microbial ecology of organic aggregates in aquatic ecosystems**. Aquatic Microbial Ecology 28: 175–211. Doi:10.3354/ame028175

Soltwedel T, Bauerfeind E, Bergmann M, Bracher A, Budaeva N, Busch K, et al (2016) **Natural variability or anthropogenically-induced variation? Insights from 15 years of multidisciplinary observations at the arctic marine LTER site HAUSGARTEN**. Ecol. Indic. 65, 89–102. Doi: 10.1016/j.ecolind.2015.10.001.

Spreen G, Kaleschke L, Heygster G (2008) **Sea ice remote sensing using AMSR-E 89 GHz channels** J. Geophys. Res., vol. 113, C02S03. Doi: 10.1029/2005JC003384.

Spring S, Scheuner C, Göker M, Klenk H-P (2015) **A taxonomic framework for emerging groups of ecologically important marine gammaproteobacteria based on the reconstruction of evolutionary relationships using genome-scale data.** Frontiers in Microbiology. 6:281. Doi: 10.3389/fmicb.2015.00281

Stein R, Macdonald RW (2004) **The Organic Carbon Cycle in the Arctic Ocean.** Springer, Ed.1. Doi: 10.1007/978-3-642-18912-8

Tamas I, Smirnova A, He Z et al (2014) **The (d)evolution of methanotrophy in the *Beijerinckiaceae*—a comparative genomics analysis**. *ISME J* **8**, 369–382 (2014). Doi: 10.1038/ismej.2013.145

Thiele S, Storesund JE, Fernández-Méndez M, Assmy P, Øvreås L (2022) **A Winter-to-Summer Transition of Bacterial and Archaeal Communities in Arctic Sea Ice.** *Microorganisms*. 10(8):1618. Doi:10.3390/microorganisms10081618

Turner JT (2015) **Zooplankton fecal pellets, marine snow, phytodetritus and the ocean's biological pump**. Prog. Oceanogr. 130, 205–248. Doi: 10.1016/j.pocean.2014.08.005

von Appen, W-J (2019): **Physical oceanography and current meter data (including raw data) from FRAM moorings in the Fram Strait, 2016-2018** [dataset bibliography]. PANGAEA, https://doi.org/10.1594/PANGAEA.904565

von Appen W-J, Waite AM, Bergmann M. *et al* (2021) **Sea-ice derived meltwater stratification slows the biological carbon pump: results from continuous observations**. *Nat Commun* **12**, 7309. Doi: 10.1038/s41467-021-26943-z

Walsh JE (2008) **Climate of the Arctic Marine Environment**. Ecological Applications, 18: S3-S22. Doi: 10.1890/06-0503.1

Wekerle C, Krumpen T, Dinter T, von Appen W-J, Iversen MH and Salter I (2018) **Properties of Sediment Trap Catchment Areas in Fram Strait: Results From Lagrangian Modeling and Remote Sensing**. Front Mar Sci. 5:407. Doi: 10.3389/fmars.2018.00407

Werner I (1997) **Grazing of Arctic under-ice amphipods on sea-ice algae**. Marine Ecology Progress Series 160, 93–99.

Wiedmann I. et al (2020) **What feeds the Benthos in the Arctic Basins? Assembling a carbon budget for the deep Arctic Ocean**. Front. Mar. Sci. 7, 544386. Doi: 10.3389/fmars.2020.00224

Wietz M, Bienhold C, Metfies K, Torres-Valdés S, von Appen WJ, Salter I, Boetius A (2021) **The polar night shift: seasonal dynamics and drivers of Arctic Ocean microbiomes revealed by autonomous sampling.** ISME Commun. Dec 11;1(1):76. doi: 10.1038/s43705-021-00074-4. PMID: 37938651; PMCID: PMC9723606.

Wietz M, Metfies K, Bienhold C, Wolf C, Janssen F, Salter I and Boetius A (2022) **Impact of preservation method and storage period on ribosomal metabarcoding of marine microbes: Implications for remote automated samplings**. Front. Microbiol. 13:999925. doi: 10.3389/fmicb.2022.999925

Wilson B, Müller O, Nordmann EL, Seuthe L, Bratbak G, Øvreås L (2017) **Changes in marine prokaryote composition with season and depth over an Arctic polar year.** Front. Mar. Sci. 4, 95. Doi:10.3389/fmars.2017.00095

Yan L (2023) **ggvenn: Draw Venn Diagram by ggplot2**. R package v. 0.1.10 https://CRAN.R-project.org/package=ggvenn

Zamani B, Krumpen T, Smedsrud LH et al (2019) Fram Strait sea ice export affected by thinning: comparing high-resolution simulations and observations. Clim Dyn 53, 3257–3270 (2019). https://doi.org/10.1007/s00382-019-04699-z

ACKNOWLEDGEMENTS

I would like to thank Dr. Christina Bienhold for accepting the role of my supervisor and for the invaluable reviews, insights, and discussions throughout the development of this thesis.

I am also grateful to Dr. Morten Iversen for kindly accepting to be the second reviewer.

Thank you Dr. Katja Metfies, Dr. Wilken-Jon von Appen, Dr. Matthias Wietz and Stefan Neuhaus for sharing data, analytical input, results, and scripts.

Thank you Max Planck Institute for Marine Microbiology, University of Bremen and Alfred Wegener Institute for Polar and Marine Research for providing the infrastructure necessary to carry out this project.

Thanks AWI for making the sea-ice data from 1979 to 2023, available via www.meereisportal.de (funding: REKLIM-2013-04) available.

Thank you MarMic community and professors, for the opportunity to realize this research

I would like to thank the HPG MPG Joint Research Group for Deep-Sea Ecology and Technology for warmly welcoming me into the group

Thank you all my MarMic classmates, for being amazing friends

A special thanks to Carlos for taking care of me, listening to endless discussions about this project, for the patience during the long nights of writing, and the emotional support. I couldn't have done it without you.

Thank you for my family who despite the distance, continue to support me in following my dreams.

Lastly, thank you to Kima for the fluffy emotional support throughout my entire academic journey.

APPENDIX 1 – SAMPLING DATA

Table S1: Sampling data and number of sequences recovered of each sample. It includes sample information (ID and data type), the start and end dates of the collection period, sampling depth (in meters) and number of sequences for 16S and 18S from the raw tables (without remove of singletons and unclassified taxa) used in alpha-diversity analysis. Samples with asterisk were removed during rarefaction for some analysis.

Sample ID	Data Type	Collection Start	Collection End	Depth [m]	Seqs 16S	Seqs 18S
Fevi34_Up01	Sediment Trap	2016-07-14	2016-07-22	196	124695	239816
Fevi34_Up02	Sediment Trap	2016-07-22	2016-07-31	196	99738	111792
Fevi34_Up03	Sediment Trap	2016-07-31	2016-08-15	196	206269	135336
Fevi34_Up04	Sediment Trap	2016-08-15	2016-08-31	196	191034	
Fevi34_Up05	Sediment Trap	2016-08-31	2016-09-15	196	79951	112572
Fevi34_Up06	Sediment Trap	2016-09-15	2016-09-30	196	146010	25278
Fevi34_Up07	Sediment Trap	2016-09-30	2016-10-31	196	206621	228280
Fevi34_Up08	Sediment Trap	2016-10-31	2016-11-30	196	126067	163724
Fevi34_Up09	Sediment Trap	2016-11-30	2016-12-31	196	118657	65967
Fevi34_Up10	Sediment Trap	2016-12-31	2017-02-28	196	134062	48234
Fevi34_Up11	Sediment Trap	2017-02-28	2017-03-31	196	114965	71300
Fevi34_Up12	Sediment Trap	2017-03-31	2017-04-17	196	205761	
Fevi34_Up13	Sediment Trap	2017-04-17	2017-05-04	196	213775	33873
Fevi34_Up14	Sediment Trap	2017-05-04	2017-05-21	196	98006	46400
Fevi34_Up15	Sediment Trap	2017-05-21	2017-06-08	196	211038	
Fevi34_Up16	Sediment Trap	2017-06-08	2017-06-25	196	284523	49304
Fevi34_Up17	Sediment Trap	2017-06-25	2017-07-07	196	109294	173419
Fevi34_Up18	Sediment Trap	2017-07-07	2017-07-19	196	128984	259163
Fevi36_Up01	Sediment Trap	2017-08-12	2017-08-21	201	164460	201078
Fevi36_Up02	Sediment Trap	2017-08-21	2017-08-31	201	87181	118850
Fevi36_Up08	Sediment Trap	2017-10-31	2017-11-30	201	132694	206665
Fevi36_Up09*	Sediment Trap	2017-11-30	2017-12-31	201	225662	4674*
Fevi36_Up11	Sediment Trap	2018-01-31	2018-02-28	201	73272	154433
Fevi36_Up15*	Sediment Trap	2018-04-30	2018-05-15	201	129918	1041*
Fevi36_Up16	Sediment Trap	2018-05-15	2018-05-31	201	48195	24933
Fevi36_Up17	Sediment Trap	2018-05-31	2018-06-15	201	100720	217468
Fevi38_Up06	Sediment Trap	2018-10-15	2018-11-01	196	84940	214017
Fevi38_Up07	Sediment Trap	2018-11-01	2018-12-01	196	234501	233350
Fevi38_Up08	Sediment Trap	2018-12-01	2019-01-01	196	249417	136694
Fevi38_Up09	Sediment Trap	2019-01-01	2019-02-01	196	136543	175634
Fevi38_Up10	Sediment Trap	2019-02-01	2019-03-01	196	89381	84943
Fevi38_Up11	Sediment Trap	2019-03-01	2019-03-16	196	105555	122739
Fevi38_Up12	Sediment Trap	2019-03-16	2019-04-01	196	148216	122074
Fevi40_Up01	Sediment Trap	2019-09-10	2019-10-01	200	49703	86871
Fevi40_Up02	Sediment Trap	2019-10-01	2019-11-01	200	107605	66342
Fevi40_Up03	Sediment Trap	2019-11-01	2019-12-01	200	88948	159907
Fevi40_Up04	Sediment Trap	2019-12-01	2020-03-01	200	162123	175109
Fevi40_Up05	Sediment Trap	2020-03-01	2020-04-01	200	65014	123401
Fevi40_Up06	Sediment Trap	2020-04-01	2020-05-01	200	178970	115309
Fevi40_Up07	Sediment Trap	2020-05-01	2020-06-01	200	173392	
Fevi40_Up08	Sediment Trap	2020-06-01	2020-07-01	200	138032	149776
Fevi40_Up09	Sediment Trap	2020-07-01	2020-07-16	200		
Fevi40_Up10	Sediment Trap	2020-07-16	2020-08-01	200	180804	
Fevi40_Up11	Sediment Trap	2020-08-01	2020-09-01	200	189036	

Fevi40_Up12	Sediment Trap	2020-09-01	2020-10-01	200	258313	
Fevi40_Up13	Sediment Trap	2020-10-01	2020-11-01	200	95532	35651
Fevi40_Up14	Sediment Trap	2020-11-01	2020-12-01	200	64154	129327
Fevi40_Up15	Sediment Trap	2020-12-01	2021-03-01	200	150260	94841
Fevi40_Up16	Sediment Trap	2021-03-01	2021-04-01	200	29730	37596
Fevi40_Up17	Sediment Trap	2021-04-01	2021-05-01	200	92781	39676
Fevi40_Up18	Sediment Trap	2021-05-01	2021-06-01	200	145561	25238
HS1_PS107_E33	RAS Amplicon	2016-08-01	2016-08-01	32.3	100836	76425
HS1_PS107_E34	RAS Amplicon	2016-08-15	2016-08-15	51.7	134773	101338
HS1_PS107_E35	RAS Amplicon	2016-09-01	2016-09-01	29.7	70329	125111
HS1_PS107_E36	RAS Amplicon	2016-09-15	2016-09-15	29.4	37157	70085
HS1_PS107_E37	RAS Amplicon	2016-10-01	2016-10-01	32.5	49069	52075
HS1_PS107_E38	RAS Amplicon	2016-11-01	2016-11-01	31.7	77001	64899
HS1_PS107_E39*	RAS Amplicon	2016-12-01	2016-12-01	32.8	7566*	26726
HS1_PS107_E40	RAS Amplicon	2017-01-01	2017-01-01	48.7	85259	73961
HS1_PS107_E41	RAS Amplicon	2017-02-01	2017-02-01	49.2	33469	100324
HS1_PS107_E42	RAS Amplicon	2017-02-14	2017-02-14	72.8	129995	117046
HS1_PS107_E43	RAS Amplicon	2017-03-01	2017-03-01	45.8	86989	88706
HS1_PS107_E44	RAS Amplicon	2017-03-08	2017-03-08	38.3	67900	77639
HS1_PS107_E45	RAS Amplicon	2017-03-15	2017-03-15	35.1	26516	115086
HS1_PS107_E46	RAS Amplicon	2017-03-22	2017-03-22	53.2	84018	161986
HS1_PS107_E47	RAS Amplicon	2017-04-01	2017-04-01	50.3	78889	109052
HS1_PS107_E48	RAS Amplicon	2017-04-15	2017-04-15	29.5	31743	94209
HS1_PS107_E49	RAS Amplicon	2017-05-01	2017-05-01	34.6	79671	136932
HS1_PS107_E50	RAS Amplicon	2017-05-15	2017-05-15	31.1	139563	98684
HS1_PS107_E51	RAS Amplicon	2017-06-01	2017-06-01	30.7	98457	111333
HS1_PS107_E52	RAS Amplicon	2017-06-15	2017-06-15	30.6	56151	50072
HS1_PS107_E53	RAS Amplicon	2017-07-01	2017-07-01	52.3	76901	93765
HS1_PS107_E54	RAS Amplicon	2017-07-08	2017-07-08	35.2	105895	62423
HS1_PS107_E55	RAS Amplicon	2017-07-15	2017-07-15	45.6	96449	42802
HS1_PS107_E56	RAS Amplicon	2017-07-22	2017-07-22	35.9	74394	100449
HS2_PS114_E1	RAS Amplicon	2017-08-15	2017-08-15	34.2	19946	65575
HS2_PS114_E2	RAS Amplicon	2017-08-30	2017-08-30	31.5	49789	33204
HS2_PS114_E3	RAS Amplicon	2017-09-14	2017-09-14	32.3	43497	82322
HS2_PS114_E4	RAS Amplicon	2017-09-29	2017-09-29	33.4	61825	97715
HS2_PS114_E5	RAS Amplicon	2017-10-29	2017-10-29	33.2	50673	66245
HS2_PS114_E6	RAS Amplicon	2017-11-28	2017-11-28	34.6	42511	70536
HS2_PS114_E7	RAS Amplicon	2017-12-28	2017-12-28	37.4	45004	91622
HS2_PS114_E8	RAS Amplicon	2018-01-27	2018-01-27	33.5	14323	92338
HS2_PS114_E9	RAS Amplicon	2018-02-11	2018-02-11	34.7	40800	
HS2_PS114_E10	RAS Amplicon	2018-02-26	2018-02-26	91.4	47882	11074
HS2_PS114_E11	RAS Amplicon	2018-03-07	2018-03-07	31.7	35665	
HS2_PS114_E12	RAS Amplicon	2018-03-16	2018-03-16	35.1	54491	127606
HS2_PS114_E13	RAS Amplicon	2018-03-25	2018-03-25	41.0	41750	88023
HS2_PS114_E14	RAS Amplicon	2018-04-03	2018-04-03	31.8	45553	112621
HS2_PS114_E15	RAS Amplicon	2018-04-12	2018-04-12	33.6	64745	53628
HS2_PS114_E16	RAS Amplicon	2018-04-21	2018-04-21	80.4	47331	74414
HS2_PS114_E17	RAS Amplicon	2018-04-30	2018-04-30	104.5	61269	106046
HS2_PS114_E18	RAS Amplicon	2018-05-12	2018-05-12	32.2	74007	55750
HS2_PS114_E19	RAS Amplicon	2018-05-24	2018-05-24	31.1	74430	21324
HS2_PS114_E20	RAS Amplicon	2018-06-05	2018-06-05	35.1	55707	40763
HS2_PS114_E21	RAS Amplicon	2018-06-17	2018-06-17	32.8	55749	14211
HS2_PS114_E22	RAS Amplicon	2018-06-29	2018-06-29	31.4	70846	73975

HS2_PS114_E23	RAS Amplicon	2018-07-08	2018-07-08	42.7	62903	108385
HS3_PS121_E28	RAS Amplicon	2018-08-01	2018-08-09	30.0	100286	222480
HS3_PS121_E29	RAS Amplicon	2018-08-17	2018-08-25	29.9	79931	128540
HS3_PS121_E30	RAS Amplicon	2018-09-02	2018-09-10	30.0	85602	194355
HS3_PS121_E31	RAS Amplicon	2018-09-18	2018-09-26	29.2	100285	184494
HS3_PS121_E32	RAS Amplicon	2018-10-04	2018-10-12	32.9	87987	192919
HS3_PS121_E33	RAS Amplicon	2018-10-20	2018-10-28	29.2	164365	100104
HS3_PS121_E34	RAS Amplicon	2018-11-05	2018-11-13	30.5	114991	108955
HS3_PS121_E35*	RAS Amplicon	2018-11-21	2018-11-29	34.9	144631	1992*
HS3_PS121_E36	RAS Amplicon	2018-12-07	2018-12-15	30.9	102872	76580
HS3_PS121_E37	RAS Amplicon	2018-12-23	2018-12-31	53.0	39121	76806
HS3_PS121_E38	RAS Amplicon	2019-01-08	2019-01-16	41.3	129790	96838
HS3_PS121_E39	RAS Amplicon	2019-01-24	2019-02-01	38.0	97288	91708
HS3_PS121_E40	RAS Amplicon	2019-02-09	2019-02-17	48.7	90019	19557
HS3_PS121_E41	RAS Amplicon	2019-02-25	2019-03-05	36.4	87922	118168
HS3_PS121_E42	RAS Amplicon	2019-03-13	2019-03-21	100.2	114177	146510
HS3_PS121_E43	RAS Amplicon	2019-03-29	2019-04-06	36.8	68972	87173
HS3_PS121_E44	RAS Amplicon	2019-04-14	2019-04-22	39.8	111098	118910
HS3_PS121_E45	RAS Amplicon	2019-04-30	2019-05-08	44.4	69371	104678
HS3_PS121_E46	RAS Amplicon	2019-05-16	2019-05-24	30.1	103644	84356
HS3_PS121_E47	RAS Amplicon	2019-06-01	2019-06-09	29.6	83898	163024
HS3_PS121_E48	RAS Amplicon	2019-06-17	2019-06-25	32.5	73324	145725
HS3_PS121_E49	RAS Amplicon	2019-07-03	2019-07-03	31.7	96455	125525
HS3_PS121_E50	RAS Amplicon	2019-07-11	2019-07-11	29.1	69317	148348
HS3_PS121_E51	RAS Amplicon	2019-07-19	2019-07-19	28.9	82637	96612
HS3_PS121_E52	RAS Amplicon	2019-07-27	2019-07-27	28.7	132581	67040
HS3_PS121_E53	RAS Amplicon	2019-08-04	2019-08-04	29.3	123424	112106
HS3_PS121_E54	RAS Amplicon	2019-08-12	2019-08-12	29.5	14175	37811
HS4_PS126_E1	RAS Amplicon	2019-09-11	2019-09-19	26.8	242359	418884
HS4_PS126_E2	RAS Amplicon	2019-09-27	2019-10-05	25.1	159537	292947
HS4_PS126_E3	RAS Amplicon	2019-10-13	2019-10-21	25.5	434194	283462
HS4_PS126_E4	RAS Amplicon	2019-10-29	2019-11-06	29.1	358714	179143
HS4_PS126_E5	RAS Amplicon	2019-11-14	2019-11-22	30.0	160489	255085
HS4_PS126_E6	RAS Amplicon	2019-11-30	2019-12-08	42.0	260992	137252
HS4_PS126_E7	RAS Amplicon	2019-12-16	2019-12-24	53.4	163722	85704
HS4_PS126_E8	RAS Amplicon	2020-01-01	2020-01-09	39.7	17016	91486
HS4_PS126_E9	RAS Amplicon	2020-01-17	2020-01-25	40.2	608857	89810
HS4_PS126_E10	RAS Amplicon	2020-02-02	2020-02-10	25.9	381303	180796
HS4_PS126_E11	RAS Amplicon	2020-02-18	2020-02-26	91.8	165372	78582
HS4_PS126_E12	RAS Amplicon	2020-03-05	2020-03-13	60.4	312519	67924
HS4_PS126_E13	RAS Amplicon	2020-03-21	2020-03-29	29.8	201448	198568
HS4_PS126_E14	RAS Amplicon	2020-04-06	2020-04-14	36.1	209612	141022
HS4_PS126_E15	RAS Amplicon	2020-04-22	2020-04-30	59.4	150160	118532
HS4_PS126_E16	RAS Amplicon	2020-05-08	2020-05-16	28.1	110182	116389
HS4_PS126_E17	RAS Amplicon	2020-05-24	2020-06-01	26.2	428562	282523
HS4_PS126_E18	RAS Amplicon	2020-06-09	2020-06-17	26.7	321287	167893
HS4_PS126_E19	RAS Amplicon	2020-06-25	2020-07-03	26.9	404587	215173
HS4_PS126_E20	RAS Amplicon	2020-07-11	2020-07-19	24.2	357352	151872
HS4_PS126_E21	RAS Amplicon	2020-07-27	2020-08-04	25.3	146667	81889
HS4_PS126_E22	RAS Amplicon	2020-08-12	2020-08-20	42.5	342844	22990
HS4_PS126_E23	RAS Amplicon	2020-08-28	2020-09-05	27.1	221917	272392
HS4_PS126_E24	RAS Amplicon	2020-09-13	2020-09-21	24.3	187120	167870

APPENDIX 2 – RAREFACTION CURVES

Figure S1: Rarefaction curves of sequencing depth and coverage of ASVs for (A - B) prokaryotes and (C - D) microbial eukaryotes. The curves were calculated by the iNEXT R package based on Hill number of order q = 0 with 100 bootstrap resamples for confidence interval estimation.

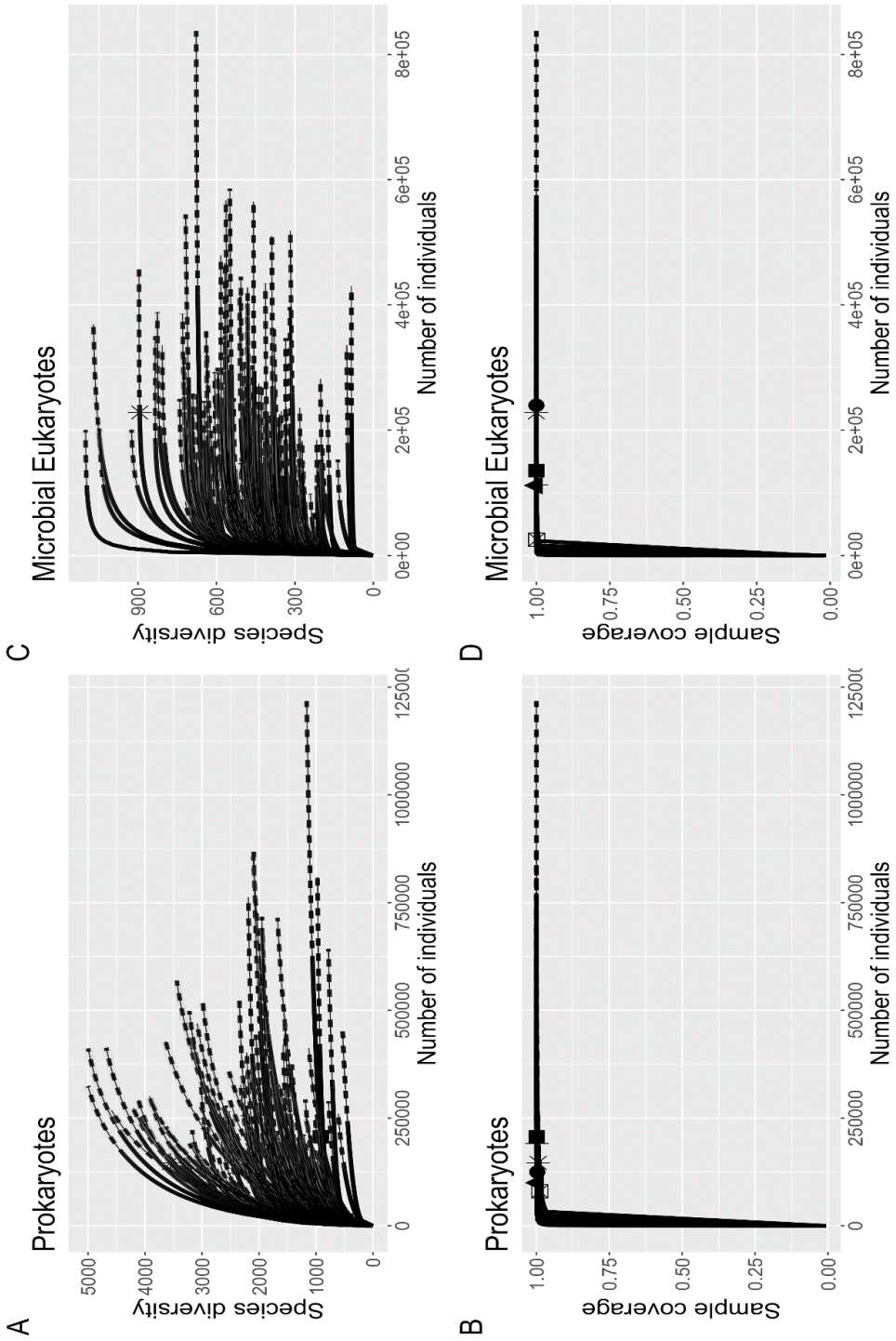

APPENDIX 3 - ALPHA DIVERSITY METRICS OVER TIME - PROKARYOTES

Figure S2: Observed ASVs and Shannon diversity metrics over the time series for prokaryotes. The upper section corresponds to surface water, while the lower section corresponds to particle-attached communities. Boxplots colors indicate seasons: red for autumn, green for spring, orange for summer, and blue for winter. The p-value is derived from the Kruskal-Wallis test. Asterisks represent significant pairwise comparisons by Wilcoxon test: * ($p \leq 0.05$), ** ($p \leq 0.01$), *** ($p \leq 0.001$), and **** ($p \leq 0.0001$).

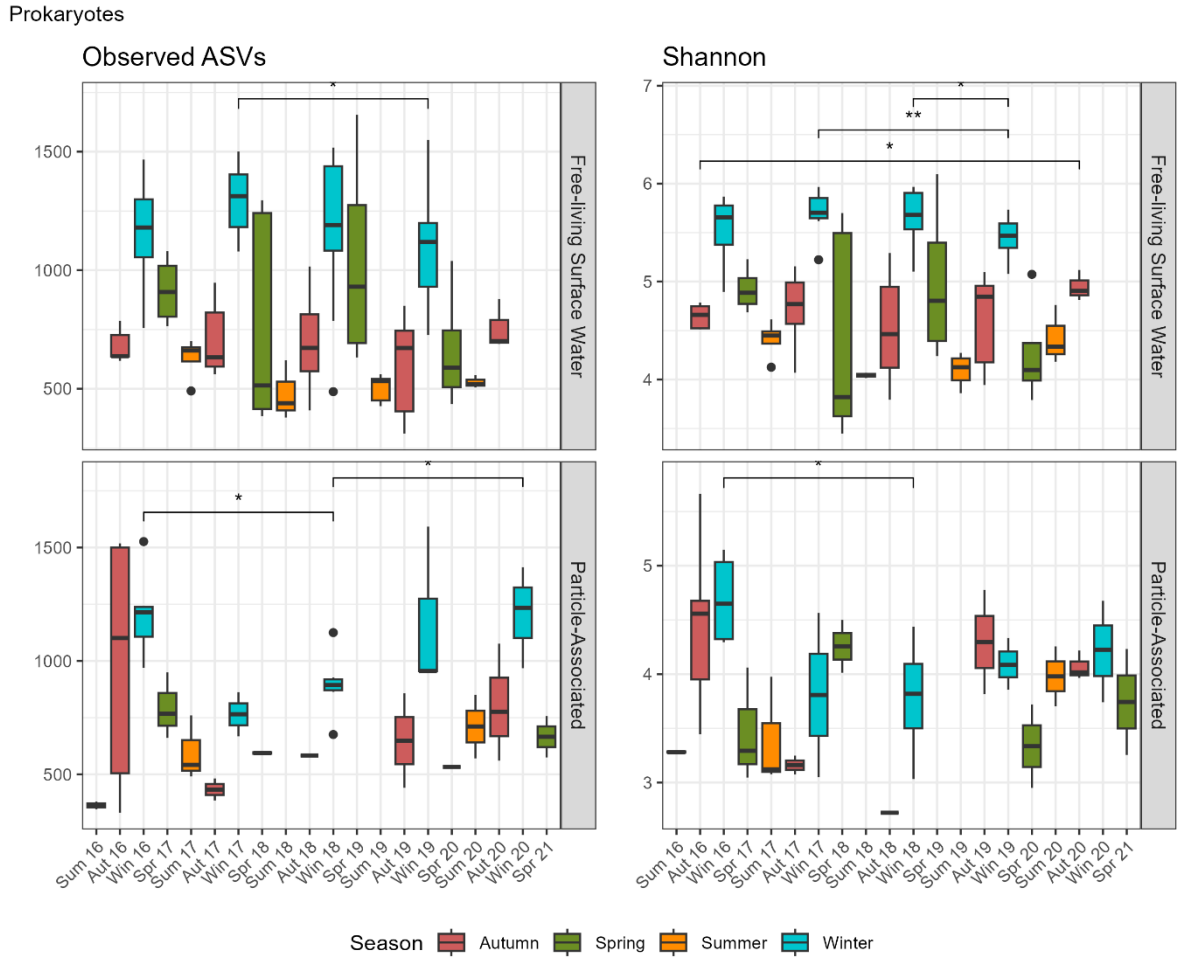

APPENDIX 4 – ALPHA DIVERSITY METRICS OVER TIME – MICRO EUKARYOTES

Figure S3: Observed ASVs and Shannon diversity metrics over the time series for microbial eukaryotes. The upper section corresponds to surface water, while the lower section corresponds to particle-attached communities. Boxplots colors indicate seasons: red for autumn, green for spring, orange for summer, and blue for winter. The p-value is derived from the Kruskal-Wallis test. Asterisks represent significant pairwise comparisons by Wilcoxon test: * ($p \leq 0.05$), ** ($p \leq 0.01$), *** ($p \leq 0.001$), and **** ($p \leq 0.0001$).

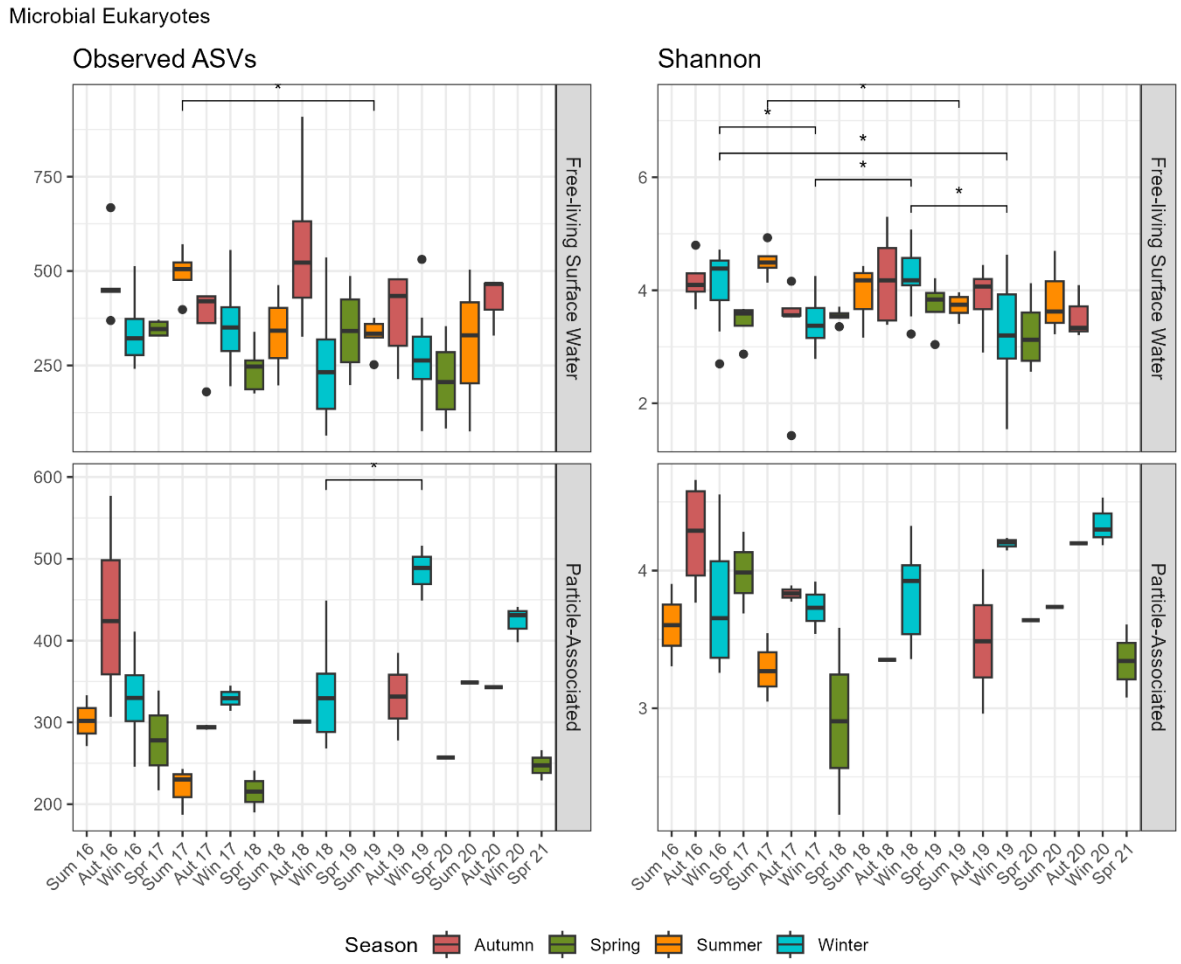

APPENDIX 5 - PARTICLE-ASSOCIATED PROKARYOTES BY SAMPLE

Figure S4: Relative abundance of the most abundant (>2%) prokaryotic families in particle-associated microbial communities by sample in Fram Strait from 2016 to 2021. It includes the samples Fevi36 Up9 and U9 15 that were later filtered out of analyses. The facets represent the seasons and the corresponding year.

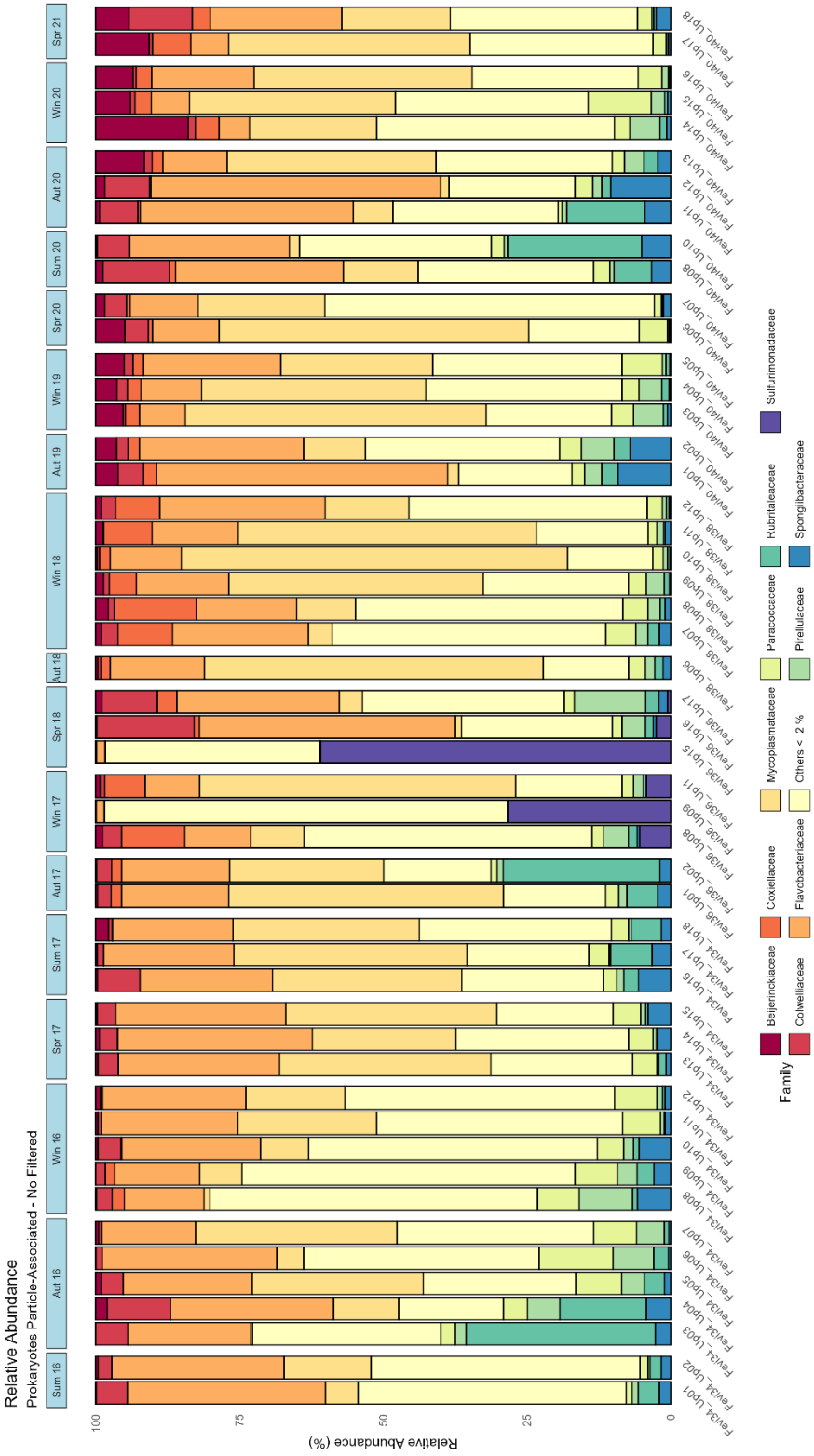

APPENDIX 6 – NMDS HABITAT

Figure S5: Two-dimensional NMDS of Bray-Curtis dissimilarity for (A) prokaryotes (B) microbial eukaryotes. Dissimilarities were calculated after Hellinger transformation. Colors represent seasons (blue for winter, green for spring, yellow for summer, and red for autumn) and symbols indicate different habitats.

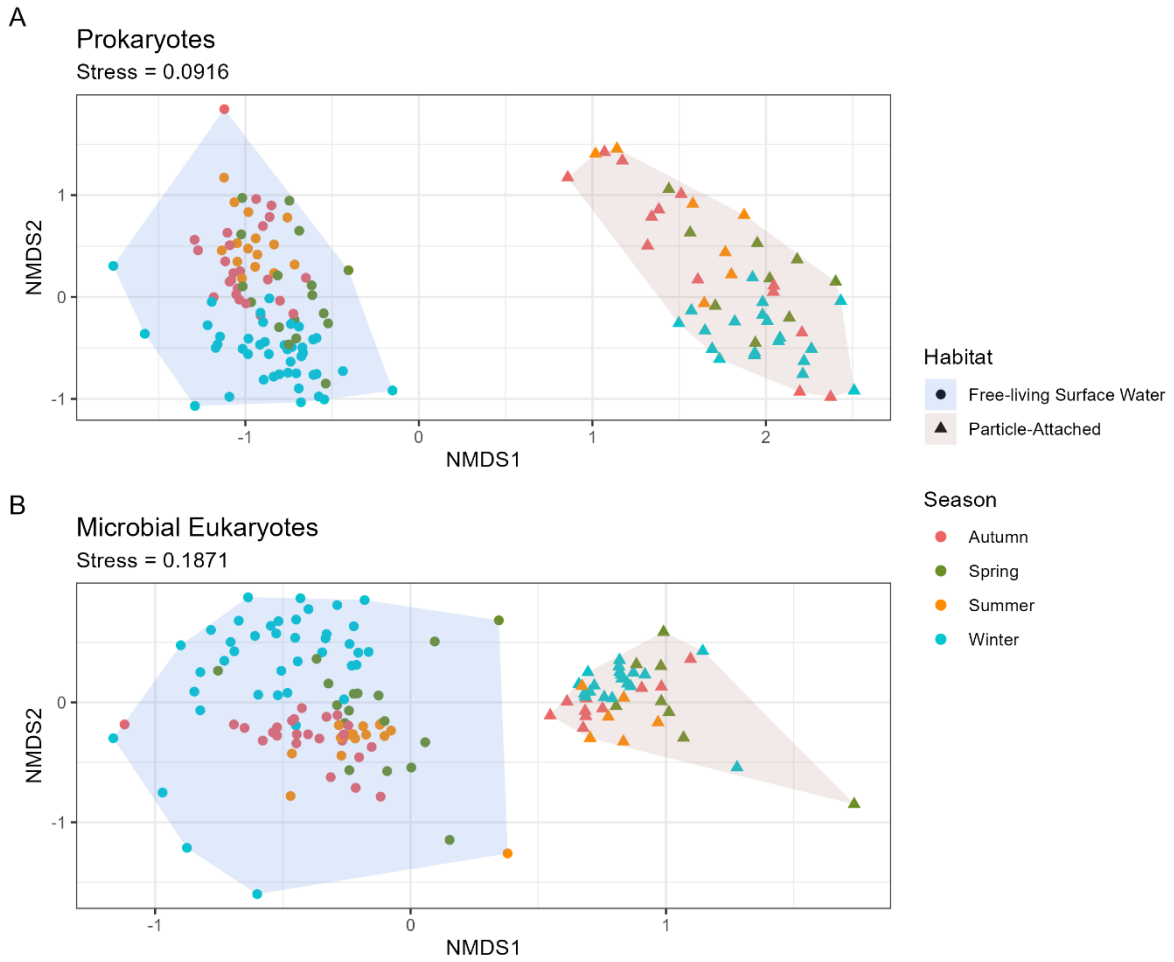

APPENDIX 7 – SHARED AND EXCLUSIVE ASVS – SURFACE WATER

Figure S6: Venn Diagrams of exclusive and shared ASVs between seasons for free-living (A) prokaryotes and (B) microbial eukaryotes from surface water. The values were rarefied in each dataset by sequencing depth using the lower number of sequences higher than 10,000.

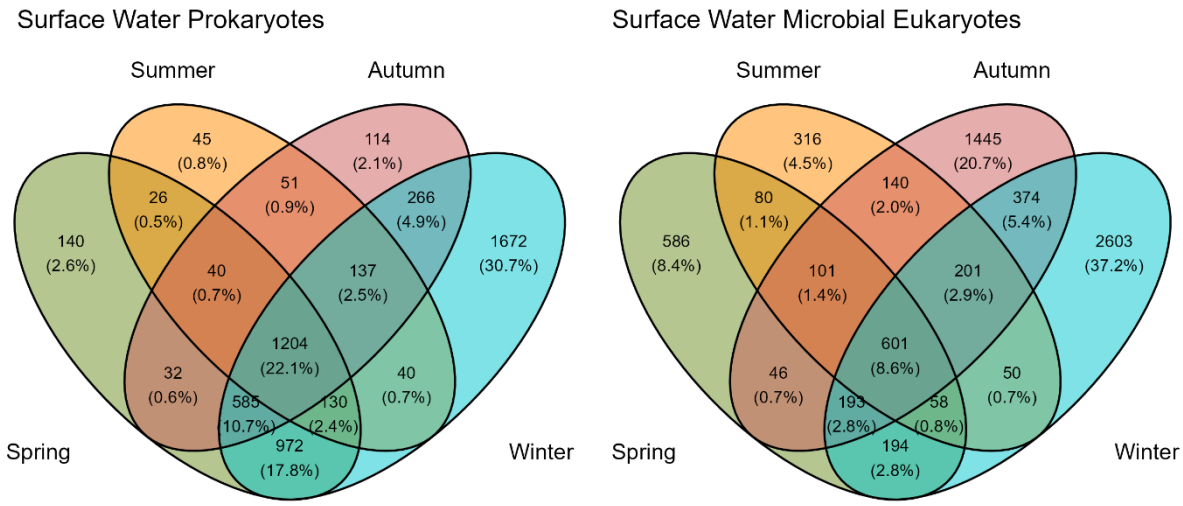

APPENDIX 8 – PERMANOVA (ADONIS) RESULTS – 1

```
#Prokaryotes Sinking Particles
Permutation test for adonis under reduced model
Permutation: free
Number of permutations: 999

adonis2(formula = otu ~ env$Season, data = otu, permutations = 999, method =
"bray")
          Df SumOfSqs      R2      F Pr(>F)
Model      3   2.3245 0.13573 2.3034  0.001 ***
Residual 44  14.8009 0.86427
Total    47  17.1254 1.00000
---
Signif. codes:  0 ‘***’ 0.001 ‘**’ 0.01 ‘*’ 0.05 ‘.’ 0.1 ‘ ’ 1

#Microbial Eukaryotes Sinking Particles
Permutation test for adonis under reduced model
Permutation: free
Number of permutations: 999

adonis2(formula = otu1 ~ env1$Season, data = otu1, permutations = 999,
method = "bray")
          Df SumOfSqs      R2      F Pr(>F)
Model      3   1.8898 0.12792 1.8091  0.001 ***
Residual 37  12.8833 0.87208
Total    40  14.7731 1.00000
---
Signif. codes:  0 ‘***’ 0.001 ‘**’ 0.01 ‘*’ 0.05 ‘.’ 0.1 ‘ ’ 1
```

APPENDIX 9 – PERMANOVA (ADONIS) RESULTS - 2

```
#Prokaryotes Surface Water
Permutation test for adonis under reduced model
Permutation: free
Number of permutations: 999

adonis2(formula = otu3 ~ env3$Season, data = otu3, permutations = 999, method
= "bray")
          Df SumOfSqs      R2      F Pr(>F)
Model      3   6.5149 0.22303 8.8986  0.001 ***
Residual  93  22.6959 0.77697
Total     96  29.2108 1.00000
---
Signif. codes:  0 ‘***’ 0.001 ‘**’ 0.01 ‘*’ 0.05 ‘.’ 0.1 ‘ ’ 1


#Microbial Eukaryotes Surface Water
Permutation test for adonis under reduced model
Permutation: free
Number of permutations: 999

adonis2(formula = otu2 ~ env2$Season, data = otu2, permutations = 999,
method = "bray")
          Df SumOfSqs     R2      F Pr(>F)
Model      3    4.116 0.1007 3.3965  0.001 ***
Residual  91   36.762 0.8993
Total     94   40.879 1.0000
---
Signif. codes:  0 ‘***’ 0.001 ‘**’ 0.01 ‘*’ 0.05 ‘.’ 0.1 ‘ ’ 1
```